1983

Time-optimal control strategies for residential heating systems using state-space techniques

Roy R. Crawford
Iowa State University

INFORMATION TO USERS

This reproduction was made from a copy of a document sent to us for microfilming. While the most advanced technology has been used to photograph and reproduce this document, the quality of the reproduction is heavily dependent upon the quality of the material submitted.

The following explanation of techniques is provided to help clarify markings or notations which may appear on this reproduction.

1. The sign or "target" for pages apparently lacking from the document photographed is "Missing Page(s)". If it was possible to obtain the missing page(s) or section, they are spliced into the film along with adjacent pages. This may have necessitated cutting through an image and duplicating adjacent pages to assure complete continuity.

2. When an image on the film is obliterated with a round black mark, it is an indication of either blurred copy because of movement during exposure, duplicate copy, or copyrighted materials that should not have been filmed. For blurred pages, a good image of the page can be found in the adjacent frame. If copyrighted materials were deleted, a target note will appear listing the pages in the adjacent frame.

3. When a map, drawing or chart, etc., is part of the material being photographed, a definite method of "sectioning" the material has been followed. It is customary to begin filming at the upper left hand corner of a large sheet and to continue from left to right in equal sections with small overlaps. If necessary, sectioning is continued again—beginning below the first row and continuing on until complete.

4. For illustrations that cannot be satisfactorily reproduced by xerographic means, photographic prints can be purchased at additional cost and inserted into your xerographic copy. These prints are available upon request from the Dissertations Customer Services Department.

5. Some pages in any document may have indistinct print. In all cases the best available copy has been filmed.

University
Microfilms
International
300 N. Zeeb Road
Ann Arbor, MI 48106

Crawford, Roy R.

TIME-OPTIMAL CONTROL STRATEGIES FOR RESIDENTIAL HEATING SYSTEMS USING STATE-SPACE TECHNIQUES

Iowa State University PH.D. 1983

Time-optimal control strategies for residential heating systems using state-space techniques

by

Roy R. Crawford

A Dissertation Submitted to the
Graduate Faculty in Partial Fulfillment of the
Requirements for the Degree of
DOCTOR OF PHILOSOPHY

Major: Mechanical Engineering

Approved:

Signature was redacted for privacy.

In Charge of Major Work

Signature was redacted for privacy.

For the Major Department

Signature was redacted for privacy.

For the Graduate College

Iowa State University
Ames, Iowa

1983

TABLE OF CONTENTS

LIST OF TABLES

LIST OF FIGURES

NOMENCLATURE

Scalars

a, b, c, d	Arbitrary coefficients used for various equations
Dis	Thermal discomfort (C)
exp(x)	Exponential of x
f_{cl}	Ratio of clothed to nude body surface area
h_c	Convective heat transfer coefficient ($W/m^2 \cdot K$)
H_u	Convergence criteria for the optimization procedure
I_{cl}	Clothing level (clo)
J	Building performance index
J_u	Energy consumption index
J_y	Indoor environmental quality index
k	Arbitrary time step
k_f	Final time step
k_i	Initial time step
L	Thermal load of the human body (met)
Max(x,y)	Function whose value is the maximum value of its arguments
Min(x,y)	Function whose value is the minimum value of its arguments
n	Order of a system
N_m	Metabolic rate (met)
p_a	Water vapor pressure in air (Pa)
p_{as}	Saturation water vapor pressure in air (Pa)
PMV	Predicted Mean Vote of thermal sensation

q	Indoor environmental weighting factor
Q_h	Electric furnace consumption (kW)
Q_l	Electric internal load (kW)
Q_s	Total horizontal solar radiation (W/m^2)
r	Energy weighting factor
RH	Relative humidity of air (%)
t	Time
T_a	Indoor dry-bulb temperature (C)
t_c	First-order time constant
T_{cl}	Clothing temperature (C)
T_{ds}	Desired standard temperature (C)
t_f	Final time
T_g	Globe temperature (C)
t_i	Initial time
T_{mr}	Mean radiant temperature (C)
T_o	Outdoor dry-bulb temperature (C)
T_s	Standard temperature (C)
T_s	Solar radiation temperature (1 C = 20 W/m^2)
T_{se}	Standard environmental temperature (C)
u	System input
u_m	Maximum system input
V	Air velocity (m/s)
y	System output
y_p	Co-state output
z	Desired system output

Vectors (bold lower case)

b	Input coefficient
c	Output coefficient
p	Co-state variable
w	Disturbance variable
x	State variable

Matrices (bold upper case)

A	System matrix

Special Units

clo	Clothing level (0.155 $m^2 \cdot K/W$)
met	Metabolic rate (58.2 W/m^2)
#	Arbitrary unit cost

Other symbols

*	Denotes optimal value
'	Denotes transpose of a vector or matrix

ACKNOWLEDGEMENTS

I express my deepest gratitude to my Major Professor, Dr. James E. Woods, for his exceptional guidance and support during this study. I am also indebted to Dr. Woods for providing many opportunities for obtaining experience in other research areas during my tenure at the Building Energy Utilization Laboratory.

I also thank the members of my advisory committee, Professors Arthur E. Bergles, R. Grover Brown, Thomas H. Kuehn, and Edmund R. Young, for sharing their valuable expertise in my area of research.

Further thanks are due to the various sources of funding for my dissertation research, which include the Engineering Research Institute, the Office of the Vice President for Research, and the Iowa State University Research Foundation.

I express a special thanks to the past and present members of the Building Energy Utilization Laboratory. The exchange of academic information and personal philosophies that I have had with these people has been especially rewarding. Very special thanks are due to Eduardo Maldonado and Gary Reynolds with whom I shared the many joys and sorrows of working towards a Ph.D.

Finally, I express my heartfelt gratitude to Elaine for her moral support and understanding throughout my graduate studies at Iowa State University.

ABSTRACT

Past research on the optimization of building performance has resulted in various control strategies which minimize building energy consumption while maintaining a specified level of indoor environmental quality (e.g., thermal comfort, mass air quality, lighting levels). The optimal control strategy proposed in this study uses a "performance index," which quantifies the "costs" of energy consumption and indoor environmental quality, to mathematically express the operating performance of a building.

A procedure is developed for deriving a dynamic system model which relates the indoor environmental quality to the energy consumption of a building. A system model is derived, semi-empirically, from actual building performance data and is converted to a finite-difference, state-space form. A mathematical optimization procedure, based on "Pontryagin's Maximum Principle", the system model, and the performance index, is developed to determine the optimal control for a building which maximizes the indoor environmental quality while minimizing the energy consumption.

The system modeling and optimization techniques are applied to a single-family residence with a forced-air, electric-resistance heating system. The resulting system

model indicates good agreement between the actual and predicted indoor environmental quality (thermal conditions). The results of the optimization of a hypothetical intermittent occupancy scenario indicate that maximum energy savings with minimum comfort penalties are realizable at the beginning and end of occupied periods. The optimization of a time-of-day electric rate strucure scenario indicates significant cost savings with only minor increases in discomfort as a result of systematically over-heating and over-cooling the structure to shift electrical loads from periods of high electric rates to periods of low electric rates.

A procedure for incorporating the optimization techniques into an actual control strategy is proposed. The practical aspects of providing weather predictions, adaptive modeling, and occupant inputs are also discussed.

INTRODUCTION

Since the beginning of time, human beings have sought shelter from their natural environment. The purpose of these early shelters was to provide a barrier which would exclude certain external elements (rain, snow, predators, etc.) and provide a buffer against certain external conditions (temperature, wind, etc.). Thus, the goal of the human quest for shelter has been, and still is, to create an indoor environment which is more amiable to the desires of its occupants. The discovery of fire gave man more control of his indoor environment and allowed civilization to expand into less temperate regions [1]. Throughout the ages, as civilization progressed and technology developed, human shelter has improved dramatically since ancient times when cave-dwellers used open fires to provide heat and to ward off predators.

Prior to this century, energy consumption in buildings was used primarily for heating and was controlled manually. By the turn of the century, the increased complexity of building systems and the demand for better performance from these systems necessitated the development of automatic controls. The United States pioneered the development and use of practical automatic controls in commercial buildings during the early 1900s, whereas the widespread acceptance of these controls in Europe did not occur until much later [1].

The earlier automatic controls were usually driven by pneumatics or electricity and were limited to local control.

Present day buildings are larger and incorporate more complex systems than ever before. Commercial building systems now exist which can control almost every aspect of the indoor environment including temperature, humidity, mass air quality, and lighting levels. The size and complexity of these systems combined with the dramatic increase in fuel prices during the 1970s has given rise to the need for even better environmental control in buildings today. Fortunately, recent advances in the fields of electronics and computers have paved the way for improving the performance of new and existing buildings through the use of more powerful controllers. These advanced controllers utilize electronic sensors and actuators coupled to central computers which can control building systems with algorithms that are more flexible and can be more sophisticated than ever before. Moreover, these computer systems can also monitor the building performance to give information which can be used for improving the various components of the building and to detect system malfunctions.

The objective of most current control algorithms is to control a given building system in a manner that will achieve a specified degree of indoor environmental quality with minimum energy consumption. Reductions in energy

consumption have been achieved in some buildings without sacrificing the quality of the indoor environment. However, further reductions in energy consumption will eventually be accompanied by a reduction in indoor environmental quality. This was demonstrated by the enactment of the Emergency Building Temperature Restrictions Act [2] which mandated a reduction in indoor environmental quality (reduced temperature setpoints during the heating season) to achieve reductions in energy consumption.

The preceding discussion indicates that the performance of a building system during normal operation depends upon two factors: energy consumption and indoor environmental quality. The relationship between these two factors depends upon the characteristics of the building systems, whereas the actual levels at which these factors are maintained depends on the manner in which the system is controlled. To assess completely the performance of a building system, consideration must be given to the output of the system (indoor environmental quality) as well as the input (energy consumption). The development of a quantitative expression of the performance of a building (i.e., a "performance index") would allow the rational comparison of different control strategies. Furthermore, this performance index, combined with a building system model, which predicts the output of the system resulting from any arbitrary input,

would provide the necessary information for determining the "optimal" control strategy for a building.

Research Objectives

The overall objective of this study is the development of optimal control strategies for buildings. This control strategy development is accomplished in three stages.

1. Derive a mathematical performance index which rationally combines the energy consumption and indoor environmental quality of a building. The objective of this study is met when the performance index is mathematically optimized to give the minimum energy consumption which results in maximum indoor environmental quality.

2. Develop a procedure for deriving a mathematical system model which relates the indoor environmental quality of a building to its energy consumption. This model requires the inclusion of all significant steady and transient effects and should be site-specific in nature. However, the modeling procedure should be general in the sense that it can be applied to any specific building within a given class with only minor modifications.

3. Develop an optimization procedure for determining the energy consumption and resulting indoor environmental quality which minimize the performance index while satisfying the system model. Develop a practical method for applying this procedure in an actual control system.

The overall procedure outlined above is described in detail in the remainder of this study. An actual single-family residence is used as a test site for obtaining data to validate portions of this study.

Background

Indoor environmental quality

The overall environmental quality in a building is affected by thermal, mass air quality, lighting, acoustic, and spatial factors [3]. Although all of these factors should be incorporated into the efficient design of a building, acoustic and spatial factors are usually determined by the design and construction of the building and normally are not directly controlled during the operation of the building. However, thermal, mass air quality, and lighting factors can be controlled during the operation of a building. Therefore, these three factors should be incorporated in the building performance index for optimization purposes if they are affected by the controlled energy consumption of the building.

Thermal factors The American Society of Heating, Refrigerating, and Air-Conditioning Engineers (ASHRAE) has developed a standard [4] for specifying thermal comfort conditions for spaces occupied by healthy persons. Thermal comfort has been defined by ASHRAE as "that condition of

mind which expresses satisfaction with the thermal environment." The ASHRAE comfort standard specifies combinations of four environmental parameters (temperature, radiation, humidity, and air movement) and two occupant parameters (clothing and activity) that result in acceptable levels of thermal comfort. This standard is based on extensive research and has been updated periodically to incorporate the latest appropriate research findings.

Numerous comfort indices have been developed for assessing thermal environments. These indices combine two or more of the six aforementioned comfort parameters into a single quantity which describes the thermal conditions of the environment with respect to the occupants exposed to the environment. One of the earliest comfort indices is the "Effective Temperature" (ET) introduced by Houghten and Yagloglou (later named Yaglou) in 1923 [5] which indicates the combined effect of dry-bulb temperature and humidity on comfort. This is an empirical index based on experimental studies of subjective human thermal responses in controlled environmental test chambers. Yaglou's results were displayed as lines of equal comfort on a psychrometric chart.

A correction to ET for radiation effects was developed by Bedford and Warner [6] in 1934 by substituting the "operative temperature" for the dry-bulb temperature. The

operative temperature (T_o) is defined as "the uniform temperature of an imaginary enclosure with which man will exchange the same dry heat by radiation and convection as in the actual environment" [7]. Bedford and Warner used the "black globe temperature" as a measure of the operative temperature. The black globe temperature (T_g) is the equilibrium temperature of a 153 mm (6 inch) diameter black globe which has approximately the same radiation and convective heat exchange as an actual person exposed to low temperature radiation. The resulting index is the "corrected effective temperature " (CET) which includes the effects of temperature, radiation, humidity.

Many other indices have been developed for describing indoor environments including the Heat Stress Index [8], Wet-Bulb Globe Temperature Index [9], and Wind Chill Index [10], however, ET was the most widely used index for over forty years after its development [7]. Inaccuracies were found in the ET model predictions with respect to relative humidity effects as early as 1947 [11].

During the 1960s extensive research was conducted at Kansas State University (KSU) on the thermal response of people to different environmental conditions [12]. In these studies, groups of people were exposed to various controlled environmental conditions and thermal sensation data were obtained using the following subjective scale:

7 = hot
6 = warm
5 = slightly warm
4 = comfortable, neutral
3 = slightly cool
2 = cool
1 = cold

Statistical methods were used to determine the significant relationships between thermal sensation and the environmental parameters. Other tests were performed to determine if other factors affected thermal comfort.

Fanger conducted similar studies at KSU and the Technical University of Denmark [13]. He used the experimental data to develop a physiological model based on an energy balance of the human body. This "comfort equation" determines conditions of thermal equilibrium for a wide range of all six comfort factors. Fanger also developed a procedure for calculating the "Predicted Mean Vote" (PMV) of the thermal response of a large group of people to various environmental conditions using a scale similar to that shown above.

Research at the Pierce Foundation [14] led to the development of the "New Effective Temperature" (ET*) scale in 1971 based on a rational physiological model which was validated with experimental data. This improved index reduced some of the errors from the old ET scale and provided better accuracy over a wider range of conditions.

A slightly modified form of the Pierce physiological model was developed at KSU for predicting thermal sensation [15]. The Pierce and KSU models incorporate an active control mechanism which results in transient capabilities and allows the quantitative prediction of thermo-regulatory mechanisms such as sweating, shivering, vasoconstriction, and vasodilation whereas the Fanger model is limited to steady-state conditions. The KSU model has been further extended to predict the effects of long-term heat acclimation [16]. All of the models perform very well at predicting neutral conditions over a wide range of environmental conditions, however, the KSU and Pierce models are more accurate as conditions deviate from thermal neutrality [17].

Gagge et al. proposed the "Standard Effective Temperature" (SET*) in 1972 [18]. Unlike ET* which only standardizes humidity, SET* is defined with standard conditions of radiation, humidity, air movement, clothing, and activity. Unlike any of the previous indices, SET* allows the comparison of completely different environments. However, the calculation procedure does not compensate for changes in the activity level.

The present-day comfort models are being refined in many areas such as the effects of localized air movement [19] and asymmetric radiative fields [20]. Recent research

has also been directed towards the effect of transient environmental conditions (e.g., fluctuating temperatures and humidity [21]) on thermal sensation.

Although most comfort studies have been limited to the six factors discussed above, recent studies have indicated effects on thermal comfort from other factors. Rohles, Bennett, and Milliken [22] found that lighting, color, and room decor have an effect on thermal comfort. Studies by Carlton-Foss and Rohles [23] indicate that some of the differences between individual perceptions of thermal sensation is related to personality factors. A study by Woods et al. [24] resulted in a correlation between thermal sensation and carbon-dioxide levels. Thus, other factors which affect thermal comfort do exist, but none have been found to be as significant as the six commonly accepted factors.

Another area of comfort research that is only recently developing is the prediction of the thermal comfort performance of buildings over long time periods. A method proposed by Hayter [25] uses the "Operative Degree Hour" defined as the time-integrated deviation of the operative temperature from comfort conditions to compare the environmental performance of different passive-solar building designs.

Another comfort performance index has been proposed by Carroll [26] for evaluating residential buildings. This index calculates the thermal discomfort at a given time as the difference between the effective temperature of the environment and a preferred temperature for the environment. The effective temperature is similar to ET* and the preferred temperature is assumed to be a function of outside temperature due to assumed changes in clothing levels with respect to weather changes. This temperature difference is integrated over time with various numerical procedures being employed to penalize undesirable transient effects. The procedure incorporates a strategy by which occupants will adjust their clothing level in response to temperature changes. The indices proposed by Hayter and Carroll have not been tested under actual occupied conditions to determine if they do give a true indication of the preferred relative weighting of discomfort over time for actual building occupants.

Mass air quality Indoor mass air quality is a topic of recent, widespread concern due to recent economic factors that have led to the reduction of ventilation air and an increase in contaminant sources. An indoor air quality standard has been developed by ASHRAE [27] which specifies maximum allowable levels for many known indoor contaminants. Some of these levels were adopted from Environmental

Protection Agency regulations regarding acceptable outdoor contaminant levels. The more commonly occurring indoor contaminants in residences and the maximum values allowed by the ASHRAE standard are shown in Table 1. This standard specifies that for some contaminants, higher concentrations are permitted over shorter time intervals, whereas for other contaminants, certain threshold limits are not allowed to be exceeded, and still other contaminants are allowed to reach

Table 1. Maximum allowable concentrations for some commonly occuring indoor contaminants (adapted from ASHRAE [27])

Contaminant	Level	Time
Carbon Monoxide	40 mg/m^3 10 mg/m^3	1 hr 8 hrs
Carbon Dioxide	4.5 g/m^3	continuous
Nitrogen Monoxide	0.5 mg/m^3 1 mg/m^3	24 hrs 30 min
Nitrogen Dioxide	100 $\mu g/m^3$	yr
Ozone	100 $\mu g/m^3$	continuous
Formaldehyde	120 $\mu g/m^3$	continuous
Sulfur Dioxide	80 $\mu g/m^3$ 365 $\mu g/m^3$	yr 24 hrs
Particulates	75 $\mu g/m^3$ 260 $\mu g/m^3$	yr 24 hrs
Radon	0.01 WL	annual average

almost any level as long as a specified long-term average level is not exceeded.

There has been a recently growing concern of the possibility of interactive effects which may cause combinations of certain contaminants to have adverse health effects when each contaminant is individually below its standard value. Although this concern has been raised by several observances of health effects, where there were no significant contamination levels [3], research has not been able to confirm this possibility.

Lighting factors For a given electrical lighting device, the lighting level is almost linearly proportional to the energy consumed. However the relationship between "visual efficiency" and lighting levels is very nonlinear [28]. As a result, the lighting levels and resulting energy consumption required for various tasks is highly variable. The control of lighting levels also requires consideration of the spectral and spatial distributions, especially when more than one lighting source is available [29].

System modeling

Extensive research has been performed in the field of dynamic building system modeling during the past forty years. Numerous analytical techniques have been developed for transient conduction heat transfer in building envelopes including the response factor and transfer function methods

of Stephenson and Mitalas [30] and Kusuda [31]. A finite-difference technique has been developed by Kuehn and Maldonado [32] which may have a slightly greater required calculation time than the transfer function method but has much greater flexibility in terms of the wall constructions that can be simulated and the amount of information that can be provided.

The extensive research that has been conducted on the dynamic performance of heating, ventilating, and air-conditioning (HVAC) equipment has been incorporated into several large computer programs for building system simulation. These programs include BLAST-2 (U.S. Army Construction Engineering Research Laboratory), DOE-2 (Lawrence Berkeley Laboratory), ECUBE-III (American Gas Association), Trace (Trane Company), and TRNSYS (University of Wisconsin). Many of these programs use quasi-steady approximations for part of the analysis to increase computational speed and reduce memory requirements. The types of buildings and analyses which can be simulated by these programs are generally limited by the techniques used.

Mehta and Woods [33] have developed a procedure for dynamically simulating building systems using classical control theory techniques which allows much greater flexibility than the previously developed techniques. The most recent advance in dynamic building simulation is the

introduction of modern control theory analysis using state-space techniques by Yi [34]. State-space techniques have also been introduced as a useful method for indoor air quality analyses [35]. These control theory techniques provide the basis for the application of a wide range of stability analysis and optimization procedures that have already been applied in other fields (e.g., communications, aeronautics, chemical processes).

Although the aforementioned building simulation procedures are useful for building performance analyses, they are either too computationally cumbersome or do not provide the necessary information for real time optimal control purposes. Furthermore, these procedures require complete, specific, a priori information about the dynamic characteristics of the building characteristics.

Janssen [36] has developed a procedure for determining the important transient and steady-state characteristics of a residential building by monitoring its dynamic response during the on and off cycles of the furnace operation. Although this procedure was developed for analysis purposes, it has potential as a modeling procedure for optimal control purposes.

Adaptive modeling techniques have been developed by Schumann [37] as a method of stabilizing the control of an air-conditioning plant. This procedure uses the actual

system operation data to obtain and correct the system model which is in turn used as the basis for an optimal control strategy which provides fast system response while maintaining stability.

Extensive research has been conducted in the field of control theory during the past twenty years [38] for the purpose of developing dynamic system models from actual system performance data (system identification). Some deterministic methods of model parameter estimation have been developed [39], however these methods are not generally useful since they require the same number of parameters as data.

Most parameter estimation procedures use stochastic methods which estimate a relatively small number of model parameters from a large quantity of data. These stochastic methods utilize an error cost function which is minimized by any of several approaches including least squares [40] and maximum likelihood estimation [41]. The most popular stochastic method is least squares which was originally developed in 1795 by Karl Friedrich Gauss who used it for astronomical calculations [38]. Since 1958, the method of least squares has been adapted to a wide variety of system identification by modifying the error cost function and the parameter calculation procedure. A few of these least square parameter estimation procedures are ordinary least

squares [41], weighted least squares [42], generalized least squares [43], and extended least squares [44]. Numerous books have been written in the field of system identification and parameter estimation by several authors including Davies [45], Eykhoff [46], Graupe [47], Mendel [48], and Sage and Melsa [39].

Optimization

The past decade has seen an increased emphasis on the development of control strategies which decrease energy consumption. Benton [49] demonstrated energy savings and improved comfort through the use of a "high performance" thermostat (low droop, fast cycling) in a residence with electric resistance baseboard heating as compared to a conventional thermostat. Stoecker et al. [50] showed that a reduction in electrical demand charges could be obtained by decreasing the gain of a proportional thermostat used to control the cooling load and letting the indoor temperature swing. The degree of reduction in demand charges was limited by the tolerable level of temperature swing.

Bloomfield and Fisk [51] have developed an "optimum start" control strategy which determines the minimum lead time required to achieve a specified temperature during intermittent heating strategies. This procedure uses Pontryagin's Minimum Principle to develop a set of equations

which are solved using linear programming techniques to determine the optimal start time.

Backus [52] and Benton [53] have developed improved heat pump control strategies which reduce the amount of auxiliary heat required for recovery during changes in thermostat setpoints. Both strategies anticipate the lead time required for the heat pump to achieve a desired space temperature, thus reducing the higher costs associated with auxiliary heating sources.

The control strategies described above attempt to minimize energy consumption while maintaining a desired, fixed temperature. Kaya [54, 55, 56] has developed an "optimum" control strategy which maintains the temperature, humidity, and air velocity of an occupied space within the ASHRAE comfort envelope with a minimum expenditure of energy. This strategy uses a steady-state optimization procedure to determine the point within the comfort envelope which will minimize energy use followed by a dynamic optimization procedure for controlling the system such that the optimal comfort point is reached in minimum time. Although this control strategy incorporates the interactive effects of three comfort factors, it still attempts to minimize energy consumption while maintaining a predetermined level of comfort.

Preliminary results from the research conducted as part of this dissertation have been recently published [57] and include the development of the first "optimal" control strategy which attempts to "minimize" energy consumption while "maximizing" thermal comfort.

PERFORMANCE INDEX

To be useful for purposes of building control strategy optimization, the performance index should

-- incorporate the relative values of energy consumption and indoor environmental quality,

-- be a scalar, mathematical function,

-- have a minimum or maximum value reflecting the optimal building performance,

-- include the building performance during the entire optimization period.

The performance index in this study uses a simple algebraic sum of energy consumption and indoor environmental quality to satisfy the first and second requirements. The third requirement is satisfied by representing the indoor environmental quality as a quantity that is zero when the conditions are optimal and positive when the conditions are degraded. Thus, the optimal system performance occurs when the performance index is minimized. The last requirement is met by integrating the performance over the optimization interval.

Indoor Environmental Quality

Thermal comfort

The six important factors which affect an occupant's thermal comfort in an enclosed space are the temperature, humidity, and motion of the ambient air, the radiant field

within the space relative to the occupant's position, and the occupant's clothing and activity level [13]. The definitions of the variables used to describe these factors in this study are given below.

T_a = dry-bulb temperature of the ambient air (C).

T_{mr} = mean radiant temperature (C), defined as the uniform temperature of an imaginary enclosure which produces the same radiative heat exchange with the occupant as the actual environment.

RH = relative humidity of the ambient air (%).

V = air velocity relative to the occupant (m/s)

I_{cl} = occupant's clothing level (clo).

N_m = occupant's activity level (met).

The units for clothing level are a measure of the thermal resistance of the clothing defined as 1 clo = 0.155 $K \cdot m^2/W$ [13]. The activity level is measured in terms of heat production per unit body surface area. The units are defined as 1 met = 58.2 W/m^2 which corresponds to sedentary activity.

Fanger model A subjective scale used by Fanger to measure occupant thermal sensation in an environment is shown below.

-3	cold
-2	cool
-1	slightly cool
0	neutral
+1	slightly warm
+2	warm
+3	hot

Fanger [13] has developed an algorithm which predicts thermal sensation as a function of the six comfort factors. This algorithm is based on the Predicted Mean Vote (PMV) for the thermal sensation (using the above scale) of a large group of human subjects subjected to various experimental conditions. The algorithm is as follows.

$$PMV = [17.6\exp(-2.1N_m)+1.6]L \tag{1}$$

$$\begin{aligned} L = {} & N_m - 0.35(0.86-0.061N_m-p_a/6670) \\ & - 0.42(N_m-1) - 0.0023N_m(44-p_a/133) \\ & - 0.0014N_m(34-T_a) \\ & - 6.8\times10^{-10}f_{cl}[(T_{cl}+273)^4-(T_{mr}+273)^4] \\ & - 0.0172f_{cl}h_c(T_{cl}-T_a) \end{aligned} \tag{2}$$

$$\begin{aligned} T_{cl} = {} & 35.7 - 1.6N_m \\ & - 6.12\times10^{-9}f_{cl}[(T_{cl}+273)^4-(T_{mr}+273)^4] \\ & + 0.155I_{cl}f_{cl}h_c(T_{cl}-T_a) \end{aligned} \tag{3}$$

$$h_c = \text{Max}[12.1V^{0.5},\ 2.39(T_{cl}-T_a)^{0.25}] \tag{4}$$

In the above equations, L is the thermal load of the body (met), T_{cl} is the clothing temperature (C), h_c is the convective heat transfer coefficient of the clothed body ($W/m^2 \cdot K$), f_{cl} is the ratio of the clothed body surface area to that of the nude body, and p_a is the water vapor pressure (Pa). All other variables are as previously defined. Fanger's algorithm also allowed for the inclusion of the

occupant's mechanical efficiency which is assumed to be always zero in this study and has been omitted from the algorithm. Equations (1-4) have also been converted to SI units for use in this study. An approximate expression for calculating f_{cl} as a function of I_{cl} was derived from data given in [13].

$$f_{cl} = 1 + 0.15I_{cl} \tag{5}$$

The water vapor pressure (p_a) is calculated from T_a and RH by the expression

$$p_a = (RH/100)p_{as} \tag{6}$$

where p_{as} is the saturation water vapor pressure (Pa) given by [7]:

$$\ln(p_{as}) = C_1/T + C_2 + C_3T + C_4T^2 + C_5T^3 + C_6\ln(T) \tag{7}$$

where

$C_1 = -5800.2206$ $\quad$ $C_4 = 0.41764768 \times 10^{-4}$

$C_2 = 1.3914993$ $\quad$ $C_5 = -0.14452093 \times 10^{-7}$

$C_3 = -0.04860239$ $\quad$ $C_6 = 6.5459673$

and $T=T_a+273$ is the absolute air temperature (K). Equation (7) is valid for T_a in the range 0 to 200 C.

Equations (1-7) contain all of the necessary information for calculating the PMV for thermal sensation,

as a function of the six comfort factors. However, equations (3) and (4) are both nonlinear functions of T_{cl} and h_c and must be solved simultaneously. A Newton-Raphson method [58] is used to obtain the solution.

The Standard Effective Temperature (SET^*) developed by Gagge [18] is defined as the dry-bulb temperature of a standard environment (uniform temperature, 50 % relative humidity, air movement resulting in a convective heat transfer coefficient of 2.9 $W/m^2 \cdot K$, clothing level of 0.6 clo, and activity level of 1 met) after one hour exposure that results in the same physiological strain as the conditions in the actual environment. Gagge's procedure for calculating SET^* does not have the capability of including activity levels different from 1 met, therefore a similar "Standard Temperature" (T_s) has been defined in this study which does incorporate variable effects of all six comfort factors.

T_s is defined as the dry-bulb temperature experienced by a "standard person" in a "standard environment" that produces the same thermal sensation as experienced by the actual person in the actual environment. The defined "standard conditions" are:

Standard Environment-- $T_{mr} = T_a$

$RH = 50\ \%$

$V = 0.1$ m/s

Standard Person-- $I_{cl} = 0.6$ clo

$N_m = 1$ met (8)

By substituting these conditions (8) into equations (1-7) and varying T_a, a relationship between T_s and PMV can be found. This relationship as shown in Fig. 1 for values of T_s between 20 and 30 C can be accurately expressed as

$$T_s = 25.4 + 2.93PMV \quad (9)$$

Equation (9) can be incorporated with the algorithm of equations (1-7) to provide a convenient means of calculating T_s.

A PMV of zero (thermal neutrality) is used as the optimal condition for thermal sensation in this study. Thus, the optimal value of T_s (denoted as T_s^*) is 25.4 C according to equation (9). Thermal discomfort (Dis) is defined in this study as the difference between the actual value of T_s and the optimal value (T_s^*).

$$Dis = T_s - T_s^* = T_s - 25.4 = 2.93PMV \quad (10)$$

This index of thermal discomfort (Dis) is merely a rational variable transformation which converts PMV to units of temperature (C). The transformation is not arbitrary since

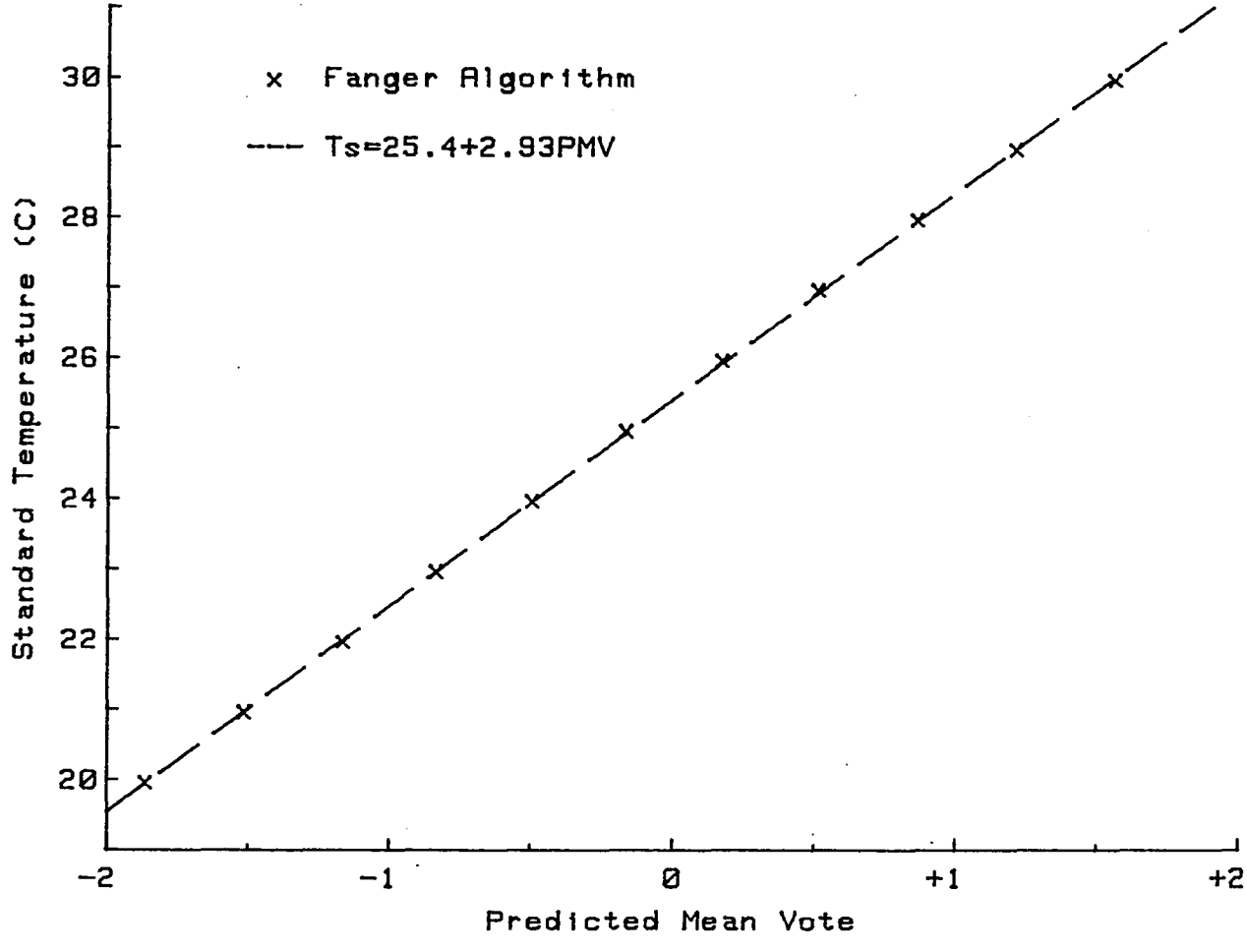

Fig. 1. Relationship between T_s and PMV calculated from the Fanger algorithm

it uses the value of 2.93 C per thermal sensation vote which was derived using the T_s definition. Thus, the value of Dis is equivalent to the negative dry-bulb temperature change required by a standard person in a standard environment to achieve optimal comfort conditions. Since Dis is based on units of temperature relative to T_s, it is not necessarily equivalent to the dry-bulb temperature change required to obtain comfort under conditions which are not standard as defined above.

Linear model Although Dis can be calculated from equations (1-10) for any values of the six comfort factors, a simplified relation would be more useful for optimization purposes. In general, Dis can be expressed as

$$Dis = f(T_a, T_{mr}, RH, V, I_{cl}, N_m) \tag{11}$$

where f is a nonlinear function of its variables as governed by the preceding equations. This equation can be linearized in the following form:

$$Dis = a_1(T_a-25.4) + a_2(T_{mr}-T_a) + a_3(RH-50) + a_4(V-0.1) + a_5(I_{cl}-0.6) + a_6(N_m-1) \tag{12}$$

In this formulation, T_a is normalized about T_s^* (25.4 C) and the remaining variables are normalized about their standard values. The method used to derive Dis, combined with the normalization used for the comfort factors,

eliminates the need for a constant term in equation (12) since Dis = 0 by definition when T_a equals T_s^* and the other comfort factors are equal to their standard values. The coefficients in equation (12) are the partial derivatives of Dis with respect to the independent variables. Values for these coefficients were calculated from the Dis algorithm using a central-differencing technique [59]. The results of these calculations are shown below.

$$\begin{aligned} a_1 &= 1.0056 \text{ C/C} & a_4 &= -4.6632 \text{ C/(m/s)} \\ a_2 &= 0.4733 \text{ C/C} & a_5 &= 5.6752 \text{ C/clo} \\ a_3 &= 0.0253 \text{ C/\%} & a_6 &= 7.5634 \text{ C/met} \end{aligned} \tag{13}$$

Each coefficient indicates the change in Dis resulting from a unit change in the factor associated with that coefficient. The first coefficient (a_1) has a value near unity (1.0056 C discomfort per C air temperature) which is logical since the derivation of Dis is based on units of air temperature. The inverses of these coefficients indicate the required change in each variable to produce a 1 C change in discomfort. These inverses also indicate the adjustment required in any of the factors to compensate for discomfort conditions which occur due to deviations in any of the other factors. The accuracy of these coefficients is dependent upon the accuracy of the Fanger algorithm from which they were derived and the deviation from the standard conditions

about which they were calculated. A similar set of "adjustment" factors has been compiled by Woods [60] for use within the region of acceptable thermal sensation (-1 < PMV < 1). In this study, a third set of adjustment factors has been calculated from information given in the thermal comfort standard set by ASHRAE [4]. These three sets of adjustment factors are compared in Table 1. The discrepancies between these factors are discussed later.

As discussed previously, the linear coefficients were derived at standard conditions. Figure 2 compares the linear Dis equation to the Fanger algorithm as each factor is varied independently from its respective standard value.

Table 2. Required change of comfort factors to obtain a 1 C change in discomfort (Dis)

Factor	Units	Required Change		
		Derived from Fanger	Derived from Literature	Derived from ASHRAE
T_a	C	1.0	1.0	1.0
$T_{mr}-T_a$	C	2.1	1.7	2.0
RH	%	40	27	27
V	m/s	-0.21	-0.47	-0.28
I_{cl}	clo	0.18	0.14	0.15
N_m	met	0.13	0.50	0.21

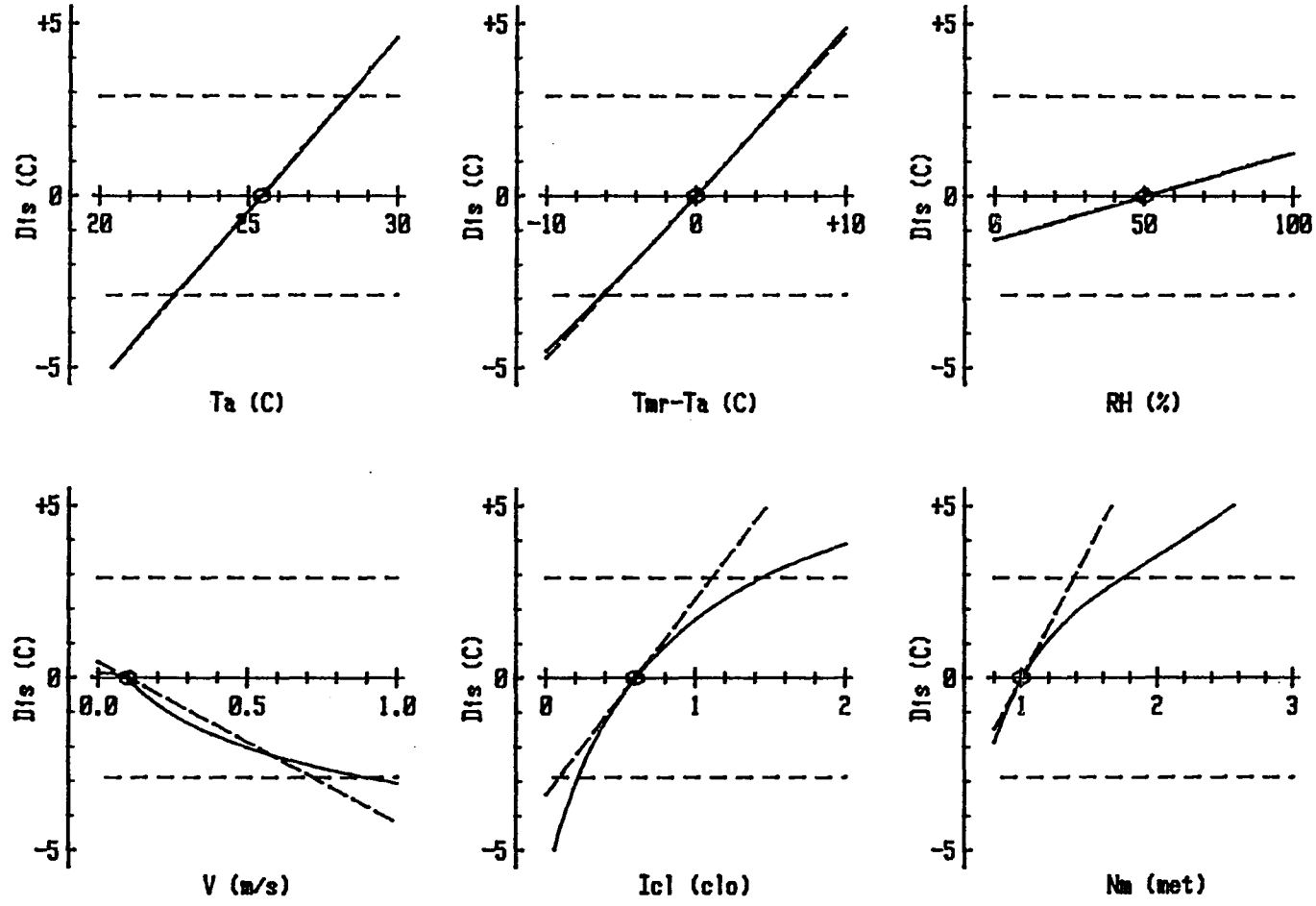

Fig. 2. Comparison of the Fanger algorithm (solid lines) and the linear discomfort equation (dashed lines) as each factor is varied about the base conditions (circled)

The horizontal dashed lines indicate the zone of 80 % thermal acceptability corresponding to a PMV between slightly cool and slightly warm. The first three factors (T_a, $T_{mr}-T_a$, RH) show strong linearity in the Fanger algorithm, however, the remaining factors (V, I_{cl}, N_m) show significant nonlinear effects. Therefore, equation (13) must be used with caution when these three factors are varied about their standard conditions. From Fig. 2, it can be seen that within the range of thermal acceptability, the maximum error in Dis of the linear model is about 1 C.

The discrepancies between the three sets of adjustment factors in Table 1 can be partially explained by examining Fig. 2. The largest difference occurs between the metabolic rate factors. In Fig. 2, the larger metabolic rate adjustment factors (0.21 and 0.50 met/C) more closely parallel the Fanger algorithm at successively higher metabolic rates. Similarly, the higher (in terms of magnitude) air velocity adjustment factors (-0.28 and -0.47 m/s/C) more closely parallel the nonlinear model at successively higher air velocities. The third largest error is between the humidity adjustment factors, however, all three factors indicate that the effect of relative humidity on comfort is small.

Figure 2 only shows the error in the linear approximation model as each comfort factor is varied independently

while the remaining factors are maintained at their standard values. During typical winter conditions in climates that require heating, humidity levels are usually lower and clothing levels are usually higher than the standard conditions used in this study. Conversely, during typical summer conditions, humidity levels are usually higher and clothing levels are usually lower. The adjustment factors in Table 2 can be recalculated with the aforementioned procedure using standardized winter and summer conditions to obtain a more accurate linear discomfort equation under these conditions. Table 3 shows the standard values for the base, winter, and summer conditions and a comparison of the

Table 3. Comparison of base, winter, and summer comfort factors and required adjustments for a 1 C increase in discomfort (Dis)

		Standard Value			Required Adjustment		
Factor	units	winter	base	summer	winter	base	summer
T_a	C	23.9	25.4	26.7	1.3	1.0	0.77
$T_{mr}-T_a$	C	0	0	0	2.7	2.1	1.7
RH	%	30	50	70	43	40	37
V	m/s	0.1	0.1	0.1	-0.30	-0.21	-0.16
I_{clo}	clo	1.0	0.6	0.3	0.25	0.18	0.12
N_m	met	1	1	1	0.14	0.13	0.12

calculated adjustment factors. The adjustment factors in this table indicate that these factors do change when the standard conditions about which they are derived change. Unlike the base case, the adjustment factors for dry-bulb temperature are not unity for the winter and summer conditions. The actual values indicate that discomfort is more sensitive to dry-bulb temperature in winter conditions and less sensitive in summer. Figures 3 and 4 compare the linearized discomfort equation (12) using the base coefficients (13) with the Fanger algorithm evaluated under winter and summer conditions, respectively. These figures show that the use of the base coefficients introduces negligible error in the prediction of optimum comfort (Dis = 0), however, the error increases as the conditions deviate from optimum.

Table 4 shows the required level of each comfort factor to produce incremental discomfort (Dis) changes of 1 C according to the linear equation (12). This table can be used to compare levels of different comfort factors which will produce equal levels of discomfort. This table also indicates the physical limits of some of the comfort factors (RH, V, N_m) which result in limits on the amount of change in discomfort that can be obtained by adjusting these factors. Since the data in Table 4 are based on the linear equation, they are subject to error. As discussed

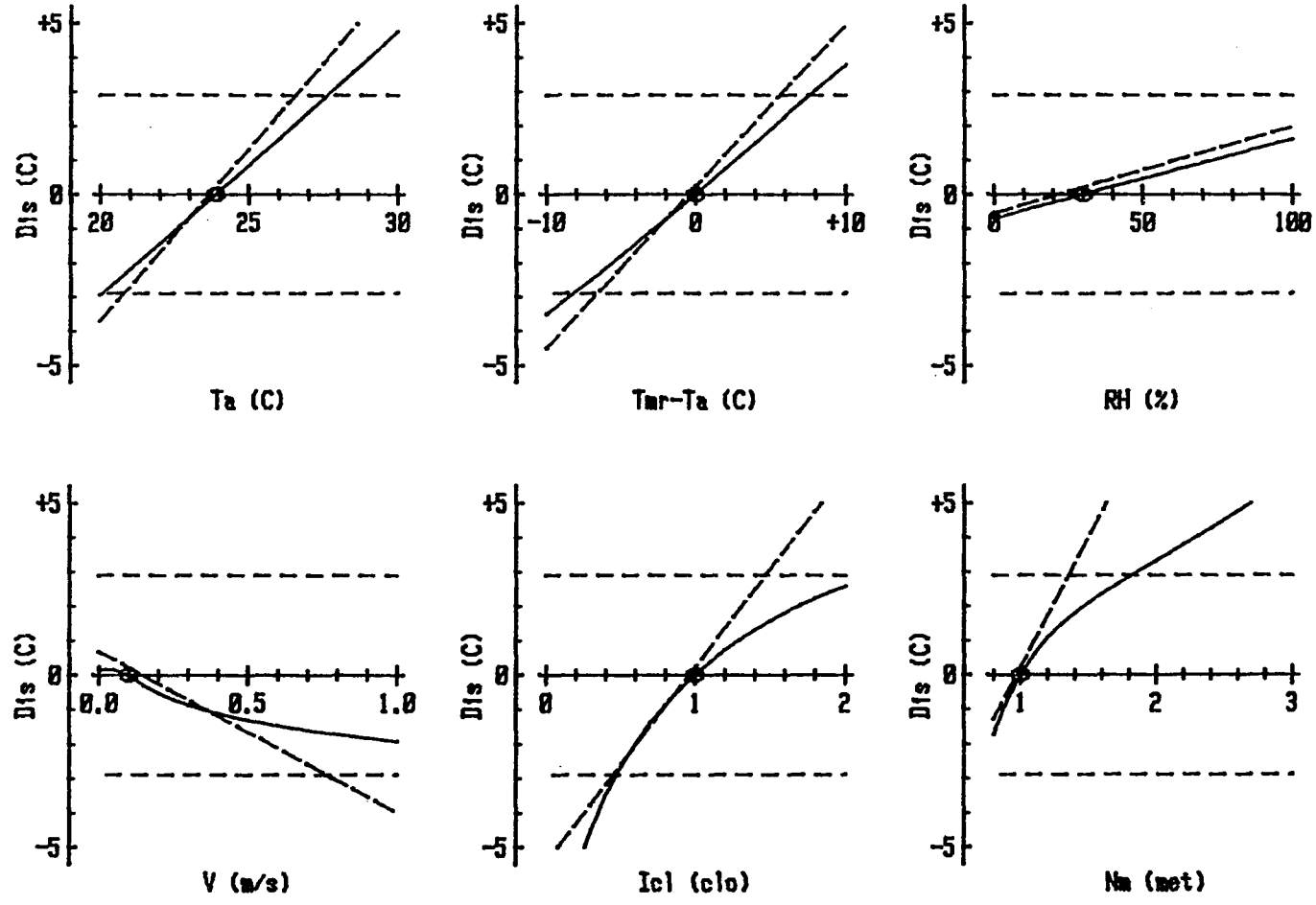

Fig. 3. Comparison of the Fanger algorithm (solid lines) and the linear discomfort equation (dashed lines) as each factor is varied about the winter conditions (circled)

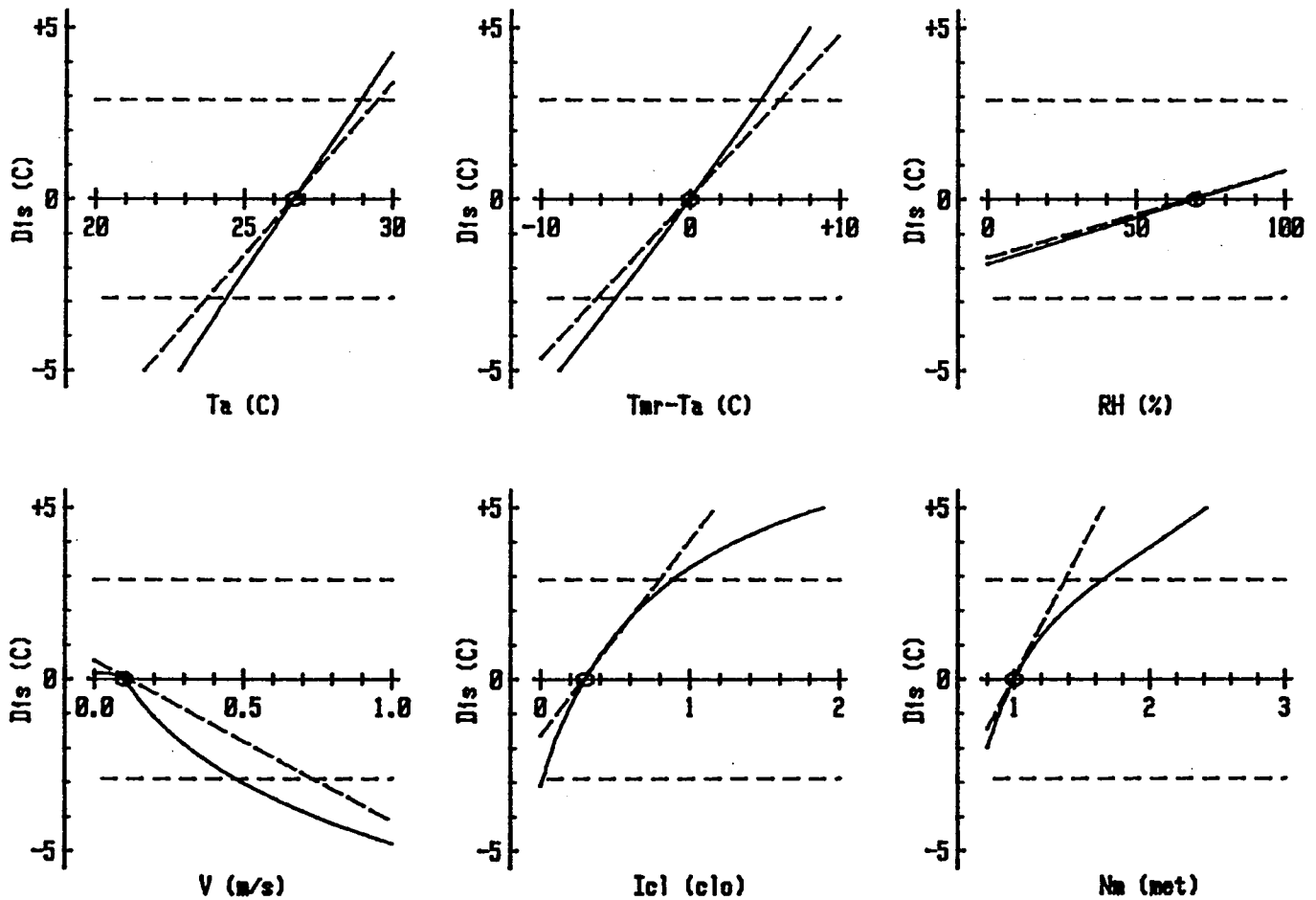

Fig. 4. Comparison of the Fanger algorithm (solid lines) and the linear discomfort equation (dashed lines) as each factor is varied about the summer conditions (circled)

Table 4. Incremental changes in Dis for various levels of each comfort factor

Incremental Change in Dis (C)	Comfort Factor Level					
	T_a (C)	$T_{mr}-T_a$ (C)	RH (%)	V (m/s)	I_{cl} (clo)	N_m (met)
-5	20.5	-10.6	--	1.17	--	--
-4	21.5	-8.5	--	0.96	--	--
-3	22.5	-6.3	--	0.74	0.07	--
-2	23.5	-4.2	--	0.53	0.25	0.74
-1	24.4	-2.1	10	0.31	0.42	0.87
0	25.4	0.0	50	0.10	0.60	1.00
+1	26.4	2.1	90	--	0.78	1.13
+2	27.4	4.2	--	--	0.95	1.26
+3	28.4	6.3	--	--	1.13	1.40
+4	29.4	8.5	--	--	1.30	1.53
+5	30.4	10.6	--	--	1.48	1.66

previously, the error generally increases as the factors are varied from their standard conditions. An error distribution was calculated for the linear equation by selecting a set of values centered about the standard conditions for each of the comfort factors except T_a in Table 4 ($T_{mr}-T_a$, RH, V, I_{cl}, N_m). The dry-bulb temperature (T_a) which results in optimum comfort (Dis = 0) was

calculated for each combination of the other five variables using the linear equation. Then the Fanger algorithm was used to calculate the discomfort as a function of each combination of the six comfort factors. These values of discomfort gave the linearization error distribution. Three error distributions were calculated by using three sets of the aforementioned five variables from Table 4. The three sets included values which resulted in incremental changes in discomfort in the ranges of ± 1, ± 2, and ± 3 C inclusive. The error distributions are given in Table 5 for each of these ranges. These distributions show that the errors in predicting optimum comfort with the linear equation increase as the comfort factors deviate from their standard values. Inspection of the data used to develop Table 5 indicates that the largest positive errors occur under conditions of high mean radiant temperature, relative humidity, air velocity, and metabolic rate, and low clothing level relative to the standard values. The largest negative errors occur under the same conditions of high air velocity and low clothing values when combined with conditions of low mean radiant temperature, relative humidity, and metabolic rate.

Equation (12) can be rewritten with negligible loss of accuracy in the following form by assuming that the coefficient, a_1, is unity.

Table 5. Optimum comfort error distributions for the linear discomfort equation for three ranges of comfort factors

Dis Error Range (C)	Percentage of Error Values		
	Allowable Range of Comfort Factors in Terms of Incremental Changes in Dis (C)		
	-1 to +1	-2 to +2	-3 to +3
above +4	0.0	0.0	0.1
+4 to +3	0.0	0.0	0.5
+3 to +2	0.0	0.2	1.8
+2 to +1	0.6	4.3	8.1
+1 to 0	76.5	51.9	39.2
0 to -1	22.8	34.8	29.9
-1 to -2	0.0	6.6	11.4
-2 to -3	0.0	1.7	4.4
-3 to -4	0.0	0.4	2.1
below -4	0.0	0.2	2.5
Total Number of Combinations	162	1125	3528

$$Dis = [T_a + a_2(T_{mr}-T_a) + a_3(RH-50) + a_4(V-0.1)] - [T_s^* - a_5(I_{cl}-0.6) - a_6(N_m-1)] \quad (14)$$

The first bracketed term is solely a function of the environment whereas the second bracketed term is solely a function of the occupant. Thus, by defining these two terms as the "standard environmental temperature" (T_{se}) and the "desired standard temperature" (T_{ds}), respectively, i.e.,

$$T_{se} = T_a + a_2(T_{mr}-T_a) + a_3(RH-50) + a_4(V-0.1) \quad (15)$$

and

$$T_{ds} = T_s^* - a_5(I_{cl}-0.6) - a_6(N_m-1) \tag{16}$$

the equation for Dis can be simplified to

$$Dis = T_{se} - T_{ds} \tag{17}$$

where Dis is now expressed as the difference between a function of the environment (T_{se}) and a function of the occupant (T_{ds}). The decoupling of the occupant and environment in this discomfort index is advantageous since it allows each effect to be considered separately.

Equation (17) is a quantitative index for an occupant's discomfort at a given time under steady-state conditions. This index gives positive values for warm discomfort, negative values for cool discomfort, and zero for optimal comfort. Squaring this index results in three advantages for this study:

1. Warm and cool discomfort will be treated as positive values resulting in an index which is optimized when it reaches its minimum value (zero).

2. Larger deviations from optimal comfort will be more greatly penalized than smaller deviations which seems intuitively desirable.

3. This form of the index simplifies the mathematics of the optimization procedure as shown in later sections.

The comfort index is finally integrated over the desired time period for the optimization to give an index (J_y) of the total discomfort during the optimization period expressed as

$$J_y = \int_{t_i}^{t_f} q(t)[y(t) - z(t)]^2 dt \qquad (18)$$

where

$y(t) = T_{se}$ at time t

$z(t) = T_{ds}$ at time t

$q(t)$ = comfort weighting factor

t_i = initial time of the optimization period

t_f = final time of the optimization period

The "discomfort weighting factor," $q(t)$, gives the relative weighting of discomfort as a function of time. This factor would have a value of zero during unoccupied periods. The units for q and thus J_y and their significance are discussed in later sections. The variables y and z are used in place of T_{se} and T_{ds}, respectively, to conform to the conventional control theory notation as will be shown in later sections. Although the variables in equation (18) are expressed as functions of time, this index is only valid if the time rates of change of T_{se} and T_{ds} are slow enough to assure the

validity of the assumption of steady-state conditions used in the derivation of equation (17).

Equation (18) expresses the discomfort of a single occupant at a single point in the indoor environment. In most cases, there are more than one occupant in a building and these occupants occupy different points in the indoor environment. If the indoor environmental conditions are relatively uniform and the occupant characteristics are similar, equation (18) is valid as a measure of the indoor environmental quality. However, when the conditions in the space are significantly different, relative to the occupants and indoor environment, the discomfort index must be expanded to include these nonuniform effects. This can be accomplished by rewriting equation (18) for each desired location and summing these terms to provide an expression which describes the total discomfort in the space as

$$J_y = \sum_{i=1}^{p} \int_{t_i}^{t_f} q_i(t)[y_i(t) - z_i(t)]^2 dt \qquad (19)$$

which can be written more compactly in matrix notation as

$$J_y = \int_{t_i}^{t_f} [\mathbf{y}(t)-\mathbf{z}(t)]'\mathbf{Q}(t)[\mathbf{y}(t)-\mathbf{z}(t)]dt \qquad (20)$$

where $\mathbf{y}(t)$ and $\mathbf{z}(t)$ are pxl vectors with elements of $y_i(t)$ and $z_i(t)$, respectively, and $\mathbf{Q}(t)$ is a pxp diagonal matrix. The diagonal elements of the $\mathbf{Q}(t)$ matrix, $Q_{ii}(t)$, correspond to the individual discomfort weighting factors ($q_i(t)$) for each of the p locations. The relative values of these weighting factors determine the relative values placed on discomfort at each of the locations.

Other factors

The index developed above only applies to the assessment of thermal sensation in a space. Other indoor environmental factors (mass air quality, acoustics, lighting, etc.) can be treated in a similar manner using the mathematical form of the index as given by equation (19). For these cases, y(t) would be a measure of the environmental factor and z(t) would be the desired level of that factor. Appropriate weighting factors, q(t), would then be applied to these factors.

Energy Consumption

The derivation for the energy consumption component of the performance index is similar to the indoor environmental quality component. When the building occupants pay for their energy consumption directly (e.g., residential homeowners), the proper energy index would be one that quantifies the total energy consumption over the

optimization time period since that is the desired quantity to be minimized. If the energy cost is based on a fixed rate relative to the total amount of energy consumed over a period of time, the energy index (J_u) can be expressed as

$$J_u = \int_{t_i}^{t_f} r(t)u(t)dt \tag{21}$$

where

$u(t)$ = rate of energy consumption at time t

$r(t)$ = energy weighting factor at time t

and t_i and t_f are as defined previously. The units for the energy weighting factor (r) are cost per unit energy consumption (e.g., \$/kWh of electricity) and the units for J_u are total energy consumption cost during the optimization period. The allowance for time dependence on r allows the inclusion of time-of-day utility rate structures.

Other utility rate structures incorporate higher rates during certain periods for higher power demands ("demand charges"). In this case, the energy weighting factor would be a function of the rate of energy consumption at a given time also, i.e., $r = r[u(t),t]$. Although these demand

charges are usually governed by a complex rate schedule, a simple index which penalizes higher energy demand levels is

$$J_u = \int_{t_i}^{t_f} r(t)u(t)^2 dt \tag{22}$$

which is identical to the previous energy index except that the rate of energy consumption is squared. The validity of this index in describing the true cost of energy consumption when demand charges exist depends upon the specific rate structure used.

Many buildings consume more than one type of purchased energy. In these cases, the energy index must include the cost of all consumed energy. The energy index of equation (19) can be extended to more than one energy source in the following form:

$$J_u = \sum_{i=1}^{m} \int_{t_i}^{t_f} r_i(k)u_i(k)dt \tag{23}$$

where

$u_i(t)$ = rate of energy consumption of the i_{th} energy source

$r_i(t)$ = energy weighting factor of the i_{th} energy source

m = number of energy sources

This equation can be expressed more conveniently as

$$J_u = \int_{t_i}^{t_f} \mathbf{r}'(t)\mathbf{u}(t)dt \qquad (24)$$

where $\mathbf{r}(t)$ and $\mathbf{u}(t)$ are mxl vectors whose elements consist of $r_i(t)$ and $u_i(t)$, respectively. If energy cost is to be minimized, the energy weighting factors would be the unit costs of each energy source. If the desire is to minimize total energy consumption, the weighting factors would be the appropriate conversions for expressing each energy source in the same units. Equation (22) can also be extended to include more than one energy source as shown below.

$$J_u = \int_{t_i}^{t_f} \mathbf{u}'(t)\mathbf{R}(t)\mathbf{u}(t)dt \qquad (25)$$

The matrix $\mathbf{R}(t)$ is a mxm diagonal matrix defined analogously to the matrix $\mathbf{Q}(t)$ in equation (20). Linear combinations of equations (24) and (25) could also be used to express the total energy consumption.

Overall Building Performance

The overall building performance can now be expressed as a single index (J) by adding the indoor environmental

quality and energy consumption (assuming no demand charges) indices of equations (20) and (24).

$$J = J_u + J_y$$

$$= \int_{t_i}^{t_f} \{r'(t)u(t) + 1/2[y(t)-z(t)]'Q(t)[y(t)-z(t)]\}dt \qquad (26)$$

The inclusion of the constant of 1/2 in the above equation is for the purpose of simplifying the mathematical derivation of the optimization procedure. The impact of this constant on the performance index can be absorbed by the indoor environmental quality weighting factors (Q).

Throughout the remainder of this study, it is assumed that the objective is to minimize building operating cost, thus J has units of cost. Consequently, the environmental weighting factors must have units of cost per unit of environmental factor. The remainder of this study is also limited to thermal comfort as the only environmental factor of interest. Therefore, the elements of the Q matrix have units of cost per unit discomfort (Dis) squared per unit time (e.g., $\$/C^2 \cdot s$). The actual values assigned to these factors depends on the "cost" of discomfort for a given situation. In some cases, this cost may be realizable such as in the workplace where environmental conditions may

affect worker productivity and the effect is quantitatively known [61]. In other cases there may be no direct cost associated with environmental conditions. Then the selection of values of the comfort weighting factors is rather arbitrary and reflects the relative value placed on comfort conditions in a space.

The performance index expressed by equation (26) was derived for continuous time. The nature of this study requires solutions which are most easily accomplished with a digital computer using finite-difference techniques. Thus the performance index must be converted from continuous to discrete time.

Values for the variables are assigned or calculated at equally spaced time steps (Δt). These time steps can be expressed as t, $t+\Delta t$, $t+2\Delta t$, etc., however, in this study the time variables have been converted to k, $k+1$, $k+2$, etc., as a shorthand notation and to distinguish variables expressed in discrete time from those expressed in continuous time. Assumptions have to be made to determine the values of variables between time steps. Since the energy consumption rates ($u(t)$) are the controlled variables in this study, it is assumed that their assigned value at one time step is maintained constant until the next time step. All other variables are assumed to vary linearly with time between time steps. These assumptions, as shown in

Fig. 5, can be used to transform the integral of equation (26) to the following summation for the performance index.

$$J = \sum_{k=k_i}^{k_f-1} \{r'(k)u(k)+1/2[y(k)-z(k)]'Q(k)[y(k)-z(k)]\}$$

$$+ 1/2[y(k_f)-z(k_f)]'Q(k_f)[y(k_f)-z(k_f)] \qquad (27)$$

This is the performance index describing the overall performance of the building which is used in the remainder of this study. The general objective of minimizing energy consumption while maximizing comfort is fulfilled when this performance index is minimized.

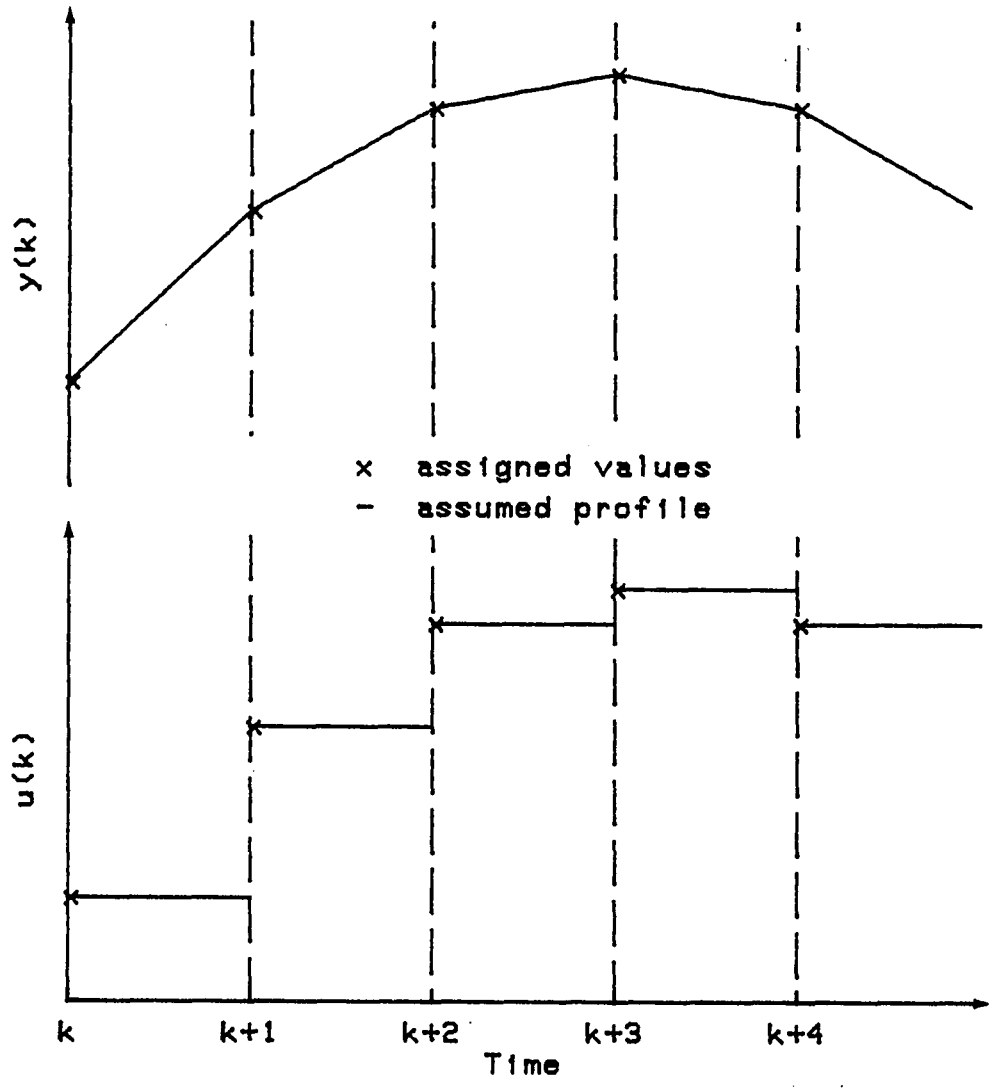

Fig. 5. Assumed profiles for the input variables (u) and output variables (y) between time steps

SYSTEM MODEL

As discussed in the previous section, the specific objective of this study is to optimize the building system performance by minimizing the performance index. To achieve this specific objective, the values of the input (**u**) and output (**y**) of the system, which result in a minimum value of the performance index, must be determined. If **u** and **y** were independent variables, the performance index would have a minimum value of zero when **u** is equal to zero and **y** is equal to **z**. However, these variables are not independent, therefore the relationship between these variables must be determined. The relationship between the input and output of the system is given by the system model.

In this section, a general form for a building system model is introduced and a method for deriving the necessary parameters of this model is developed. The modeling procedure is then validated with data from an actual single-family residence.

General Model Form

The system model must relate the output of the system, **y**, to the controlled input, **u**, and to all uncontrolled inputs or disturbances, **w**, (e.g., ambient weather conditions, internal loads) which significantly affect the performance of the system. The time-dependent nature of the

inputs, coupled with the thermal capacity of the building structure, requires a dynamic system model that can predict these transient effects.

Mathematically, the outputs of a dynamic system at a given time depend on the past outputs as well as the past (controlled and uncontrolled) inputs. For simplicity, it is assumed that the system can be adequately described by a linear, stationary (time-invariant) model and that the system has one output, one controlled input, and q disturbances. With these assumptions, the system can be described in discrete time with an "AutoRegressive Moving Average" (ARMA) model [62] expressed as

$$y(k) = \sum_{i=1}^{n_y} a_i y(k-i) + \sum_{i=1}^{n_u} b_i u(k-i) + \sum_{j=1}^{q} \sum_{i=1}^{n_{wj}} d_{ij} w_j(k-i) \qquad (28)$$

where $w_j(k)$ is the jth disturbance at time k and n_y, n_u, and n_{wj} are the number of time steps backwards in time that are necessary for describing the transient behavior due to y, u, and w_j, respectively. The system parameters, a_i, b_i, and d_{ij} are determined by the characteristics of the system

being modeled. This model can be expanded to include systems with more than one input and output.

The use of equation [28] requires knowledge of the system parameters. These parameters can be estimated by a theoretical analysis of the entire system. However, this method of "system identification" [46] requires separate analyses for different systems, is mathematically tedious and complex, and results in unknown error. A conceivably simpler system identification method would allow calculation of these parameters from output, input, and disturbance data obtained during the actual system operation and would thus eliminate the theoretical analysis. This system identification algorithm would be general in nature to be applicable to a large class of systems (e.g., single-family residences with a single heating source). Finally this algorithm would provide a system model that is only sufficiently complex to provide the necessary accuracy for the optimization.

The modeling procedure used in this study allowed the addition of one independent variable at a time to the model given by equation (28) using a recursive least squares method. A statistical test was used to determine the significance of the contribution of each variable in reducing the model error. If this significance was low, the variable was dropped from the model, otherwise it was

retained. Each possible independent variable was tested in this manner until a final model was obtained. The statistical procedure used is given in Appendix A.

Equation (28) can be transformed into the following simplified matrix form using state-space techniques.

$$\mathbf{x}(k+1) = \mathbf{A}\mathbf{x}(k) + \mathbf{b}u(k) + \mathbf{w}(k) \tag{29}$$

$$y(k) = \mathbf{c}'\mathbf{x}(k) \tag{30}$$

The matrices **A**, b, and c have order nxn, nx1, and nx1, respectively, and contain the system parameters defined by equation (28). The nx1 vector w(k) describes the q uncontrolled inputs to the system (e.g., outdoor temperature, solar radiation, internal loads). The "state" vector **x**(k) is comprised of the necessary information for predicting the output of the system from one time step to the next. In this case, the state of the system is defined by the past inputs and outputs of the system. All other variables are as previously defined. Extensive model analysis [62] and optimization procedures [63] have been developed for system models in this form. The details of the transformation from equation (28) to equations (29) and (30) are shown in a subsequent section for the specific case used in this study.

ERH Experimental Data

The modeling procedures developed in this section were validated with actual system performance data from the Iowa State University Energy Research House (ERH).

Site description

The ERH is a furnished, single-family residence (Fig. 6) located at 2136 Torey Pines Road in Ames, Iowa. This building was designed as an energy-conscious research facility and contains three living levels within a cubical structure. The total floor area is 222 m^2 and includes three bedrooms, living room, family room, kitchen, laundry, mechanical room, and one and a half baths. A three story greenhouse is located along the entire south wall of the ERH. The layout of the ERH is shown in Fig. 7.

The envelope of the ERH consists of insulated wood-frame above-grade walls, double pane windows, insulated concrete below-grade walls, earth-bermed concrete walls, flat insulated roof, and an insulated concrete slab for the lower level floor. Previous research at the ERH has shown that the product of the overall heat transfer coefficient and the total surface area (UA) is 0.23 kW/K [64] and the infiltration rates are in the range of 0.1 to 0.3 air changes per hour depending on wind speed and direction [65]. All of the windows, with the exception of the kitchen, have

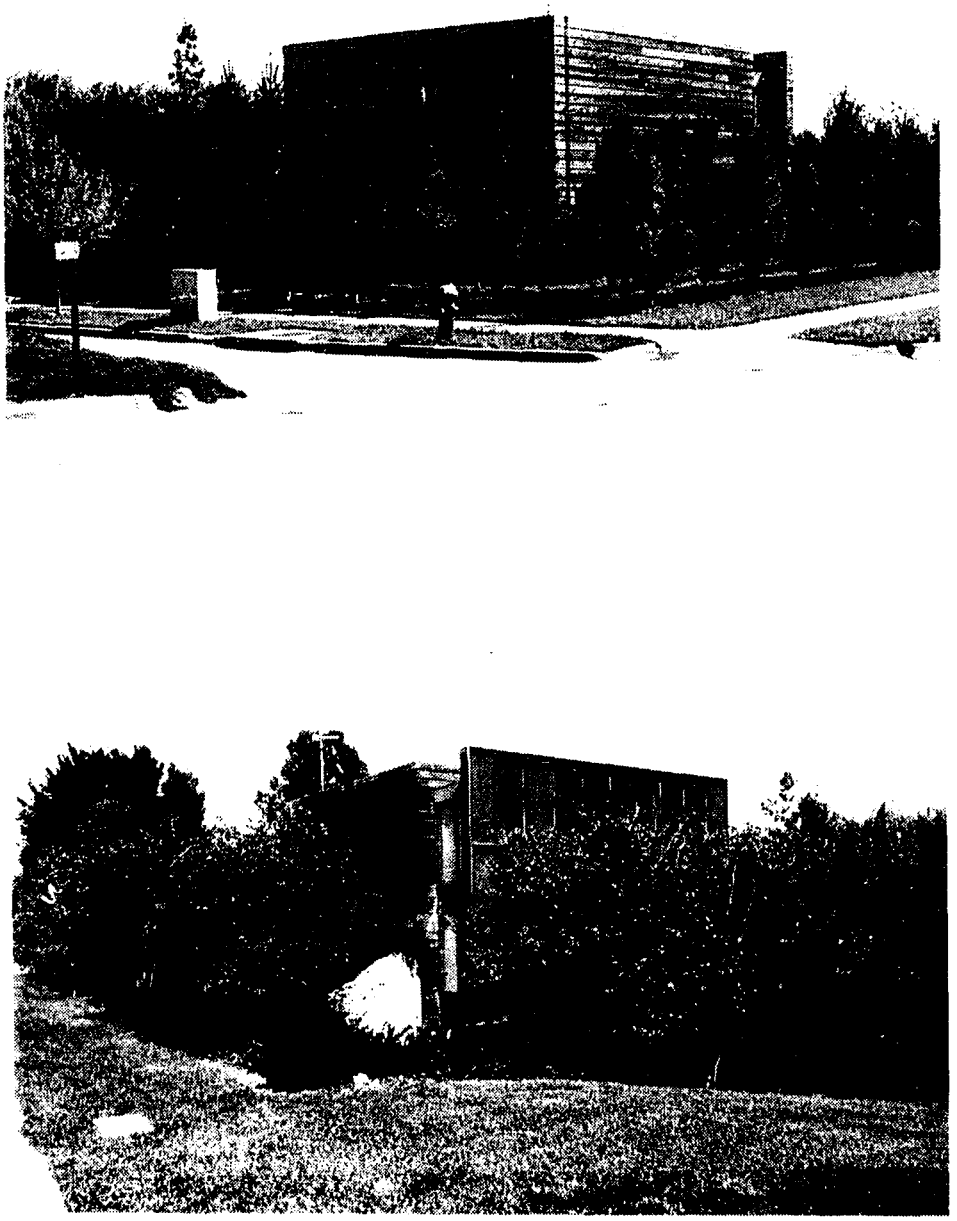

Fig. 6. North (top photo) and south (bottom photo) views of the Energy Research House

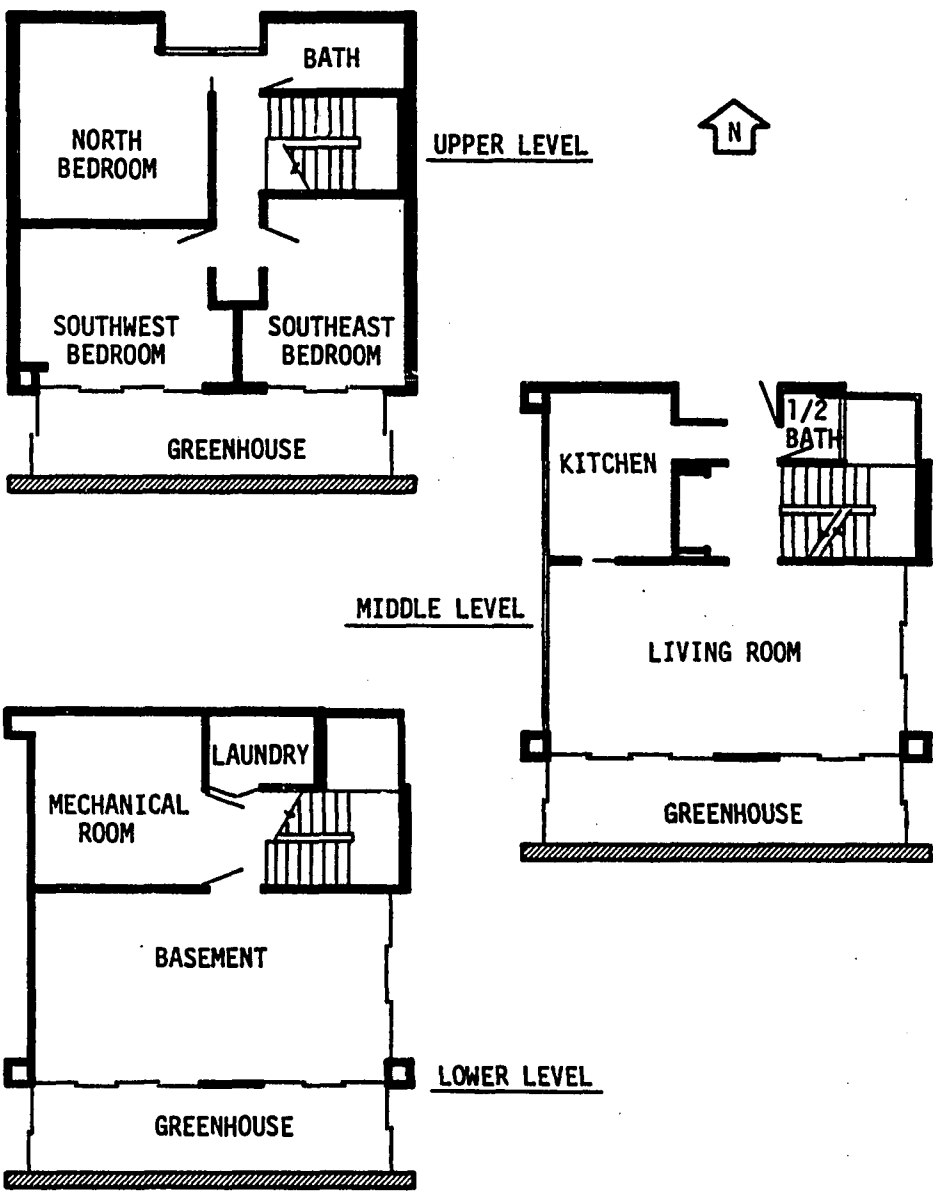

Fig. 7. Floor plan of the Energy Research House

installed window coverings which were in the closed position during the entire study.

The ERH contains various types of mechanical equipment for heating, cooling, and ventilating the indoor environment. This equipment includes a heat pump, electric resistance furnace, active liquid-cooled solar collectors, energy storage tanks, outside air economizer, and separate forced-air and radiant distribution systems. The test period was during winter conditions which required space heating. To simplify system modeling, only the electric resistance furnace (12 kW fixed measured capacity) with the forced-air distribution system was used for heating and infiltration was the only means of ventilation during the test period. The main part of the ERH was heated uniformly by the forced-air system and the greenhouse was not heated by mechanical means. Nobody lived in the ERH during the test period and the only occupancy allowed was for purposes of brief routine equipment maintenance.

Measurements

Three categories of measurements were taken during the experimental study of the ERH: indoor environmental quality, energy consumption, and ambient weather conditions. Indoor environmental quality was limited to thermal conditions at a point near the center of the living room as shown in Fig. 8 and excluded other factors such as lighting,

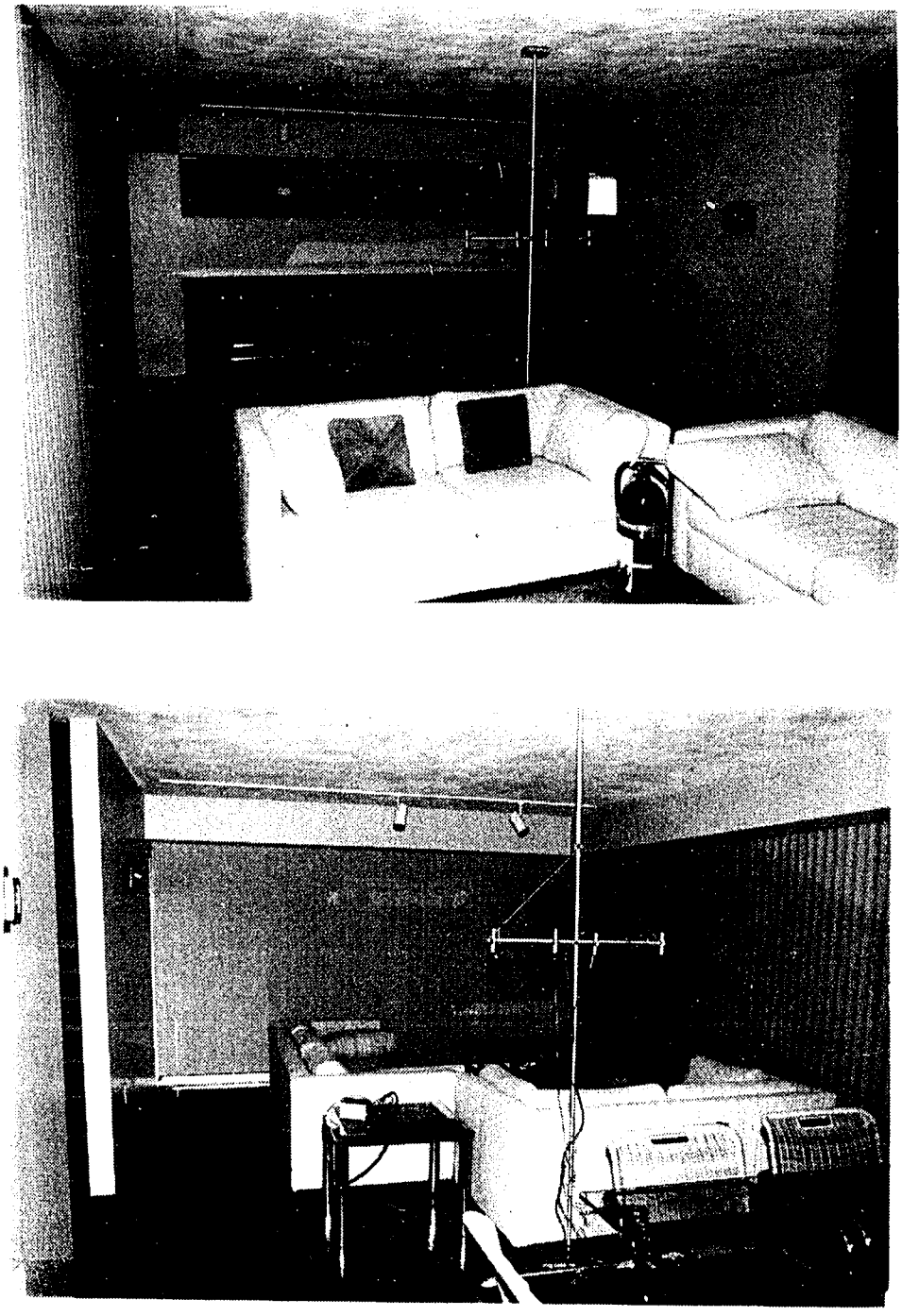

Fig. 8. Interior views of the living room from the east (top photo) and west (bottom photo) sides

acoustics, and mass air quality. Based on previous data taken, it was assumed that the indoor air velocity was negligible (less than 0.2 m/s). During the ERH tests, no energy was expended to control humidity levels in the house and no significant humidity sources existed since the ERH was unoccupied. Therefore, the effect of humidity changes on thermal comfort during the winter conditions tested was assumed negligible and humidity effects were not considered in the modeling procedure. The thermal conditions that were measured were dry-bulb and globe temperature. Yellow Springs Instruments (YSI Model 91) temperature transducers (thermistors) were used for these measurements and are shown in Fig. 9.

The globe temperature sensor used in this study was a 15 cm diameter, hollow, black, copper sphere with an internal temperature sensor. Previous research [6] indicates that the measurement by this sensor approximates the operative temperature of the room. The assumption of negligible humidity and air movement effects results in the globe temperature being approximately equal to the Standard Environmental Temperature (T_e).

The only purchased energy consumption in this study was electricity. Total electrical consumption was monitored as well as the electrical consumption of the electric furnace with Scientific Columbus (Exceltronic XL-A2) watt

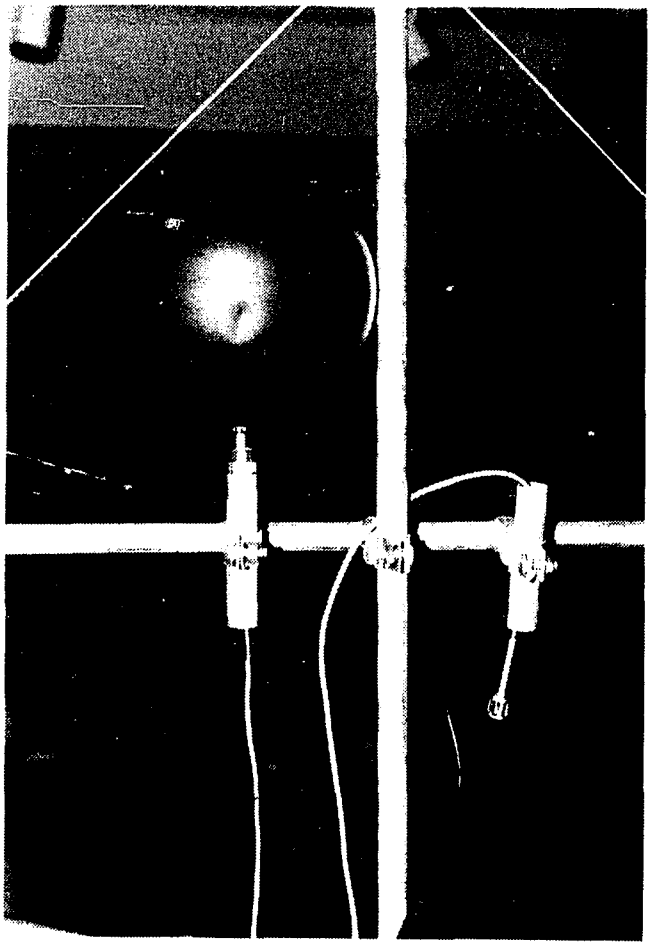

Fig. 9. Globe temperature sensor (left) and dry-bulb temperature sensor (right) used for indoor environmental measurements

transducers. The domestic water heater was disabled during the test period and the active solar system was restricted to charging the energy storage tanks. Since these storage tanks were well insulated and located underground beneath the greenhouse, their effect on the thermal loads were considered negligible. Differences between total electrical consumption and electricity consumed for heating were caused by instrumentation and computers, brief periods of lighting during equipment tests, and electrical valves and pumps used by the solar system. This parasitic consumption resulted in an internal electrical load which was treated as a disturbance to the system.

Weather conditions were measured with a Climatronics modular weather station with sensors located on the roof of the ERH. The conditions monitored were dry-bulb temperature and total horizontal solar radiation. These variables were also considered disturbances to the system.

An Analog Devices (MACSYM II) computerized data acquisition system was used to measure the signals from all of the aforementioned data points. Energy consumption and solar radiation were monitored at six-second intervals. These readings were averaged and recorded at fifteen-minute intervals on a Techtran Datacassette (Model 818). The other measured points were monitored and recorded at fifteen-minute intervals on the same device. Backup readings were

also recorded on paper with a DecWriter (model LA 35) printer. The fifteen-minute data collection interval was selected on the basis of being the shortest time interval that could be feasibly collected and stored with the existing equipment. A summary of the nomenclature used to describe the data collected is given in Table 6.

Data were collected continuously during a thirty-day period from January 20 to February 18, 1983. The dry-bulb temperature sensor used for the thermal comfort measurements was also used as the sensor for the control of the electric furnace through use of the MACSYM II computer. A simple

Table 6. Summary of data collected for the ERH system model

	Measurement	Location	Variable	Units
1.	Indoor Dry-bulb Temperature	Living Room	T_a	C
2.	Indoor Globe Temperature	Living Room	T_g	C
3.	Outdoor Dry-bulb Temperature	Roof	T_o	C
4.	Total Horizontal Solar Radiation	Roof	Q_s	W/m^2
5.	Electric Furnace Consumption	Mechanical Room	Q_h	kW
6.	Internal Load (Electrical)	Mechanical Room	Q_l	kW

on-off control strategy, which maintained the temperature within a predetermined deadband about a setpoint, was used to control the furnace operation. Arbitrary temperature setpoints and deadbands were selected and changed throughout the test period to insure a wide range of dynamic test conditions. The indoor temperature was always maintained between 15 and 20 C.

The on-off control of the furnace, when combined with narrow temperature deadbands, resulted in the furnace cycling at shorter periods than the fifteen-minute data sampling interval. Thus, the integrated energy consumption values during these conditions were between zero and the furnace capacity (12 kW). For this study, it was assumed that the furnace was "modulated" at partial capacity during these periods of short cycling. In the remainder of this study, it was assumed that the furnace operated at partial capacity in the same manner. This assumption is more valid for an electric furnace than for a combustion furnace or heat pump since the inefficiencies associated with the intermittent operation of an electric furnace are usually less than those associated with either of the other two.

Model Results

Although the modeling procedure described in Appendix A can be used to determine the number of parameters that are significant in the system model, it gives no indication of

the amount of data that is necessary to accurately predict these parameters. The ERH data from the entire thirty-day test period were used to determine the significant parameters using the aforementioned procedure. These parameters were then recalculated for shorter time periods than the original thirty-day period to determine the amount of data necessary for producing an accurate system model.

The primary goal of the ERH system model development was to predict the globe temperature as a function of the other monitored variables since this is the variable that predicted thermal comfort in the performance index. However, it was also advantageous to include the indoor dry-bulb temperature as a predicted variable as it provided additional information about the dynamic state of the system.

The ERH system model was developed in two parts. First a model of the form of equation (28) was derived using the procedure of Appendix A for predicting the indoor dry-bulb temperature as a function of the other variables shown in Table 6 with the exception of globe temperature. Then another model was derived to predict the globe temperature as a function of the other variables including dry-bulb temperature. This two-step procedure allowed the model errors associated with the two outputs to be treated independently.

Dry-bulb temperature

The general equation for modeling the dry-bulb temperature of the ERH using the measured variables shown in Table 6 can be rewritten from equation (28) as

$$T_a(k) = \sum_{i=1}^{n_1} a_{1i}T_a(k-i) + \sum_{i=0}^{n_3} a_{3i}T_o(k-i) + \sum_{i=1}^{n_4} a_{4i}T_s(k-i) + \sum_{i=1}^{n_5} a_{5i}Q_h(k-i) + \sum_{i=1}^{n_6} a_{6i}Q_l(k-i) \quad (31)$$

where the a's are the parameters to be determined and the n's are the numbers of significant past time steps for each of the independent variables. The parameter names have been arbitrarily redefined to provide consistency with the variables used for the ERH system model. The solar radiation variable in this equation has been transformed to T_s which is defined as the total horizontal radiation (Q_s) divided by an arbitrary factor of 20 $W/m^2 \cdot C$. Thus, 1 C of solar radiation corresponds to 20 W/m^2 of total horizontal solar radiation. This variable transformation was used to rescale the solar radiation values to the same magnitude as the other variables to reduce computational errors in the

model development. The units for T_s were arbitrarily selected to be in terms of temperature for convenience. This transformation is not the same as the "sol-air" temperature as has been used in other analyses [7].

Equation (31) does not allow the inclusion of the variables T_s, Q_h, or Q_l at the current or future time steps since it is impossible for those values to have an effect on T_a. However, the model does permit the possible inclusion of T_o at the current time step since this temperature may be at least as indicative of the temperature during the past time step as the temperature at the preceding time step.

The aforementioned modeling procedure is entirely empirical and requires no physical insight into the nature of the physical process being modeled. However, knowledge of the physical process can improve the accuracy of the model and should be incorporated whenever possible [46]. For the case of the ERH, it is known that under steady-state conditions with no heating sources ($Q_h = Q_l = T_s = 0$), the indoor dry-bulb temperature should be equal to the outdoor dry-bulb temperature ($T_a = T_o$). Applying these conditions to equation (31) resulted in the following condition for the model parameters:

$$T_a = \sum_{i=1}^{n_1} a_{1i} T_a + \sum_{i=0}^{n_3} a_{3i} T_o$$

or

$$1 = \sum_{i=1}^{n_1} a_{1i} + \sum_{i=0}^{n_3} a_{3i} \qquad (32)$$

Equation (32) imposed a constraint on the model parameters which forced the general model form of equation (31) to provide the proper steady-state performance. To assure that the modeling procedure satisfied this constraint, equation (32) was used to express one of the parameters as a linear combination of the others. This expression was then substituted for one of the parameters in the general equation, thus reducing by one the number of parameters calculated by the modeling procedure in Appendix A.

Although one parameter was eliminated from the general equation, it was still in the model, implicitly, as a combination of the other parameters. The independent variable associated with the "eliminated" parameter explicitly appeared in the model even if it had no significance on the model accuracy. Thus, the parameter selected for elimination from the model had to be one that corresponded to an independent variable that was significant in predicting the model output as this variable could not be eliminated from the model during its development.

Although the indoor dry-bulb temperature was known to be affected by past values of the outdoor dry-bulb

temperature, the actual time step at which this value was most significant was not obvious. However, the indoor dry-bulb temperature at a given time step was highly correlated with its value at the previous time step since the amount by which it could change during one time step was limited due to the finite capacity of the electric furnace and the thermal capacity of the building. Therefore, the parameter corresponding to the first preceding indoor dry-bulb temperature (a_{11}) was selected as the parameter to be eliminated.

The use of equation (32) to eliminate a_{11} from equation (31) resulted in the following model form:

$$\begin{aligned} T_a(k)-T_a(k-1) = & \sum_{i=2}^{n_1} a_{1i}[T_a(k-i)-T_a(k-1)] \\ & + \sum_{i=0}^{n_3} a_{3i}[T_o(k-i)-T_a(k-1)] \\ & + \sum_{i=1}^{n_4} a_{4i}T_s(k-i) + \sum_{i=1}^{n_5} a_{5i}Q_h(k-i) \\ & + \sum_{i=1}^{n_6} a_{6i}Q_l(k-i) \end{aligned} \qquad (33)$$

The elimination of a_{11} resulted in the independent variable $T_a(k-1)$ being subtracted from all of the temperature terms

in the above equation with the exception of T_s. Thus, the dependent variable was transformed to the change in indoor dry-bulb temperature from one time step to the next. Although the dependent and independent variables had been altered in the model above, the modeling procedure in Appendix A was still applicable. The only difference was that the error in predicting the change in indoor dry-bulb temperature rather than the actual dry-bulb temperature was minimized by the procedure. However, the steady-state rationalization used to derive this dynamic model form helped control steady-state error as long as the outdoor dry-bulb temperature was not eliminated during the model development.

All thirty days of data were used to determine the significant parameters in the above model. The actual initial time used was 12:15 a.m. of the second day and the final time was midnight of the thirtieth day. The data for the first day, defined as day 0, were reserved for use as initial values for the independent variables, thus allowing past values to be used in the model for up to 96 previous time steps (24 hours) without changing the initial time for the dependent variables. This resulted in 2784 time steps (29 days) for the model development.

An F-test [66] was used to determine the significance of each added variable in the model development in reducing

the mean squared error of the model (see Appendix A). A relatively high significance level (p) of 0.01 was used for the F-test to reduce the total number of parameters allowed in the model development. The F-test was based on 1, 2784-n-1 degrees of freedom at each stage of the model development with n being the number of parameters in the system model not including the parameter being tested. If the value of n is small relative to 2784, the critical value of F (F_c) is approximately 6.7 [66]. Thus, only parameters which resulted in calculated value of F greater than 6.7 were retained in the model. Tables 7 and 8 show the results of these significance tests on the variables tested in this case. The seven variables listed in Table 7 were the only variables that were found to be significant in the model development. These significant variables were the electrical furnace consumption for the five previous (k-1 through k-5) time steps, the outdoor dry-bulb temperature at the current (k) time step, and the solar radiation during the second (k-2) previous time step.

The standard deviations shown in Table 7 for this model were calculated as the square root of the mean squared error which in turn was calculated as the sum of the squared error between the predicted and actual values of the dependent variable at each time step divided by the degrees of freedom. The number of degrees of freedom (2777) was calculated by

Table 7. Summary of significant variables in the development of the indoor dry-bulb temperature model ($p=0.01$, $F_c=6.7$)

Model Order	Variable	F	Standard Deviation of Model Error (C)
1	$Q_h(k-1)$	---[a]	0.433
2	$Q_h(k-2)$	7872.0	0.221
3	$Q_h(k-3)$	777.0	0.196
4	$Q_h(k-4)$	312.6	0.185
5	$Q_h(k-5)$	81.2	0.183
6	$T_o(k)$	639.9	0.165
7	$T_s(k-2)$	20.7	0.164

[a]An F-test cannot be performed for the first stage of the model development since there is no previous model error for comparison. However, a t-test indicates that this variable is significant (see Table 9 and the accompanying text).

subtracting the number of model parameters (7) from the total number of time steps (2784) used in the model development. Because the dependent variable used in this model was the change in dry-bulb temperature from one time step to the next, the calculated standard deviation was not the model error in predicting the actual value for the indoor dry-bulb temperature.

Table 8 shows some of the variables that tested as insignificant during the model development. These variables

Table 8. Summary of insignificant variables in the development of the indoor dry-bulb temperature model ($p=0.01$, $F_c=6.7$)

Main Variable[a]	F	Main Variable	F
$Q_l(k-1)$	2.8	$T_s(k-4)$	0.3
$T_a(k-2)$	0.3	$T_s(k-8)$	0.4
$Q_h(k-6)$	5.6	$T_s(k-12)$	0.0
$T_o(k-1)$	1.5	$T_s(k-16)$	0.7
$T_o(k-4)$	0.0	$T_s(k-20)$	1.6
$T_o(k-8)$	0.0	$T_s(k-24)$	2.5
$T_o(k-12)$	0.5	$T_s(k-28)$	3.7
$T_o(k-16)$	1.0	$T_s(k-32)$	4.1
$T_o(k-20)$	0.4	$T_s(k-36)$	4.0
$T_o(k-24)$	0.3	$T_s(k-40)$	3.7
$T_o(k-28)$	0.2	$T_s(k-44)$	2.3
$T_o(k-32)$	0.2	$T_s(k-48)$	1.4

[a]The variable $T_a(k-1)$ which was subtracted from the variables, T_a and T_o, in the model is omitted in this table.

were individually tested against the model consisting of the seven variables shown in Table 7. The internal load and indoor dry-bulb temperature were not found to be significant in the model development for any previous time steps.

During the model development, it was observed that the order in which the variables were tested played an important role in determining their significance. As an example, the outdoor dry-bulb temperature at any previous time step during the past several hours was significant in the model development as long as no other outdoor dry-bulb temperature variable was already included in the model. However, when one of these variables was included in the model, all others were determined to be insignificant during the subsequent model development. A similar behavior was exhibited by the solar radiation data. For the outdoor dry-bulb temperature variables it was found that the most recent value of the variables had the highest initial significance when added to the model containing none of these variables at other time steps. Thus, the variable, $T_o(k)$, was added to the model first. For the solar radiation variables, the second previous (k-2) time step was the most significant variable and was added to the model first.

Although no values of outdoor dry-bulb temperature and solar radiation other than those described above were accepted as statistically significant at the p=0.01 level, the calculated F-values for these variables during the past time steps produced an interesting pattern which may have some physical significance as shown in Table 8. Although the significance was highest for each of these variables at

a more recent time step as discussed previously, another peak level of significance occured at a more previous time step. This behavior can be explained by the thermal storage capacity of the building envelope. Thus, the immediate effect of these external loads (outdoor dry-bulb temperature and solar radiation) had the highest significance in the model development, however a lagged effect also appeared to exist. The time lag for the outdoor dry-bulb temperature and solar radiation appeared to be approximately four and eight hours, respectively. However, this lagged effect was not sufficiently significant to be included in the model development.

Table 9 shows the values for the parameters associated with the significant variables shown in Table 7. This table also shows the calculated t-values for these parameters (see Appendix A). The t-test indicated if the associated parameter was significantly different than zero. A significance level (p) of 0.01 was also used for this test and the associated degrees of freedom were essentially infinity resulting in a critical value for t (t_c) of 2.3 [67]. Calculated values of t with magnitudes greater than this critical value indicated that the associated parameter was not zero at the significance level tested. All of the parameters shown in Table 9, including the first parameter,

Table 9. Parameters and t-values for the indoor dry-bulb temperature model (p=0.01, t_c=2.3)

Independent Variable	Parameter Name	Parameter[a] Value	t
$Q_h(k-1)$	b_{11} (a_{51})[b]	0.1870	146.3
$Q_h(k-2)$	b_{12} (a_{52})	-0.1103	-71.8
$Q_h(k-3)$	b_{13} (a_{53})	-0.02083	-13.5
$Q_h(k-4)$	b_{14} (a_{54})	-0.01485	-9.7
$Q_h(k-5)$	b_{15} (a_{55})	-0.006893	-5.4
$T_o(k)-T_a(k-1)$	b_{16} (a_{30})	0.005186	25.5
$T_s(k-2)$	b_{17} (a_{42})	0.002114	4.5

[a]The units for the first five parameters are C/kW and the units for the last two are C/C.

[b]The symbols in parentheses are the parameter names as defined in equation (33). The other symbols are redefinitions which are used in subsequent model formulations.

which could not be tested with an F-test as indicated in Table 7, were significant at the 0.01 level.

The final form of the equation for predicting the indoor dry-bulb temperature as a function of the seven significant variables and parameters is

$$T_a(k)-T_a(k-1) = b_{11}Q_h(k-1) + b_{12}Q_h(k-2) + b_{13}Q_h(k-3) + b_{14}Q_h(k-4) + b_{15}Q_h(k-5) + b_{16}[T_o(k)-T_a(k-1)] + b_{17}T_s(k-2) \quad (34)$$

or equivalently,

$$T_a(k) = (1-b_{16})T_a(k-1) + b_{11}Q_h(k-1) + b_{12}Q_h(k-2) + b_{13}Q_h(k-3) + b_{14}Q_h(k-4) + b_{15}Q_h(k-5) + b_{16}T_o(k) + b_{17}T_s(k-2) \quad (35)$$

The correspondence between the parameter definitions in this equation with the parameters in equation (33) is given in Table 9.

Globe temperature

The procedure used to develop the indoor dry-bulb temperature model was applied in an almost identical manner to develop a model for predicting the globe temperature. A rationalization was also used in this model to force the indoor and outdoor dry-bulb temperatures and the globe temperature to be equal under steady-state conditions with no heating sources. The dependent variable used was the difference between the globe and indoor dry-bulb temperatures as this quantity reflected the radiant

temperature effect on thermal comfort. The general form of the model equation is shown below.

$$
\begin{aligned}
T_g(k)-T_a(k) = & \sum_{i=1}^{n_1} a_{1i}[T_a(k-i)-T_a(k)] \\
& + \sum_{i=1}^{n_2} a_{2i}[T_g(k-i)-T_a(k)] \\
& + \sum_{i=0}^{n_3} a_{3i}[T_o(k-i)-T_a(k)] \\
& + \sum_{i=1}^{n_4} a_{4i}T_s(k-i) + \sum_{i=1}^{n_5} a_{5i}Q_h(k-i) \\
& + \sum_{i=1}^{n_6} a_{6i}Q_l(k-i) \qquad (36)
\end{aligned}
$$

The significant variables as determined from the modeling procedure are shown in Table 10. Actual indoor dry-bulb temperature data were used in the model development rather than predicted values from the indoor dry-bulb temperature model. The standard deviations shown in this table are for the prediction of the difference between the globe and indoor dry-bulb temperatures. Thus, the error in predicting the actual globe temperature is a combination of the errors from the indoor dry-bulb temperature and globe temperature models. One of the significant variables shown in Table 10

Table 10. Summary of significant variables in the development of the globe temperature model ($p=0.01$, $F_c=6.7$)

Model Order	Variable	F	Standard Deviation of Model Error (C)
1	$Q_h(k-1)$	---[a]	0.330
2	$Q_h(k-2)$	114.5	0.324
3	$T_g(k-1)-T_a(k)$	4111.7	0.206
4	$T_o(k)-T_a(k)$	71.4	0.203
5	$T_a(k-1)-T_a(k)$	167.7	0.197

[a]An F-test cannot be performed for the first stage of the model development since there is no previous model error for comparison. However, a t-test indicates that this variable is significant (see Table 12).

for the globe temperature model development is the indoor dry-bulb temperature at the previous time step. This term may not significantly improve the model accuracy since it will propagate any errors resulting from the indoor dry-bulb temperature model. The effect of this term on the overall accuracy of predicting the globe temperature was not significant as shown in a subsequent section.

A summary of some of the insignificant variables tested is shown in Table 11. These tests were based on the fourth-order globe temperature model which contained the first four significant variables shown in Table 10 and excluded the indoor dry-bulb temperature at the previous time step. In

Table 11. Summary of insignificant variables in the development of the globe temperature model ($p=0.01$, $F_c=6.7$) based on the fourth-order model

Main Variable[a]	F	Main Variable	F
$T_g(k-2)$	0.9	$T_o(k-4)$	2.0
$T_s(k-1)$	0.2	$T_o(k-8)$	0.9
$T_o(k-1)$	1.1	$T_o(k-12)$	0.4
$Q_h(k-3)$	5.4	$T_o(k-16)$	1.3
$Q_l(k-1)$	0.5	$T_o(k-20)$	0.5
		$T_o(k-24)$	0.2

[a]The variable $T_a(k)$ which was subtracted from the variables T_g, T_a, and T_o in the model is omitted in this table.

this model, the internal load and solar radiation terms were not significant at any previous time step tested. The outdoor dry-bulb temperature showed a secondary peak significance at a four hour previous time step in a similar manner as shown by the indoor dry-bulb temperature model. However this effect was also insignificant at the level used in the model development.

The values of the model parameters and associated t values for the fourth-order and fifth-order globe temperature models are shown in Table 12. The effect of the inclusion of the fifth variable, $T_a(k-1)$, on the values of the model

Table 12. Parameters and t-values for the indoor globe temperature model (p=0.01, t_c=2.3)

Independent Variable	Parameter Name	Model Order=4		Model Order=5	
		Parameter Value	t	Parameter Value	t
$Q_h(k-1)$	b_{21} $(a_{51})^a$	-0.0818	-52	-0.0808	-53
$Q_h(k-2)$	b_{22} (a_{52})	-0.00484	-3	0.0143	7
$T_g(k-1)-T_a(k)$	b_{23} (a_{21})	-0.0256	-31	0.217	12
$T_o(k)-T_a(k)$	b_{24} (a_{30})	-0.00548	-9	-0.00422	-7
$T_a(k-1)-T_a(k)$	b_{25} (a_{11})	---	---	-0.0236	-13

[a]The symbols in parentheses are the names used for the parameters in equation (36). The other symbols are the redefinitions for the parameters which are used in subsequent model formulations.

parameters is shown in this table. The form of the globe temperature equation can be written for the fifth-order case as

$$\begin{aligned} T_g(k)-T_a(k) = {} & b_{21}Q_h(k-1) + b_{22}Q_h(k-2) \\ & + b_{23}[T_g(k-1)-T_a(k)] \\ & + b_{24}[T_o(k)-T_a(k)] \\ & + b_{25}[T_a(k-1)-T_a(k)] \end{aligned} \tag{37}$$

or equivalently as

$$T_g(k) = (1-b_{23}-b_{24}-b_{25})T_a(k) + b_{21}Q_h(k-1) + b_{22}Q_h(k-2) + b_{23}T_g(k-1) + b_{24}T_o(k) + b_{25}T_a(k-1) \quad (38)$$

where the values for the parameters are given in the appropriate column of Table 12. The fourth-order model can be expressed with the same equation by setting b_{25} to zero and changing the remaining parameters to the appropriate values given in Table 12.

Combined model

As discussed previously, the standard deviations for the model development do not give a true indication of the model accuracy in simultaneously predicting indoor dry-bulb and globe temperatures. Furthermore, the errors that are shown for the development are based on model comparisons with the actual data that were used to derive the model. Therefore, the previous analysis indicated the accuracy of the model in "fitting" the actual building performance data, but did not indicate the accuracy of the model in "predicting" the future performance of the building.

The analysis for determining the model variables required for adequate prediction of the transient system behavior indicated that only relatively short-term transient effects (approximately one hour or less) were significant.

Although the variables considered in this study were tested for significance in the model for up to twenty-four preceding hours, no other significant effects were found. However, transient effects with longer "time constants" do exist in actual buildings (e.g., below-grade heat transfer) which are not accounted for in the above model and result in model error. Furthermore, some system characteristics that may vary with time (e.g., thermal properties of the structure, infiltration rate), can cause errors due to the time-invariant assumption used in the model development. A third source of error may be the linear model assumption, as in the selection of total horizontal solar radiation as a disturbance variable. The physical arrangement of the ERH may result in solar radiation having a different effect at different times of day due to the window and wall orientation and at different times of the year due to changes in the position of the sun in the sky. Finally, errors may exist in the model predictions due to errors in predicting the future values of the disturbance variables, especially weather.

The reduction of the model errors that occur on a short-term time basis (less than one day) would probably require additional measurements (e.g., individual wall temperatures, wind speed and direction) and more sophisticated models containing more variables. However,

this additional complexity may be impractical to implement and unnecessary in terms of required accuracy for an actual optimal control strategy.

The long-term model errors that gradually occur over time periods greater than a day could possibly be reduced by incorporating an adaptive model in the control strategy. A simple means of providing an adaptive model could be obtained by periodically recalculating the model parameters with the above procedure using the most currently available data. The required accuracy of this adaptive model depends partly on the amount of time into the future that is required of the model predictions by the optimal control strategy. The relatively fast dynamic response of the building being modeled would probably require no more than one day of prediction in the control strategy. Therefore, it is necessary to determine how many previous periods of data are required for the system model development to insure accurate prediction of the system performance for one day into the future.

The indoor dry-bulb and globe temperature models were compared to the actual data using the parameter values derived from the full 29 days of data. This comparison was made by initializing the model at the beginning of the first day of the 29-day period with actual data from the previous day. Actual disturbance and heat input data were used as

inputs to the model and the dry-bulb and globe temperatures were calculated during the one-day period and compared to the actual data. The errors between the predicted and actual dry-bulb temperature were summarized by calculating the "root mean squared" (RMS) error which is the square root of the arithmetic mean over a one-day period (96 time steps) of the squared error at each time step. The errors between the predicted and actual values of the difference between the globe and dry-bulb temperature at each time step were also summarized using the RMS error for the fourth-order and fifth-order models. These error calculations were repeated for each day during the 29-day period and are summarized in Table 13.

Although the fourth-order and fifth-order globe temperature models have considerably different values for the parameters as shown in Table 12, the RMS errors for these models are nearly identical as shown in Table 13. Thus, to reduce model complexity without significantly sacrificing accuracy, the fourth-order globe temperature was used throughout the remainder of this study.

Graphical comparisons of the indoor dry-bulb temperature model and the fourth-order globe temperature model using the 29-day model parameters are shown in Appendix B for each of the 29 days shown in Table 13.

Table 13. Summary of daily RMS model errors using the 29 day model development

Day	RMS Error (C) for $T_a(k)$	RMS Error (C) for $T_g(k)-T_a(k)$	
		Fourth-Order	Fifth-Order
1	0.562	0.499	0.498
2	0.635	0.457	0.455
3	0.587	0.423	0.422
4	0.160	0.392	0.391
5	0.850	0.542	0.540
6	0.401	0.498	0.497
7	0.543	0.348	0.346
8	0.503	0.323	0.322
9	0.157	0.404	0.403
10	0.667	0.375	0.373
11	0.477	0.455	0.454
12	0.841	0.476	0.475
13	0.742	0.523	0.522
14	1.413	0.464	0.463
15	0.441	0.532	0.531
16	0.932	0.497	0.491
17	1.320	0.498	0.496
18	0.598	0.502	0.500
19	0.699	0.523	0.521
20	0.501	0.533	0.531
21	0.499	0.574	0.572
22	0.460	0.529	0.527
23	0.515	0.494	0.493
24	0.320	0.545	0.544
25	1.105	0.357	0.356
26	1.135	0.433	0.433
27	0.756	0.479	0.477
28	0.982	0.457	0.457
29	0.470	0.365	0.364
Ave.[a]	0.743	0.478	0.477

[a]These "averages" are the root mean squared averages of the daily RMS errors in each column.

Table 13 shows that the accuracy of the 29-day model was better for some days than others. The figures in Appendix B indicate that part of the error was due to consistently high or low predictions during some of the days. These "steady-state" errors indicate that some long-term effects may have existed, and thus affected the long-term accuracy of the model.

To determine the amount of data required for the model development, the accuracies of models using different amounts of data for their development were compared. The model parameters were calculated using a specified number (n) of consecutive days of data from day i-n to day i-1. Then the predictions of the resulting model were compared to the actual data for the ith day. The RMS model errors were calculated for days n+1 through 29 using this procedure with the model development always being based upon the n days previous to the day being tested. As the number of days used in the model development (n) increased, the number of days available to test the model (29-n) decreased. These results, as shown in Table 14, indicate that the model was improved considerably when using two days for its development as compared to one day. Additional days in the model development resulted in smaller improvements until minimum RMS errors for dry-bulb and globe temperatures were obtained for the five-day model development. The inclusion

Table 14. Summary of the effect of the number of previous days used for the model development on the accuracy of the model in predicting the performance of the following day

Number of Days for Model Development	Number of Days for Model Predictions	RMS Errors (C)	
		$T_a(k)$	$T_g(k)-T_a(k)$
1	28	0.934	0.856
2	27	0.788	0.532
3	26	0.816	0.481
4	25	0.786	0.449
5	24	0.763	0.434
6	23	0.792	0.434
7	22	0.789	0.440
8	21	0.792	0.449
9	20	0.797	0.457
10	19	0.821	0.468
11	18	0.820	0.474
12	17	0.833	0.475
13	16	0.850	0.473
14	15	0.834	0.475
15	14	0.842	0.472
16	13	0.831	0.473
17	12	0.742	0.474
18	11	0.760	0.476
19	10	0.781	0.473
20	9	0.802	0.469
21	8	0.845	0.458
22	7	0.879	0.449
23	6	0.926	0.442
24	5	0.987	0.419
25	4	0.913	0.434
26	3	0.794	0.436
27	2	0.792	0.416
28	1	0.480	0.368

of additional days in the model development past this minimum point degraded the model accuracy. This trend indicated that the model was adapting to long-term changes

in the system characteristics. The actual minimum values for the model errors occurred when the maximum number of days (28) was used for the model development. However, this case only allowed for one day of prediction in the calculation of the RMS errors. Therefore, the information towards the bottom of Table 14 is not as reliable since it is based on less prediction data and must be interpreted with caution.

As indicated previously, the greatest model improvement occurred when two days were used in the model development instead of one. Further improvements were obtained by using up to five days in the model development, however the additional storage and computational effort in an actual control strategy implementation may not be justified by the slight improvement in model accuracy. Therefore, it was assumed that two days of data in the model development provided sufficient accuracy for this study.

Tables 15 and 16 show the calculated parameter values for the indoor dry-bulb temperature and globe temperature models, respectively, for each day during the 29-day period when two days were used in the model development. The indoor dry-bulb temperature model parameters which correspond to the more recent heat inputs (b_{11}, b_{12}) and the outdoor dry-bulb temperature (b_{16}) had less variability with respect to the particular days for which they were

Table 15. Parameter values for the indoor dry-bulb temperature model using two days for the model development

Day[a]	Parameters						
	b_{11} (C/kW)	b_{12} (C/kW)	b_{13} (C/kW)	b_{14} (C/kW)	b_{15} (C/kW)	b_{16} (C/C)	b_{17} (C/C)
1	0.19	-0.13	-0.001	-0.013	-0.0137	0.0044	0.0009
2	0.19	-0.13	-0.012	-0.007	-0.0100	0.0050	0.0037
3	0.19	-0.13	-0.002	-0.008	-0.0117	0.0052	0.0039
4	0.19	-0.12	-0.010	-0.014	-0.0102	0.0055	0.0000
5	0.21	-0.10	-0.036	-0.022	0.0141	0.0050	0.0019
6	0.18	-0.11	-0.024	0.006	-0.0203	0.0047	0.0007
7	0.18	-0.12	-0.008	-0.007	-0.0132	0.0056	0.0014
8	0.18	-0.11	-0.019	-0.004	-0.0124	0.0058	0.0023
9	0.18	-0.12	-0.009	-0.011	-0.0088	0.0058	0.0022
10	0.18	-0.12	-0.014	-0.003	-0.0133	0.0056	0.0032
11	0.18	-0.10	-0.048	0.019	-0.0225	0.0052	0.0032
12	0.21	-0.10	-0.056	-0.010	-0.0108	0.0060	0.0007
13	0.20	-0.09	-0.053	-0.029	0.0096	0.0059	-0.0014
14	0.20	-0.08	-0.061	-0.025	0.0076	0.0055	0.0006
15	0.19	-0.09	-0.046	-0.023	-0.0017	0.0055	0.0029
16	0.19	-0.11	-0.005	-0.043	-0.0009	0.0050	0.0045
17	0.19	-0.11	-0.024	-0.018	-0.0132	0.0046	0.0037
18	0.21	-0.09	-0.056	-0.023	-0.0004	0.0054	0.0030
19	0.21	-0.09	-0.050	-0.050	0.0198	0.0058	0.0007
20	0.20	-0.09	-0.039	-0.027	-0.0030	0.0055	0.0017
21	0.20	-0.11	-0.028	-0.026	-0.0105	0.0053	0.0033
22	0.20	-0.10	-0.035	-0.031	-0.0020	0.0053	0.0026
23	0.20	-0.09	-0.050	-0.017	-0.0023	0.0054	0.0000
24	0.17	-0.09	-0.034	0.004	-0.0195	0.0039	0.0007
25	0.18	-0.11	-0.013	-0.023	0.0032	0.0038	0.0024
26	0.18	-0.11	-0.012	-0.025	0.0030	0.0044	0.0031
27	0.19	-0.11	-0.013	-0.027	0.0057	0.0056	0.0045
28	0.19	-0.11	-0.017	-0.029	0.0097	0.0054	0.0032
29[b]	0.19	-0.11	-0.021	-0.015	-0.0069	0.0052	0.0021

[a]Number corresponds to the first day of the two-day data period used for the model development.

[b]This row contains the parameters from the 29-day model development.

Table 16. Parameter values for the globe temperature model using two days for the model development

Day[a]	Parameters			
	b_{21} (C/kW)	b_{22} (C/kW)	b_{23} (C/C)	b_{24} (C/C)
1	-0.093	0.0154	-0.031	-0.0094
2	-0.093	0.0069	-0.023	-0.0023
3	-0.098	0.0126	-0.037	-0.0166
4	-0.084	-0.0053	-0.011	0.0047
5	-0.075	-0.0196	-0.024	-0.0060
6	-0.087	-0.0017	-0.014	-0.0012
7	-0.092	0.0082	-0.017	-0.0037
8	-0.084	0.0046	-0.008	0.0097
9	-0.087	0.0047	-0.027	-0.0085
10	-0.088	0.0049	-0.032	-0.0104
11	-0.077	-0.0130	-0.026	-0.0062
12	-0.074	-0.0231	-0.014	0.0012
13	-0.075	-0.0210	-0.035	-0.0130
14	-0.057	-0.0341	-0.023	-0.0049
15	-0.064	-0.0249	-0.027	-0.0061
16	-0.087	0.0049	-0.029	-0.0062
17	-0.075	-0.0076	-0.047	-0.0153
18	-0.064	-0.0277	-0.025	-0.0053
19	-0.052	-0.0352	-0.013	0.0068
20	-0.070	-0.0154	0.008	0.0293
21	-0.069	-0.0156	0.043	0.0625
22	-0.059	-0.0226	0.033	0.0521
23	-0.071	-0.0163	0.000	0.0231
24	-0.082	-0.0133	-0.004	0.0183
25	-0.074	-0.0089	-0.007	0.0146
26	-0.087	-0.0043	-0.074	-0.0518
27	-0.091	-0.0001	-0.080	-0.0571
28	-0.080	0.0016	-0.017	0.0056
29[b]	-0.082	-0.0048	-0.026	-0.0055

[a]Number corresponds to the first day of the two-day data period used for the model development.

[b]This row contains the parameters from the 29-day model development.

calculated than the other parameters. In general, the parameters that were the most significant in the 29-day model development had the lowest variability during the two-day model development for both the indoor dry-bulb temperature and globe temperature models.

ERH Model Interpretation

The values of the parameters that were determined during the model development indicate the dynamic and steady-state characteristics of the system. For the purposes of this discussion, parameter values from the 29-day model development as shown in Tables 9 and 12 are used.

Dry-bulb temperature

To demonstrate the meaning of the various dynamic model parameters, the indoor dry-bulb temperature model given by equation (34) with the parameter values from the 29-day model development is shown below.

$$\begin{aligned} T_a(k) - T_a(k-1) = {} & (0.1870C/kW)Q_h(k-1) \\ & - (0.1103C/kW)Q_h(k-2) \\ & - (0.02083C/kW)Q_h(k-3) \\ & - (0.01485C/kW)Q_h(k-4) \\ & - (0.006893C/kW)Q_h(k-5) \\ & + (0.005186C/C)[T_o(k)-T_a(k-1)] \\ & + (0.002114C/C)T_s(k-2) \end{aligned} \qquad (39)$$

This equation relates the change in indoor dry-bulb temperature over a fifteen-minute period to the electrical heat input and the outdoor weather conditions. The maximum total horizontal solar radiation that was available during the test period was about 600 W/m^2 which is equivalent to a value of T_s of 30 C. Equation (39) indicates that this maximum level of radiation results in only a 0.06 C change in the indoor dry-bulb temperature. The minimum outdoor dry-bulb temperature during the test period was about -20 C. This outdoor temperature, combined with an indoor dry-bulb temperature of 20 C results in a predicted change of only -0.2 C in the indoor dry-bulb temperature. However, the electric furnace used during these tests has a capacity of 12 kW which results in a predicted change of 2.2 C in the indoor dry-bulb temperature during the first time period that the furnace is operated after a 1.25 hour off period. Equation (39) predicts that if the furnace is further maintained at full capacity and the effect of the outdoor dry-bulb temperature and solar radiation is neglected, the resulting indoor dry-bulb temperature increases will be 0.9, 0.7, 0.5, and 0.4 C during the next four fifteen-minute time intervals, respectively. This apparent reduction in the heating effect of the furnace on the indoor air can be explained by heat transfer to the adjacent surfaces within the space (e.g., walls, furniture) as the air temperature

rises higher than the temperature of these surfaces. When the furnace is switched off, the same effect occurs in a reverse manner. Thus, the five electric furnace parameters actually reflect the thermal capacity of the ERH interior.

The indoor dry-bulb temperature model as expressed by equation (39) can be simplified to the following form under steady-state conditions.

$$Q_h = (0.15kW/C)(T_a-T_o) - (0.062kW/C)T_s \quad (40)$$

This equation indicates a UA value of 0.15 kW/K for the ERH which is considerably lower than the value of 0.23 kW/K that was indicated by previous testing under steady-state conditions [64]. This difference indicates the error associated with the dynamic model in predicting steady-state results.

The maximum possible solar radiation during the test period (T_s = 30 C) can supplement the electrical heating by about 1.9 kW under steady-state conditions as indicated by equation (40).

Under conditions of no electrical heating during the past 1.25 hours and no solar radiation during the past 0.5 hours, equation (39) for the indoor dry-bulb temperature reduces to the following form.

$$T_a(k) = 0.9948T_a(k-1) + 0.0052T_o(k) \quad (41)$$

The coefficient of the indoor dry-bulb temperature variable at the previous time step (0.9948) indicates the characteristics of the dynamic response of the model. This coefficient is related to the "time constant" (t_c) of a first-order system in continuous time by the expression [62],

$$\exp(-\Delta t/t_c) = 0.9948 \qquad (42)$$

where Δt is the time step (15 minutes) used in the model equation. Equation (42) can be solved for t_c to give a time constant of 48 hours for the first-order response of the indoor dry-bulb temperature to changes in the outdoor dry-bulb temperature. This seemingly high time constant is indicative of the relatively high insulating value of the ERH structure.

Globe temperature

The characteristics of the globe temperature model are indicated by equation (37) with the parameters from the 29-model development as shown below.

$$\begin{aligned} T_g(k) - T_a(k) = &- (0.08177C/kW)Q_h(k-1) \\ &- (0.004841C/kW)Q_h(k-2) \\ &- (0.02564C/C)[T_g(k-1)-T_a(k)] \\ &- (0.005480C/C)[T_o(k)-T_a(k)] \end{aligned} \qquad (43)$$

The negative parameters indicate that the globe temperature will generally be less than the indoor dry-bulb temperature when the outdoor dry-bulb temperature is less than the indoor dry-bulb temperature. This effect is indicative of the interior surfaces of the exterior walls being slightly cooler than the indoor dry-bulb temperature which causes a cooling effect on the globe sensor due to radiant heat exchange.

The coefficient for the globe temperature at the previous time step (-0.02564) results in damped oscillations for the globe temperature response. These oscillations have a period of two time steps (30 minutes) and are damped exponentially with a four-minute time constant. The oscillating behavior of the model can be explained by modeling errors due to the selected sampling rate which is long relative to the cycling of the furnace and has no physical significance to the actual system behavior. However, these oscillations are not noticeable in the model predictions because of the relatively high rate at which they are damped. The four-minute time constant coincides with the time constant of the globe temperature sensor.

The negative coefficients for the heat input terms of equation (43) indicate that the difference between the indoor globe and dry-bulb temperatures becomes more negative when the heat is turned on. This effect can be explained by

the interior surface temperatures and the resulting mean radiant temperature rising at a slower rate than the indoor dry-bulb temperature as was also indicated by the indoor dry-bulb temperature model.

The globe temperature model as given by equation (43) can be expressed under steady-state conditions as shown below.

$$T_g = (1.0055C/C)T_a - (0.0130C/C)T_o - (0.0866)Q_h \qquad (44)$$

Equation (40) can be used to eliminate Q_h from equation (44) to give the following equation which relates the globe temperature to the indoor and outdoor dry-bulb temperatures during steady-state heating conditions with no solar radiation.

$$T_g = 0.9925T_a + 0.0075T_o \qquad (45)$$

This expression indicates that the outdoor dry-bulb temperature has very little effect on the steady-state globe temperature. This effect is indicative of the high insulating value of the outside walls which results in the inside surface temperatures being very near the indoor dry-bulb temperature under steady-state conditions.

State-Space Representation

The final step in the model development is the transformation of the indoor dry-bulb and globe temperature

equations to the state-space formulation given by equations (29) and (30) for use in the system optimization procedure. The expressions for predicting the indoor dry-bulb and globe temperatures as given by equations (35) and (38), respectively, are rewritten below for convenience.

$$T_a(k) = (1-b_{16})T_a(k-1) + b_{11}Q_h(k-1) + b_{12}Q_h(k-2) + b_{13}Q_h(k-3) + b_{14}Q_h(k-4) + b_{15}Q_h(k-5) + b_{16}T_o(k) + b_{17}T_s(k-2) \quad (46)$$

$$T_g(k) = (1-b_{23}-b_{24})T_a(k) + b_{21}Q_h(k-1) + b_{22}Q_h(k-2) + b_{23}T_g(k-1) + b_{24}T_o(k) \quad (47)$$

The desired state-space form for the model as given by equations (29) and (30) are also rewritten below.

$$\mathbf{x}(k+1) = \mathbf{A}\mathbf{x}(k) + \mathbf{b}u(k) + \mathbf{w}(k) \quad (48)$$

$$y(k) = \mathbf{c}'\mathbf{x}(k) \quad (49)$$

The output of the model, y(k), is defined as the globe temperature, $T_g(k)$, since this is the variable that was assumed to be indicative of the effect of the indoor environment on thermal sensation. The controlled input, u(k), is defined to be the electrical consumption of the electric furnace, $Q_h(k)$.

Equation (18) relates the state of the system at one time step to the state, controlled input, and disturbances at the previous time step. The output of the system is a

linear combination of the state. Although the indoor dry-bulb temperature model given by equation (46) includes the outdoor dry-bulb temperature at the first previous time step and the solar radiation at the second previous time step, both of these variables can be incorporated in the disturbance vector at a single time step as their values are independent of the dynamics of the system or the manner in which it is controlled. The variables in equations (46) and (47) other than the disturbances or the controlled input must be incorporated in the state vector, $\mathbf{x}(k)$, for the output equation (49) to be valid as an expression for calculating the output of the system. Thus, the state of the system must include the variables, $T_a(k)$, $T_g(k)$, $Q_h(k-1)$, $Q_h(k-2)$, $Q_h(k-3)$, and $Q_h(k-4)$, which results in a sixth-order system for the state-space representation. Although it is valid to use each of these six variables separately as a state variable, the following state representation is equally as valid and is used in this study to reduce the mathematical complexity of the system matrices.

$$\mathbf{x}(k) = \begin{bmatrix} T_a(k) \\ T_g(k)-(1-b_{23}-b_{24})T_a(k) \\ Q_h(k-1) \\ Q_h(k-2) \\ Q_h(k-3) \\ Q_h(k-4) \end{bmatrix} \tag{50}$$

This state representation results in the following expressions for the system matrices, **A**, **b**, and **c**, and the disturbance vector, **w**(k).

$$\mathbf{A} = \begin{bmatrix} 1-b_{16} & 0 & b_{12} & b_{13} & b_{14} & b_{15} \\ 1-b_{23}-b_{24} & b_{23} & b_{22} & 0 & 0 & 0 \\ 0 & 0 & 0 & 0 & 0 & 0 \\ 0 & 0 & 1 & 0 & 0 & 0 \\ 0 & 0 & 0 & 1 & 0 & 0 \\ 0 & 0 & 0 & 0 & 1 & 0 \end{bmatrix} \tag{51}$$

$$\mathbf{b} = \begin{bmatrix} b_{11} \\ b_{21} \\ 1 \\ 0 \\ 0 \\ 0 \end{bmatrix} \qquad \mathbf{c} = \begin{bmatrix} 1-b_{23}-b_{24} \\ 1 \\ 0 \\ 0 \\ 0 \\ 0 \end{bmatrix} \tag{52, 53}$$

$$w(k) = \begin{bmatrix} b_{16}T_o(k) + b_{17}T_s(k-2) \\ b_{24}T_o(k) \\ 0 \\ 0 \\ 0 \\ 0 \end{bmatrix} \tag{54}$$

This state-space representation is used as the form for the system model in the optimization procedure developed in the next section.

OPTIMIZATION

The objective of the system optimization is to determine the control history, u(k), for $k = k_i, k_i+1, \ldots k_f-1$, that minimizes the performance index given by

$$J = \sum_{k=k_i}^{k_f} \{r(k)u(k)+1/2q(k)[y(k)-z(k)]^2\} + 1/2q(k_f)[y(k_f)-z(k_f)]^2 \quad (55)$$

subject to

$$\mathbf{x}(k+1) = \mathbf{A}\mathbf{x}(k) + \mathbf{b}u(k) + \mathbf{w}(k) \quad \text{for } k = k_i, \ldots k_f-1 \quad (56)$$

$$\mathbf{x}(k_i) = \mathbf{x}_i \quad (57)$$

$$0 < u(k) < u_m, \text{ for } k = k_i, \ldots k_f-1 \quad (58)$$

$$y(k) = \mathbf{c}'\mathbf{x}(k), \text{ for } k = k_i+1, \ldots k_f \quad (59)$$

The previous sections were devoted to the development of the performance index (55) and the system model (56). In this section, a procedure is developed for determining the optimal performance of a building by adapting known optimal control theory techniques.

Mathematical Conditions

Pontryagin's Minimum Principle [68] is an optimization procedure that results in a set of mathematical conditions

for the optimal control history for a system modeled in continuous-time. A similar procedure, known as the "discrete maximum principle" has been developed for use in discrete-time problems [63]. Although this is a procedure for maximizing a function, it is equally applicable to problems that require the minimization of a function. The discrete maximum principle uses a Lagrange multiplier approach to obtain a "Hamiltonian" function defined as

$$\begin{aligned} H[\mathbf{x}(k), u(k), \mathbf{p}(k+1), k] = & \\ & r(k)u(k) + 1/2q(k)[\mathbf{c}'\mathbf{x}(k)-z(k)]^2 \\ & + \mathbf{p}'(k+1)[\mathbf{A}\mathbf{x}(k) + \mathbf{b}u(k) + \mathbf{w}(k)] \end{aligned} \tag{60}$$

The variable, $\mathbf{p}(k)$, is an nx1 vector which is commonly called the "co-state" of the system and is governed by the equation,

$$\begin{aligned} \mathbf{p}(k) &= \frac{\partial H[\mathbf{x}(k), u(k), \mathbf{p}(k+1), k]}{\partial \mathbf{x}(k)} \\ &= q(k)\mathbf{c}[\mathbf{c}'\mathbf{x}(k)-z(k)] + \mathbf{A}'\mathbf{p}(k+1) \\ &\qquad \text{for } k = k_i \ldots k_f \end{aligned} \tag{61}$$

with

$$\mathbf{p}(k_f+1) = \mathbf{0} \tag{62}$$

A necessary condition for the optimal solution of the above equations is that the values for the control history at each time step, $u(k)$, must minimize the Hamiltonian as defined by

equation (60) at each time step when evaluated at the optimal values for the state and co-state variables. By denoting the optimal value for each of the variables with a "*", the set of necessary conditions for the optimal control strategy is the state equation,

$$\mathbf{x}^*(k+1) = \mathbf{A}\mathbf{x}^*(k) + \mathbf{b}u^*(k) + \mathbf{w}(k)$$
$$\text{for } k = k_i, \ldots k_f-1$$
$$\mathbf{x}^*(k_i) = \mathbf{x}_i \tag{63}$$

the co-state equation,

$$\mathbf{p}^*(k) = q(k)\mathbf{c}[\mathbf{c}'\mathbf{x}^*(k)-z(k)] + \mathbf{A}'\mathbf{p}^*(k+1)$$
$$\text{for } k = k_i+1, \ldots k_f$$
$$\mathbf{p}^*(k_f+1) = \mathbf{0} \tag{64}$$

and the control equation,

$$[r(k)+\mathbf{b}'\mathbf{p}^*(k+1)]u^*(k) = \text{Min}\{[r(k)+\mathbf{b}'\mathbf{p}^*(k+1)]u(k)\} \tag{65}$$

for

$$0 < u(k) < u_m \quad \text{and} \quad k = k_i, \ldots k_f-1$$

Inspection of the control equation (65) gives the following conditions for the optimal control history:

$$u^*(k) = \begin{cases} 0, \text{ if } r(k)+b'p^*(k+1) > 0 \\ u_m, \text{ if } r(k)+b'p^*(k+1) < 0 \\ \text{indefinite, if } r(k)+b'p^*(k+1) = 0 \end{cases} \quad (66)$$

Thus, the optimal control input cannot be directly evaluated with the control equation at any time step where the quantity, $r(k)+b'p^*(k+1)$, is equal to zero.

Equations (63-65) are a set of necessary, but not sufficient, conditions for the optimal control history. Thus, solutions may exist to these equations that are not optimal. Furthermore, these equations do not guarantee that an optimal solution exists, nor do they guarantee that the optimal solution is unique. Therefore, if equations (63-65) can be solved simultaneously to obtain a solution, other methods must be used to determine if the solution is optimal.

Steady-state solution

The steady-state solution to the optimization problem is easily obtained and provides some insight into the dynamic solution. The state and co-state equations can be rewritten under steady-state conditions as

$$\mathbf{x} = (\mathbf{I}-\mathbf{A})^{-1}(\mathbf{bu}+\mathbf{w}), \quad (67)$$

$$y = \mathbf{c}'\mathbf{x} \quad (68)$$

$$\mathbf{p} = \mathbf{q}(\mathbf{I}-\mathbf{A}')^{-1}\mathbf{c}(\mathbf{c}'\mathbf{x}-z), \quad (69)$$

where the "*" notation from equations (63) and (64) have been omitted for brevity. The matrix I is the nxn identity matrix. For the optimal steady-state control input to have a value other than zero or its maximum, the following condition from equation (66) must be satisfied.

$$r+b'p = 0 \tag{70}$$

Equations (67-70) can be solved simultaneously to give the optimal system output and control input as

$$y = z - g_1(r/q), \tag{71}$$

$$u = g_1(y-g_2), \tag{72}$$

where

$$g_1 = [c'(I-A)^{-1}b]^{-1}, \tag{73}$$

$$g_2 = c'(I-A)^{-1}w. \tag{74}$$

The parameter, g_2, gives the effect of the disturbance variables, w, on the steady-state heat input. For the case of the ERH with no solar radiation, g_2 reduces to the outdoor dry-bulb temperature. The system output for the ERH is the globe temperature, thus the parameter g_1 is the overall heat transfer coefficient for the system based on indoor globe temperature rather than indoor dry-bulb temperature as indicated by equation (72). Since g_1 is positive for the ERH, equation (71) indicates that the

optimal steady-state indoor globe temperature (y) is always less than the desired temperature (z) and this difference is linearly proportional to the ratio of the energy weighting factor (r) and to the discomfort weighting factor (q). This difference is also affected by the overall heat transfer coefficient (g_1). Thus, equation (71) indicates that optimal steady-state conditions depend on the cost of energy (r), the cost assigned to discomfort (q), and the thermal performance characteristics of the system (g_1). Although the optimal control input, u, does depend on outdoor conditions as shown by equation (72), the optimal comfort conditions are independent of the outdoor conditions.

Dynamic solution

Obtaining the dynamic solution of equations (63-65) is not a straightforward task for several reasons. Equation (65) indicates that the control input can be determined directly from the co-state variables to be zero or its maximum value under certain conditions. However, the control input cannot be directly evaluated from this equation when the quantity, $r(k)+b'p^*(k+1)$, is zero, which is the only condition that will permit the control input to have an intermediate value. Physical reasoning indicates that the optimal control input should have intermediate values during at least some intervals of the

optimization period, therefore, a method for determining these intermediate values is probably required.

The state equation (63) has a known initial condition and can be solved in the forward time direction as was demonstrated during the model testing. However, the **A** matrix in the state equation is not invertible, thus it cannot be solved backwards in time. Consequently, the co-state equation (64) has a known final condition and can only be solved in the backwards-time direction. Thus, equations (63) and (64) define a "two-point boundary-value" problem which cannot be solved directly by marching through time.

Steepest descent method The problems associated with the simultaneous solution of equations (63-65) indicate that an iterative method is required. A "steepest descent" method [68] exists for solving two-point boundary-value problems with unconstrained inputs. This is an iterative method which has been extended in this study for use in solving the problem with constrained inputs.

The steepest descent algorithm and the modifications used in this study are as follows:

1. Select an initial control history, $u^i(k)$, for $k = k_i, \ldots k_f-1$. Physical insight should be used to select a control history which is as close to the optimal control history as can be practically determined as this will affect the number of iterations required to obtain convergence.

2. Use the control history, u^i, to solve the state equation (63) by marching forward in time from the initial condition at time step k_i to the final time step, k_f. Save the calculated values of the state variables, $\mathbf{x}^i(k)$, at each time step.

3. Solve the co-state equation (64) by marching backwards in time from the final condition at time step, k_f+1, to the initial time step, k_i, using the saved values of the state variables from step 2. At each time step, calculate and save the quantity, $r(k)+\mathbf{b}'\mathbf{p}^i(k+1)$.

4. Calculate a new control history, u^{i+1}, as a function of the old history, u^i, with the expression,

$$u^{i+1}(k) = u^i(k) - g \frac{\partial H^i}{\partial u}(k), \quad k = k_i, \ldots k_f \tag{75}$$

where

$$\frac{\partial H^i}{\partial u}(k) = r(k) + \mathbf{b}'\mathbf{p}^i(k+1) \tag{76}$$

and g is a postive constant which controls the rate of convergence. The development of equation (76) assures that the performance index will be reduced if the step size, g, is not too large. The selection of the step size is discussed later.

5. As the steepest ascent algorithm was developed for the case of unconstrained input, the calculated values for u^{i+1} from the previous step may violate the input constraints. Thus, it is necessary to replace any negative values of $u^{i+1}(k)$ with zero and any values which exceed u_m must be replaced with u_m.

6. If the desired level of convergence has not been achieved, replace u^i with u^{i+1} and begin a new iteration at step 2. Otherwise, terminate the procedure and output the desired results. A method for calculating the level of convergence is described below.

Step size selection The step size, g, for calculating the change in the control variable at each iteration determines the rate of convergence of the steepest ascent algorithm. At each iteration, there exists an optimal value of g that will maximize the decrease in the performance index. Smaller or larger values of g will result in less decrease in the performance index, thus reducing the rate of convergence. Excessively large values of g may result in increases in the performance index and cause the optimization procedure to diverge. The difficulty in selecting the optimal value of g is further compounded by the fact that this optimal value varies with each iteration. Thus, the convergence rate of this optimization procedure is

strongly dependent on the method used to select g at each iteration.

The optimal value for g can be determined using a single variable search at each iteration [68]. This procedure starts with an arbitrary value for g which is used to calculate a new control history (steps 4 and 5). This control history is used to calculate a new state trajectory (step 2) which in turn is used to calculate a new value for the performance index. Other values of g are used in the same manner until a minimum value for the performance index is obtained. The procedure then resumes at step 6. Although this single variable search method should require the least number of iterations of the overall optimization procedure, the amount of calculation required to find the optimal value of g at each iteration may be excessive. Thus, a trade-off exists between the computational time required by the single variable search for the optimal value of g at each iteration and the computational time due to the number of required iterations.

A procedure was developed in this study which combined the single variable search method for g with the overall optimization procedure. Although the optimal value of g varied with each iteration, it was assumed in this procedure that this variation occurred in an orderly manner. This assumption was based on preliminary testing of the

optimization procedure with arbitrary values of g which indicated that the optimal value of g (g^*) was relatively small during the first iterations and generally increased with additional iterations. This preliminary testing also supported the assumption that the performance index (J) at first decreased and then increased with increasing values of g for each iteration. This assumed relationship between J and g during any one iteration is qualitatively shown in Fig. 10. During subsequent iterations, it was assumed that g^* increases and $J(g^*)$ decreases with respect to the values shown in Fig. 10. The above assumptions were used to develop the following procedure for selecting g at each iteration of the optimization procedure.

1. Select an arbitrary value of g for the first iteration and calculate the corresponding value for the performance index, J(g). Compare this value to the initial value of the performance index J(0). If J(g) is less than J(0), proceed to step 2. Otherwise skip step 2 and proceed to step 3.

2. Increment g by a predetermined amount, Δg, and calculate $J(g+\Delta g)$. If $J(g+\Delta g)$ is less than J(g) proceed to step 2a, otherwise proceed to step 2b.

2a. This situation is represented by Region A of Fig. 10. Use the value of $g+\Delta g$ for the step size and

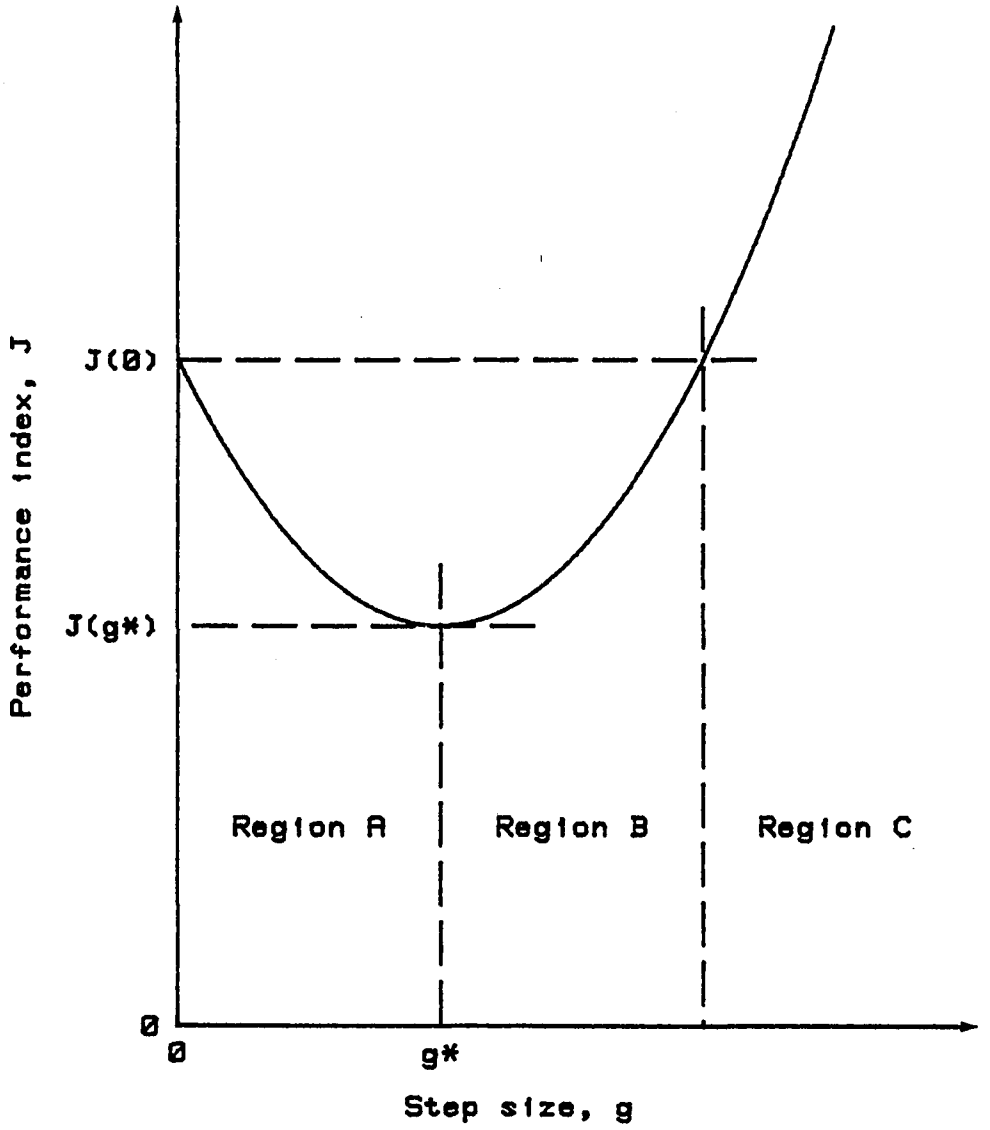

Fig. 10. Assumed relationship between J and g at each iteration of the steepest ascent algorithm

continue the iteration process using $g+2\Delta g$ as the initial step size for the next iteration.

2b. This situation is represented by Region B of Fig. 10. Use the value of g for the step size and continue the iteration process using $g-\Delta g$ as the initial step size for the next iteration.

3. The performance index is actually increased in this case as shown by Region C of Fig. 10. Incrementally decrease g by g until the performance index is decreased to a value below J(0). Then continue with the iteration process using $g-\Delta g$ as the initial step size for the next iteration.

The step size increment, Δg, should be somewhat greater than the expected change in g^* from one iteration to the next. This will allow g to reach g^* after a number of iterations if the initial guess for g is low as indicated by Region A of Fig. 10. When g approaches g^*, it should oscillate between Regions A and B during subsequent iterations. Preliminary testing indicated that the incremental increases in g^* are better described by an exponential relationship than a linear one. Further testing indicated that a good convergence behavior could be obtained with the relation,

$$\log_{10}(g+\Delta g) = \log_{10}(g) + 0.25 \qquad (77)$$

or equivalently,

$$g+\Delta g = 10^{+0.25}g = 1.778g \tag{78}$$

and

$$g-\Delta g = 10^{-0.25}g = 0.562g \tag{79}$$

Other preliminary tests using equations (78) and (79) for the changes in step size, g, resulted in values of g in Regions A and B during most of the iterations. Occasionally, values of g occurred in Region C, however the procedure described above was satisfactory for returning g to Regions A and B during subsequent iterations. Although this procedure for selecting the step size does not determine the optimal value at each iteration, it does attempt to adjust the step size at each iteration in the optimal direction for the next iteration.

Convergence criteria A convergence criteria is necessary to determine when the iteration process is complete. The steepest ascent algorithm [68] for unconstrained input uses the following criteria to determine convergence.

$$H_u = \sum_{k=k_i}^{k_f-1} \frac{\partial H}{\partial u}(k)^2 = 0 \tag{80}$$

In an actual optimization by a digital computer, the steepest descent algorithm would end when H_u is less than a predetermined, small, positive value. Equation (80) does not provide a valid convergence criteria for the case of constrained input because H_u is not zero for optimal conditions if the optimal control input is u_m or zero at any time step as indicated by the optimal conditions given by equation (66). For this case of constrained input, optimal conditions occur when

$$\frac{\partial H}{\partial u}(k) = r(k) + b'p(k+1) = \begin{cases} >0, \text{ for } u(k) = u_m \\ <0, \text{ for } u(k) = 0 \\ 0, \text{ for } 0<u(k)<u_m \end{cases} \tag{81}$$

Thus, the convergence criteria of equation (80) is transformed to

$$H_u = \sum_{k=k_i}^{k_f-1} h[u(k)][r(k) + b'p(k+1)]^2 \tag{82}$$

where

$$h[u(k)] = \begin{cases} 0, \text{ for } u(k) = 0 \text{ or } u(k) = u_m \\ 1, \text{ for } 0<u(k)<u_m \end{cases} \tag{83}$$

Equations (82) and (83) are used to calculate the convergence criteria for the case of constrained input used

in this study. When this convergence criteria is less than a predetermined, positive value, the iteration process is assumed to be complete.

A computer program was developed from the above procedure to obtain optimal solutions for the performance of the ERH. This program was written in BASIC for solution on a Hewlett-Packard System 35 (model number HP9835A) desktop computer. A listing of the program is in Appendix C.

Optimization Results

The optimization procedure was applied to several hypothetical cases using the ERH system model to obtain information on the sensitivity of the various optimization parameters. These hypothetical cases also indicated the nature of the optimal performance for two scenarios. For the first scenario (intermittent occupancy), it was assumed that the house was unoccupied for twelve hours during the day and occupied for twelve hours at night. Electrical utility rates were assumed constant during the entire period. For the second scenario (time-of-day utility rate structure), it was assumed that daytime electrical utility rates were twice as high as the nighttime rates and the house was occupied at all times. For both scenarios, it was assumed that the outside dry-bulb temperature was 0 C and the solar radiation was 0 W/m^2 at all times. During all

occupied periods, it was assumed that the desired standard temperature (z) was 20 C.

Intermittent occupancy

The discomfort weighting factors, q(k), were defined as the "cost" of discomfort at time step k. During unoccupied periods, q(k) was equal to zero and during occupied periods q(k) had a postive value with units of cost per degrees of discomfort squared per time step (15 minutes). For this scenario, it was assumed that the cost of discomfort was constant during the occupied periods.

Figure 11 is a graphical representation of the discomfort for an arbitrary time period. This figure shows the discrete values for discomfort at each time step and the assumed linear relation between time steps. During the time period, k_a to k_b, q is assumed to be a fixed value, q_{ab}, and during the subsequent time period, k_b to k_c, q is assumed to be a different fixed value, q_{bc}. The total cost of discomfort (J_y) during the time period from k_a to k_c can be calculated by analytically integrating the cost-weighted discomfort over this time period. This integration results in the expression

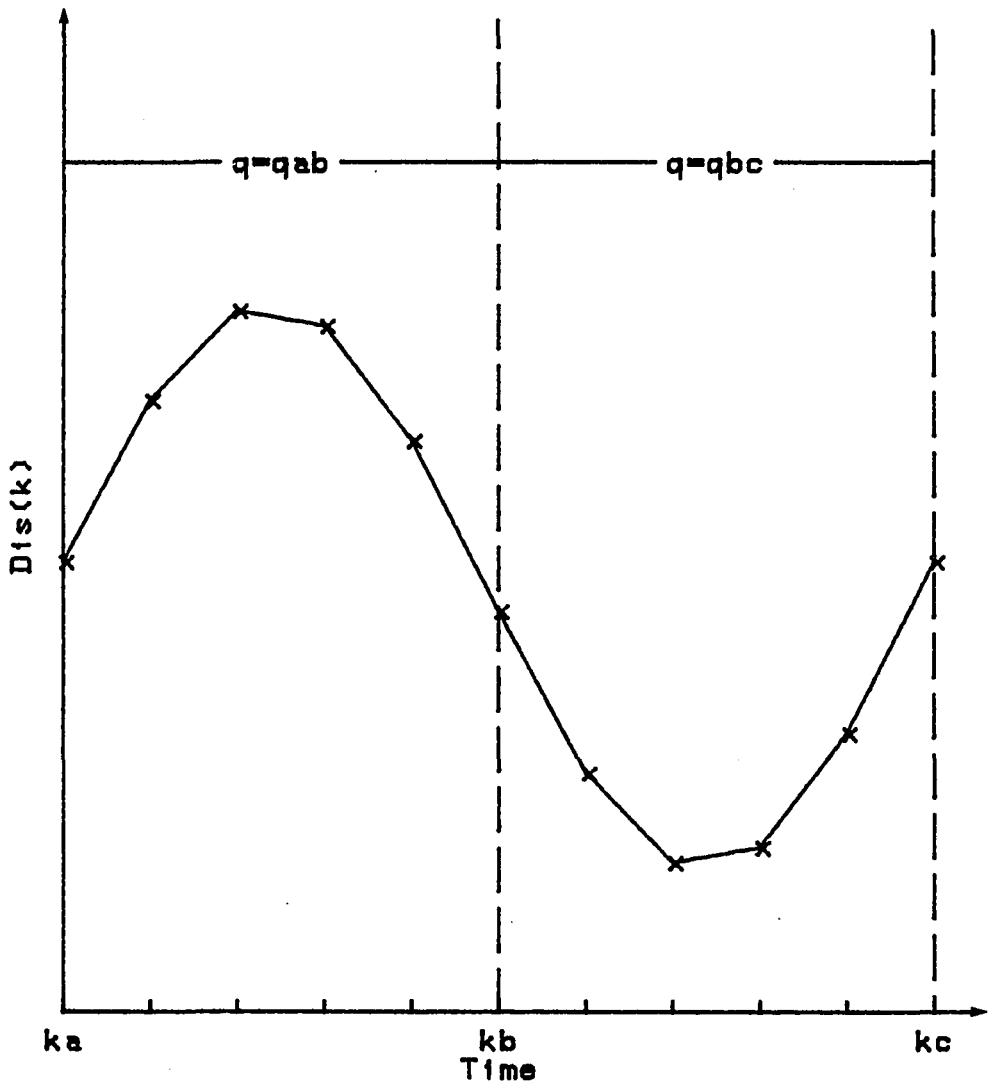

Fig. 11. Assumed arbitrary discomfort (Dis) profile with a step change in the discomfort weighting factor (g)

$$J_y = 1/2 q_{ab} Dis^2(k_a) + q_{ab} \sum_{k=k_a+1}^{k_b-1} Dis^2(k)$$

$$+ 1/2(q_{ab}+q_{bc}) Dis^2(k_b)$$

$$+ q_{bc} \sum_{k=k_b+1}^{k_c-1} Dis^2(k) + 1/2 q_{bc} Dis^2(k_c) \qquad (84)$$

which can be rewritten as

$$J_y = \sum_{k=k_a}^{k_c} q(k) Dis^2(k) \qquad (85)$$

where

$$q(k) = \begin{cases} 1/2 q_{ab}, & \text{if } k=k_a \\ q_{ab}, & \text{if } k_a<k<k_b \\ 1/2(q_{ab}+q_{bc}), & \text{if } k=k_b \\ q_{bc}, & \text{if } k_b<k<k_c \\ 1/2 q_{bc}, & \text{if } k=k_c \end{cases}$$

Equation (85) is the same form as that used in the discomfort index. Thus, the value for q(k) at the beginning or end of the optimization period is one-half of the defined value of q(k) during the adjacent time step and the value for q(k) at any time step which corresponds to a change in

comfort weighting is the simple average of the defined values for q(k) during the preceding and proceeding time steps.

For this scenario, it was assumed that the ERH was only occupied from 6:00 p.m. to 6:00 a.m. During this period, it was assumed that q(k) had a fixed value, q_c. The optimization period was assumed to be a two-day period with an initial time of midnight (k=0) and a final time of midnight, 48 hours later (k=192). The values for q(k) for the two-day period are given below.

$$q(k) = \begin{cases} 0, \text{ for } 24<k<72 \text{ and } 120<k<168 \\ q_c, \text{ for } 0<k<24,\ 72<k<120, \text{ and } 168<k<196 \\ q_c/2, \text{ for } k=24,\ 72,\ 120,\ 168, \text{ and } 196 \end{cases} \quad (86)$$

A value is not assigned to q(0) because the discomfort at time zero is a function of the initial state of the system and is not affected by the optimization process.

The performance index is a linear function of r(k) and q(k). Thus, both of these factors can be multiplied by a common scaling factor without affecting the optimal solution. As a result of this linearity, the units used for expressing the cost of the energy consumption and discomfort are completely arbitrary as long as they are consistent. Therefore an arbitrary unit for cost, defined by the symbol "#", was used in this study. For this scenario, the

values for the energy weighting factor are assumed to be constant with respect to time and have a value of 1 #/kW per fifteen-minute time interval. Since it is assumed that the heat input, u(k) is constant during the time period, k to k+1, the unit of #/kW per fifteen minute-interval is equivalent to 4 #/kWh. The corresponding units for q_c are $\#/C^2$ per fifteen-minute time interval.

Initial conditions for the state vector, $\mathbf{x}(0)$ were arbitrarily chosen to be the steady-state values for the system state during the period from time step 0 to time 24 as calculated by equations (67-69). The initial control history for each scenario consisted of the steady-state value during occupied periods and a value of zero during unoccupied periods.

The first intermittent occupancy scenario was simulated using the dynamic optimization procedure with a value for q_c of 1 $\#/C^2$. This resulted in steady-state values for the indoor dry-bulb temperature, globe temperature, and heat input of 20.0 C, 19.8 C, and 3.0 kW, respectively. The results of the dynamic optimization procedure are shown in Fig. 12. In this figure, the "co-state output", $y_p(k)$ is defined as

$$y_p(k) = \mathbf{b}'\mathbf{p}(k+1), \tag{87}$$

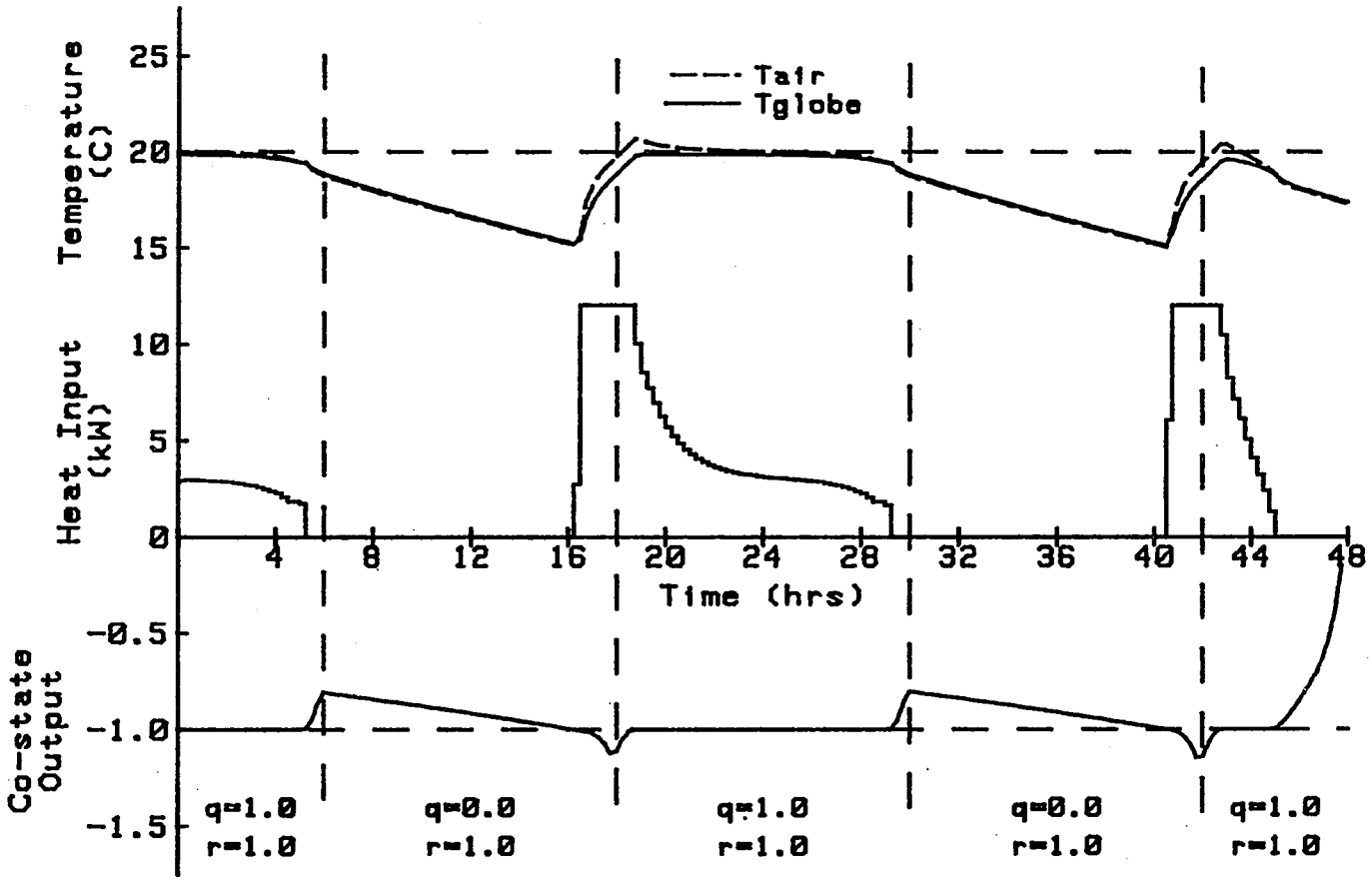

Fig. 12. Results of the intermittent occupancy optimization scenario

maintained at their steady-state values at the beginning of According to the optimal conditions given by equation (66), $y_p(k)$ should be equal to $-r(k)$ when $u(k)$ is an intermediate value and $y_p(k)$ should be greater than or less than $r(k)$ when $u(k)$ is zero or u_m, respectively. Figure 12 indicates that these optimal conditions were satisfied by the dynamic optimization procedure.

The optimal control strategy indicated by Fig. 12 has several interesting features. The indoor temperatures were the optimization period until approximately one hour prior to the end of the occupied period when the temperatures were allowed to drift by switching off the heat input. The temperatures continued to drift until about two hours prior to the start of the next occupied period at which time the heat was controlled to full capacity. The heat was maintained at full capacity, causing the indoor dry-bulb temperature to exceed the desired temperature (20 C), until the globe temperature reached its steady-state value. The globe temperature was maintained at this value by reducing the heat input until steady-state values were also obtained for the indoor dry-bulb temperature and heat input near the end of the first day.

The optimal control strategy for the second day was almost identical to the first day until the last four hours when the heat input was reduced to zero and the temperatures

were allowed to drift for the remaining optimization period. This behavior was caused by the omission of any discomfort penalties for the day following the optimization period and indicates that it is not "economical" to expend energy at the end of the optimization period if the stored energy is not utilized during the subsequent period. As a result, the predicted system performance at the end of the two-day period is not optimal if the future performance of the system is taken into account. Therefore, the following optimal control strategies are presented in terms of the first day performance of a two-day optimization period.

Figure 13 compares the optimal control strategies for q_c equal to 0.5, 1, and 5 \#/C^2. These values for q_c resulted in similar steady-state globe temperatures of 19.70, 19.85, and 19.97 C, respectively. However, the case with the highest discomfort penalty (q_c = 5 \#/C^2) maintained the steady-state globe temperature throughout almost the entire occupied periods, whereas the case with the lowest discomfort penalty (q_c = 0.5 \#/C^2) did not achieve the steady-state globe temperature until more than one hour after the beginning of the occupied periods and allowed the globe temperature to begin drifting nearly four hours before the end of the occupied periods. Thus, the optimization procedure indicated that greater energy savings can be

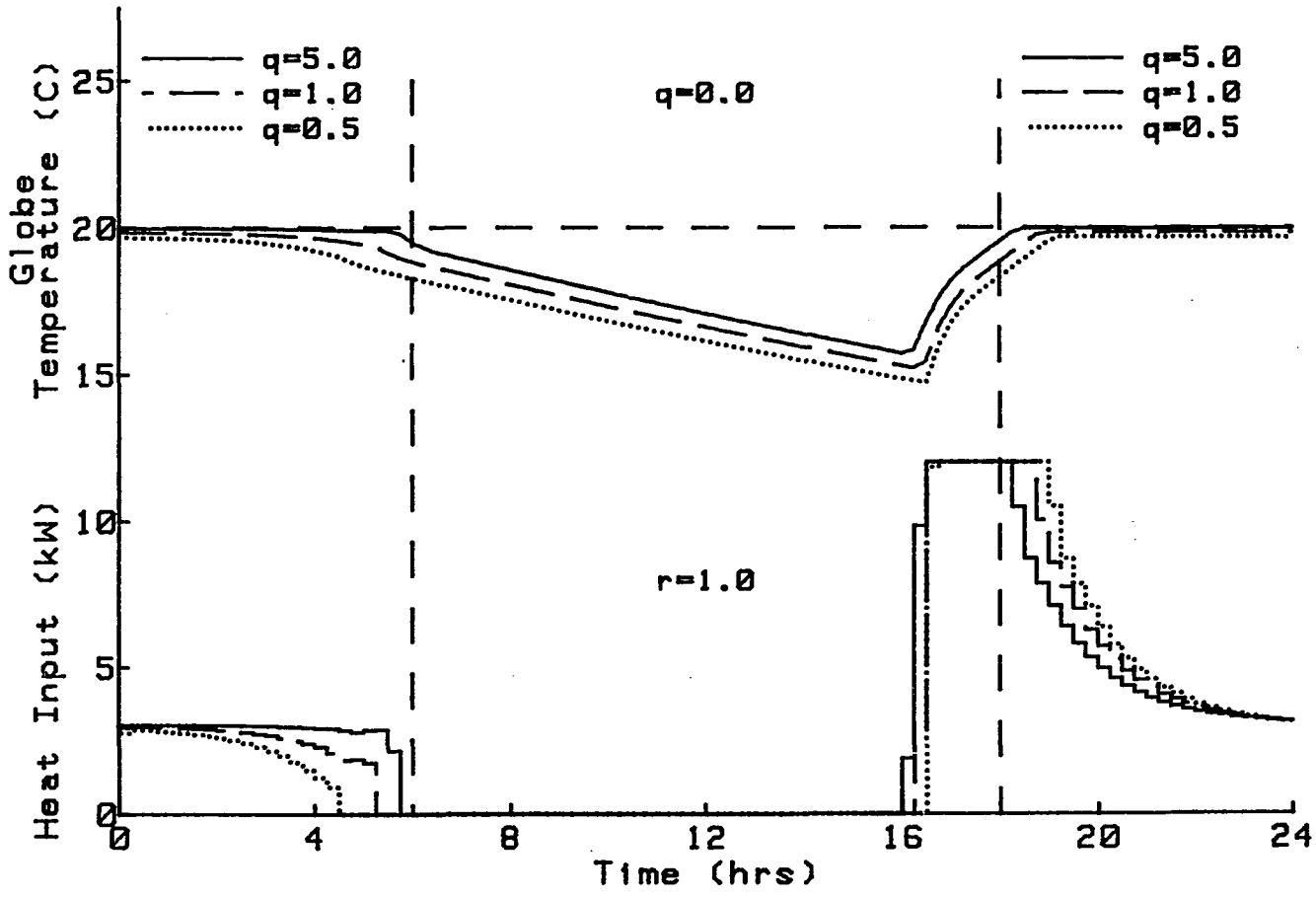

Fig. 13. Effect of the discomfort weighting factor on the intermittent occupancy optimization scenario

obtained by allowing higher discomfort at the beginning and end of each occupied period rather than during the interim.

The effect of outdoor temperature on the intermittent occupancy scenario is shown in Fig. 14. The solid line is identical to the case shown in Fig. 12 with an outdoor dry-bulb temperature of 0 C and the dashed lines are for a constant outdoor dry-bulb temperature of 10 C. This figure indicates that as the outdoor dry-bulb temperature increased, the globe temperature was brought to its steady-state value earlier at the beginning of the occupied periods and was allowed to drift earlier towards the end of the occupied period.

The optimal control strategy for a time-varying outdoor dry-bulb temperature is shown in Fig. 15. For this scenario, the outdoor dry-bulb temperature (T_o) varied sinusoidally with a mean value of 0 C and an amplitude of 5 K as indicated by the following equation.

$$T_o(k) = 5\sin[(k-36)(\pi/48)] \tag{88}$$

In this equation T_o has units of C with a maximum value of 5 C at 3:00 p.m. (k=60) and a minimum value of -5 C at 3:00 a.m. (k=12). Figure 15 compares the optimal control strategy for this time-varying outdoor temperature with the constant outdoor temperature (0 C) case shown in Fig. 12.

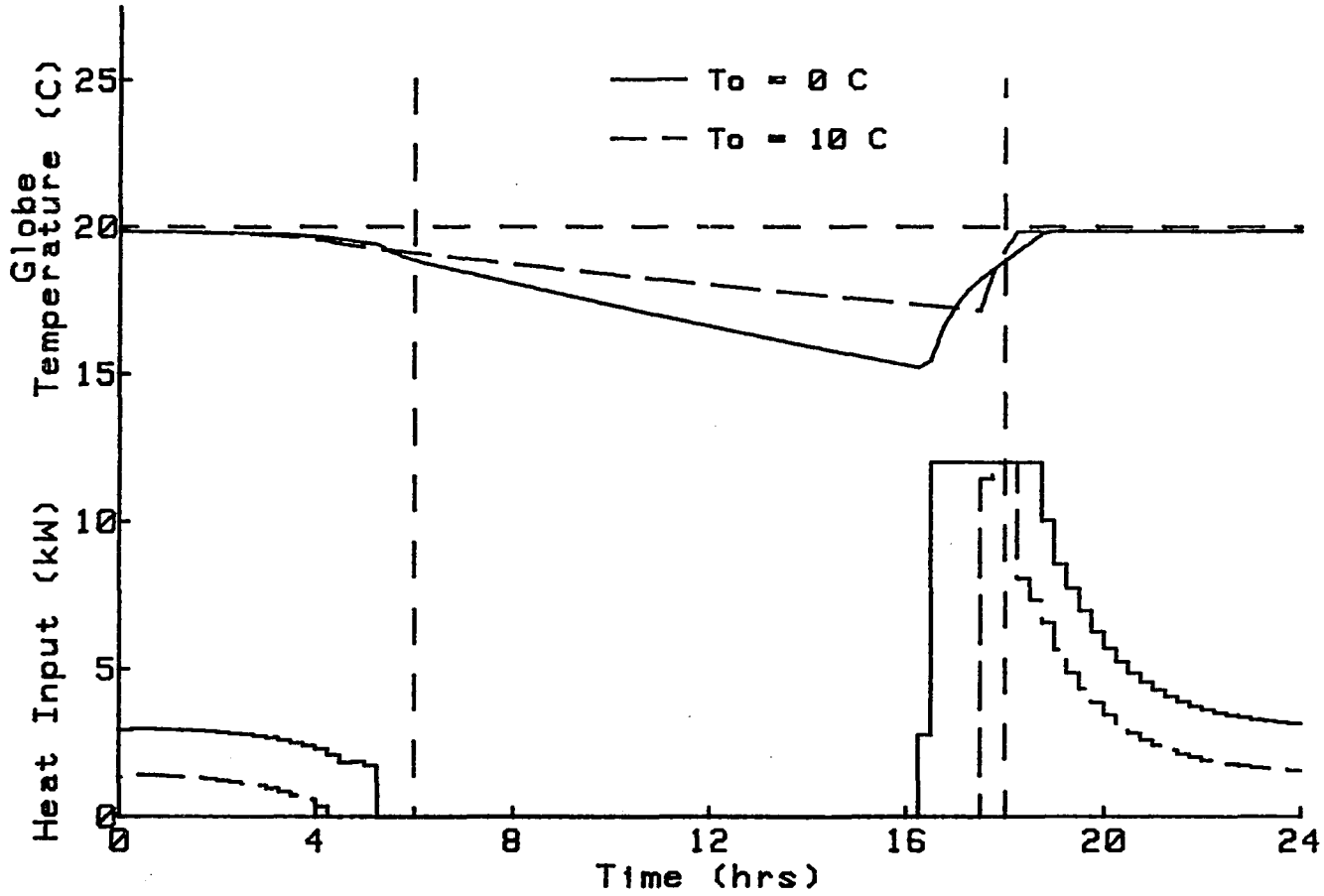

Fig. 14. Effect of outdoor dry-bulb temperature on the intermittent occupancy optimization scenario

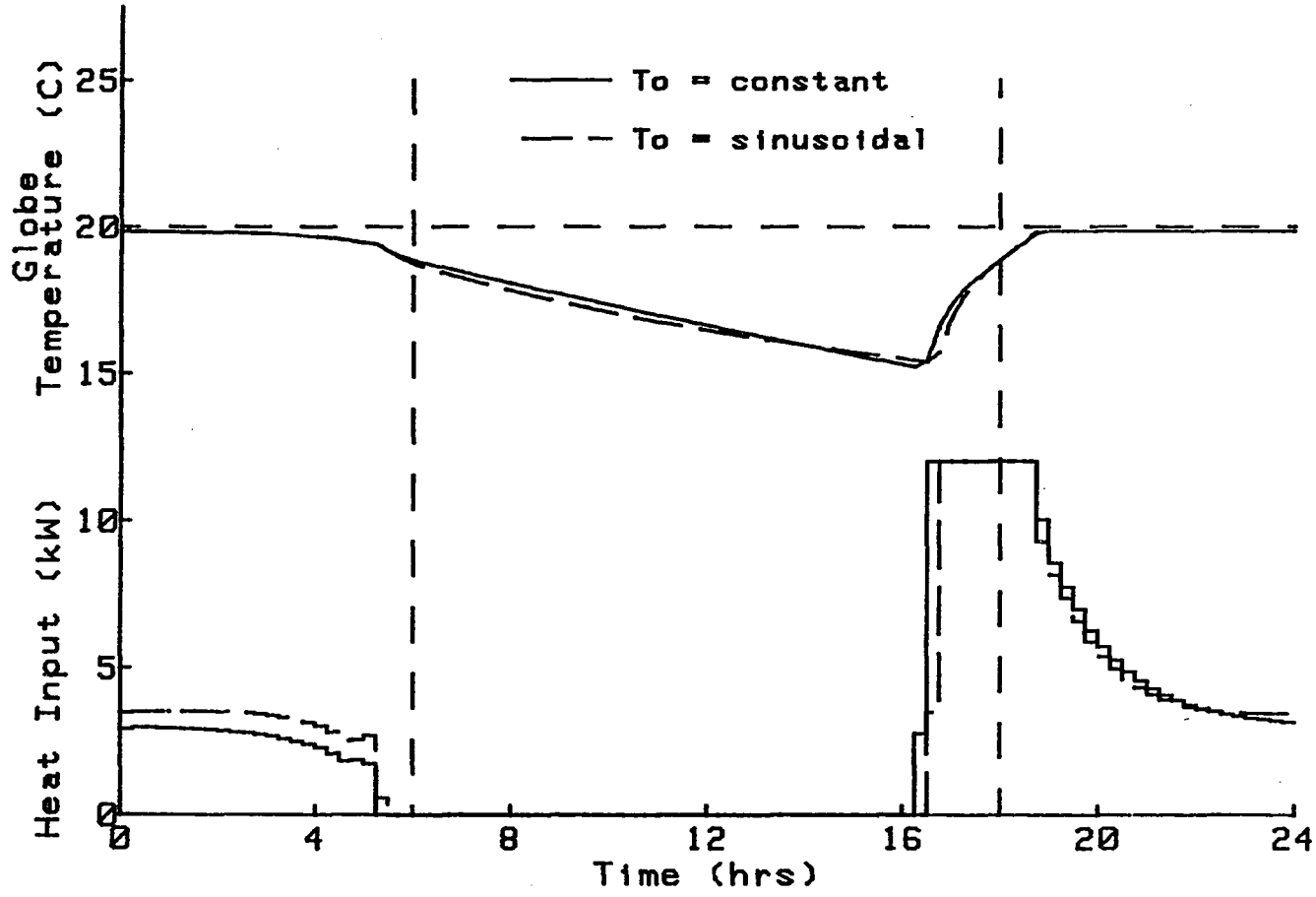

Fig. 15. Effect of time-varying outdoor temperature on the intermittent occupancy optimization scenario

Although the heat input was somewhat different for the two cases, the globe temperature profiles were almost identical.

The effect of solar radiation on the optimal control strategy is indicated in Fig. 16 by comparing the case shown in Fig. 12 with no solar radiation with an identical case which included solar radiation. The values used for the total horizontal radiation were from the actual measurements obtained from day 24 of the ERH data. These measurements were recorded during a cloudless day in February. Figure 16 indicates that the inclusion of solar radiation had an effect on the optimal control input and the optimal globe temperature profile.

Time-of-day electric rates

For this scenario, q(k) was held at a fixed arbitrary value during the entire optimization period and r(k) was varied with time according to an arbitrary electrical rate structure. The assumed rate structure had an electrical rate that was twice as high during the daytime hours of 6:00 a.m. to 6:00 p.m. as the rate during the remaining nighttime hours. These costs were assumed to be 1 and 0.5 ¢/kW, respectively. Thus, the values for r(k) at each time step were defined as shown below.

$$r(k) = \begin{cases} 1, \text{ for } 24 \leq k \leq 71 \text{ and } 120 \leq k \leq 167 \\ 0.5, \text{ otherwise} \end{cases} \tag{89}$$

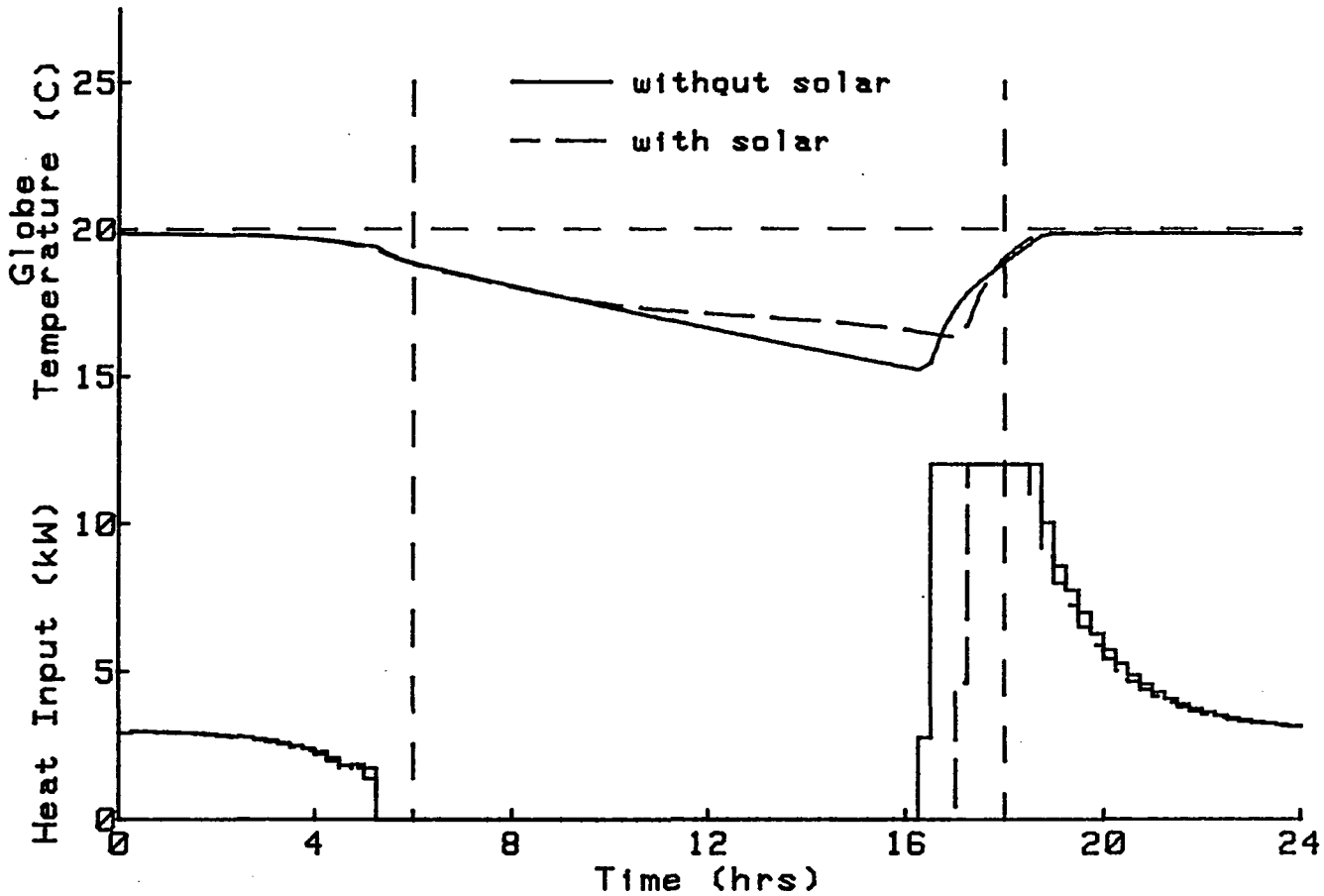

Fig. 16. Effect of solar radiation on the intermittent occupancy optimization scenario

The optimization results for this scenario for q = 1 $\#/C^2$ are shown in Fig. 17. These results indicate that the optimal control strategy used the thermal capacity of the building to shift the electrical load from high rate periods to low rate periods each time the electrical rates changed by systematically allowing the temperature to rise and drift.

The magnitude of the electrical load shift depended on the value of the discomfort weighting factor as shown in Fig. 18 which compares the case of Fig. 17 (q = 1 $\#/C^2$) to a case with q = 2 $\#/C^2$ and to a reference case where r = 1 \#/kW and q = 1 $\#/C^2$ throughout the entire optimization interval. Table 17 compares the energy consumption, energy costs, and the average discomfort for the first day of the optimization period for each of the three cases shown in Fig. 18. The average discomfort was calculated as the root mean square of the discomfort at each time step. The electrical costs for the base case in Table 17 were calculated using the time-of-day electrical rate structure for comparison purposes. These results indicate that although electrical consumption was nearly identical for the three cases, electrical costs were reduced by 10 and 17 % for the high and low comfort cases, respectively, compared to the base case. The resultant increases in discomfort are 0.18 and 0.43 C for the high and low comfort cases,

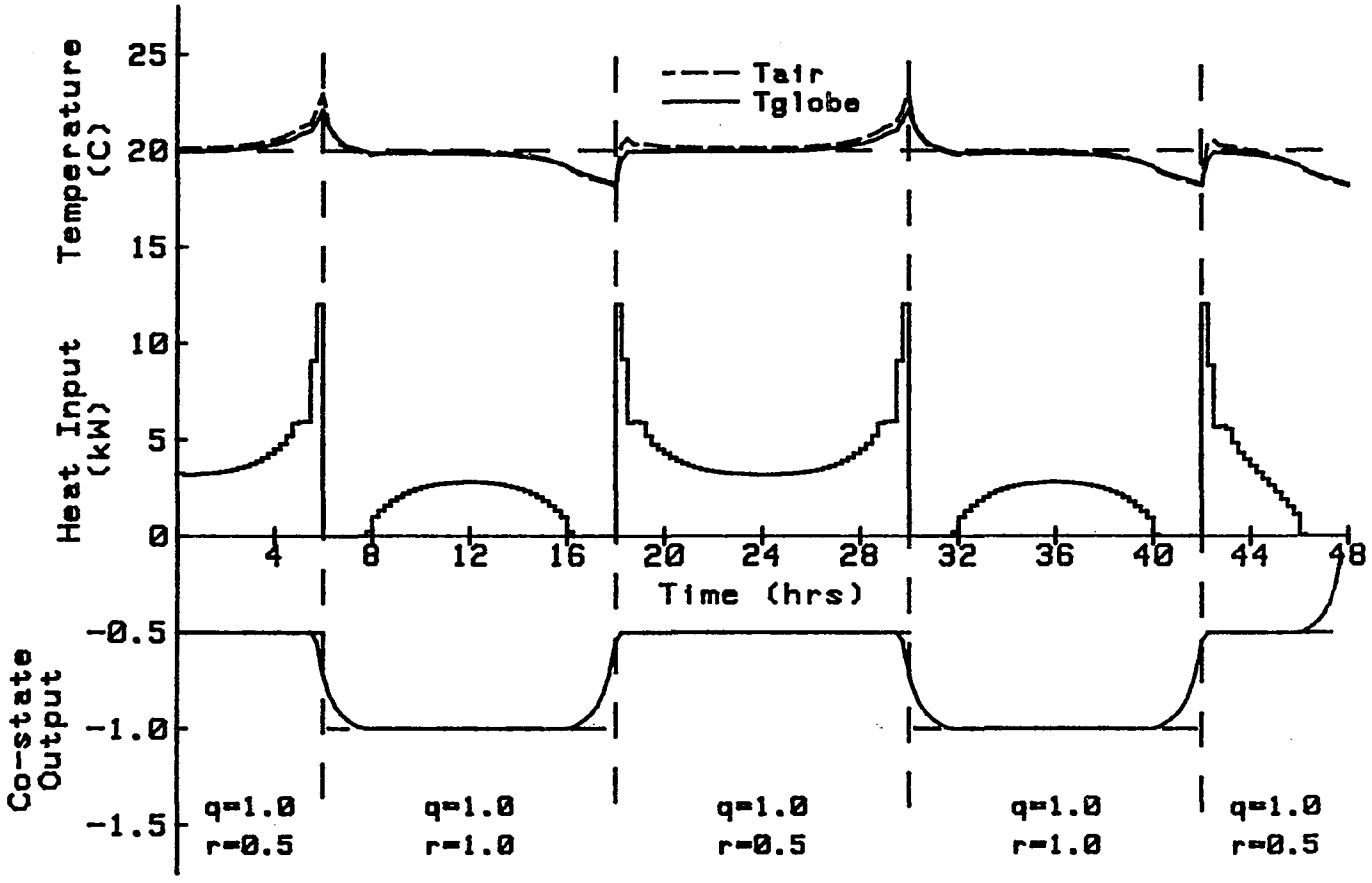

Fig. 17. Results of the time-of-day electric rate structure scenario

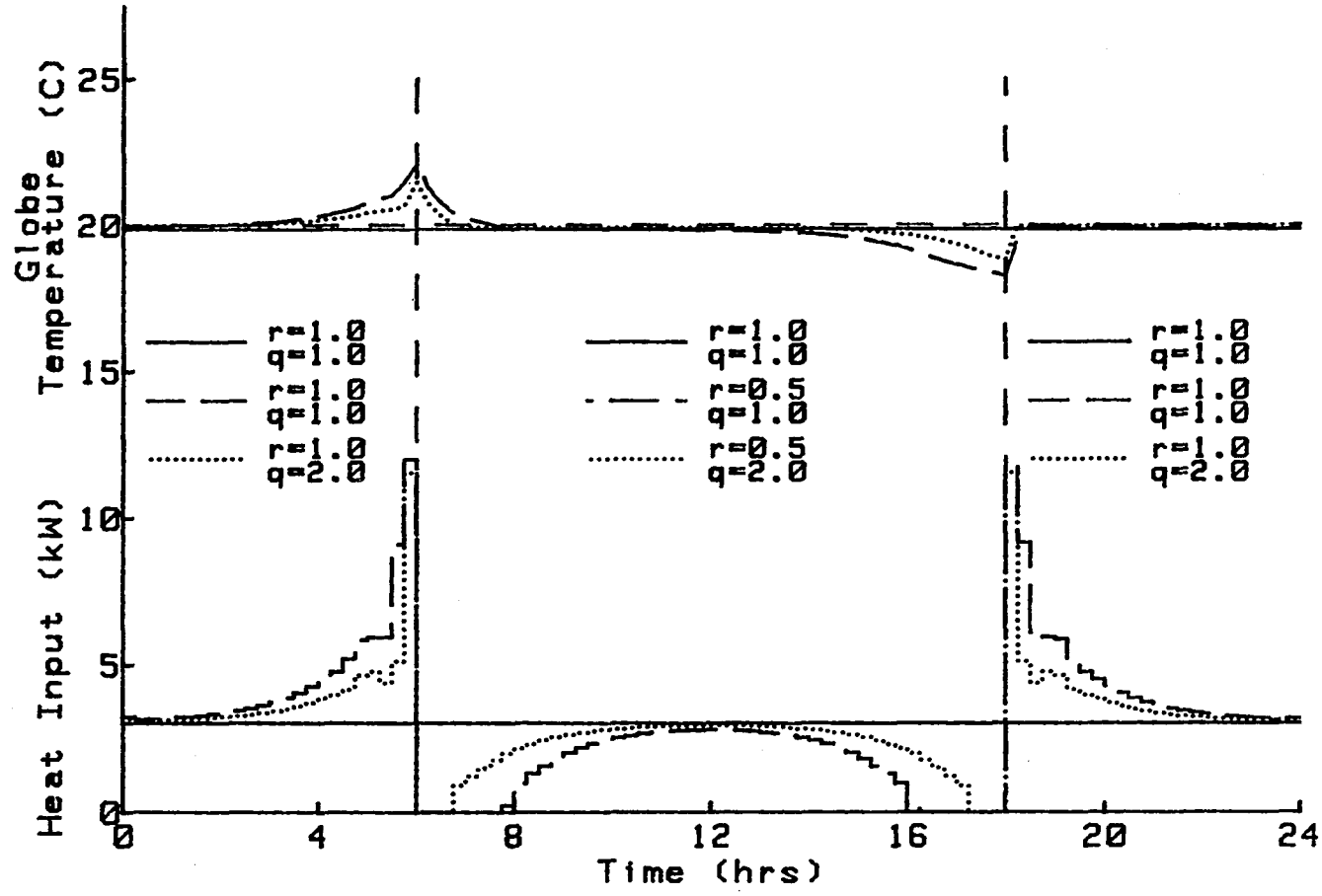

Fig. 18. Effect of the discomfort weighting factor on the time-of-day electric rate structure scenario

Table 17. Summary of the optimization results for the time-of-day electric rate structure scenario

Case	Electrical Consumption (MJ)	Electrical[a] Cost (#)	Average Discomfort (C)
Base[b]	262	218	0.15
High Comfort[c]	263	197	0.33
Low Comfort[d]	262	182	0.58

[a]All electrical costs, including the base case are calculated in terms of the time-of-day electrical rate structure.

[b]Constant electrical rate structure (r=1 #/kW) and constant discomfort weighting factor (q = 1 #/C^2).

[c]Time-of-day electrical rate structure with q = 2 #/C^2.

[d]Time-of-day electrical rate structure with q = 1 #/C^2.

respectively. These results indicate that the optimal control strategy can result in considerable energy cost savings with only a small sacrifice in comfort.

DISCUSSION

The preceding sections described the general development of the performance index, the system model, and the optimization procedure. Data from the ERH were used to derive an actual system model and the optimization procedure was applied to this model with assumed occupancy patterns, electrical rate structures, and weather conditions. The results of these simulations indicated the nature of the optimal performance of the ERH as defined in this study. However, these results may differ from the ideal situation when the optimization procedure is applied in an actual control strategy.

Control Strategy Application

The implementation of the above procedures as a real-time control strategy requires several modifications and additions to the above procedures. Some of the important changes are listed below.

1. The optimization procedure provides information about the optimal temperature profiles and the optimal control history. A procedure is needed to incorporate this information into a control strategy for governing the actual operation of the system.

2. A more efficient algorithm for the modeling and optimization procedures is necessary to reduce the

computational requirements to a level that can be achieved by a relatively inexpensive microprocessor.

3. The modeling procedure requires the use of sufficient instrumention for obtaining the necessary data for the real-time model development.

4. Any significant deviations between the predicted and actual system performance that occur in the optimization process due to inaccuracies in the system model or weather predictions must be accounted for by the control strategy. Therefore, sensors are required for monitoring the actual indoor environmental conditions to provide a feedback of the accuracy of the control strategy.

5. A method for predicting the necessary weather variables is required for the optimization procedure. This may also require additional instrumentation if on-site weather data are utilized in the weather predictions.

6. Provisions must be incorporated into the control strategy for the input of the necessary occupant parameters which include occupancy periods, personal comfort requirements (clothing and activity levels), and the desired weighting for discomfort (q).

An optimal control strategy is proposed based on the information presented in the previous sections. This control strategy would require a microprocessor-based control system that can monitor and store the necessary

indoor environmental and disturbance variables and can control the necessary system inputs. The microprocessor would also have to be capable of performing the necessary calculations for the model development and optimization procedures. The control strategy would periodically update the system model with past system performance data and use this information to optimize the system performance for a future time period. The predicted optimal system performance would then be used to control the system until the model is again updated and a more current optimization is performed.

The calculated optimal control input could be used directly to control the actual system. However, any errors in the system model or weather predictions would cause differences between the desired and actual system output. Conversely, the predicted optimal system output could be used as a variable "setpoint" for a conventional on-off or proportional control strategy. Errors in the system model or weather predictions would then result in differences between the predicted optimal and the actual control input. Since the optimization results for the ERH optimization scenario indicated that variations in outdoor temperature have a greater effect on the optimal control input than on the optimal system output (see Figs. 15 and 16), the second control strategy outlined above appears to be a better

method of compensating for possible errors in the overall control strategy implementation.

The latter optimal control strategy can be described in terms of three time periods as defined below.

t_{cal} = amount of time required to perform the necessary calculations for the model development and system optimization

t_{mod} = time period of past data required for the model development

t_{opt} = future time period for which the system is optimized

During a time interval defined as t to $t+t_{cal}$, the system model would be developed from data obtained during the time period, $t-t_{mod}$ to t. This system model would be used to optimize the predicted system performance during the future time period, $t+t_{cal}$ to $t+t_{cal}+t_{opt}$. During this calculation time interval (t to $t+t_{cal}$), the predicted optimal output from the previous calculation time interval would be used as the reference control signal. The length of the calculation time interval may require a variable reference signal. This procedure would then be repeated for the next calculation time interval.

During each calculation interval, the necessary system performance data must be collected and stored and the appropriate weather predictions must be made. Any changes in the energy weighting factors, r(k), discomfort weighting factors, q(k), or the desired levels of the indoor

environmental quality, z(k), for future time steps should also be accounted for during the calculation process.

The calculation time interval should be as small as possible to permit the system model and optimization procedure to adapt quickly to changing conditions which result in errors in the optimization process, although no real advantage would result from having a calculation time interval that is shorter than the time step used for the model development and optimization procedure.

As it is likely that the calculation interval would be significantly shorter than the time period of data required for the model development, the model development procedure could be improved in terms of required computation time by using a recursive modeling procedure which adds the most recent data to the model development at each time interval and eliminates the most past data, thus reducing the amount of required calculation.

The optimization time interval must be at least as long as the calculation time interval, since the optimal results from the previous calculation interval are used as the control setpoints during the current calculation time interval. The ERH optimization scenarios indicated that results were not valid near the end of the optimization period (see Fig. 12) because the optimization procedure did not account for the future performance of the system. Thus,

the length of the optimization time period should exceed that of the calculation time period by an amount that is sufficient to eliminate the effects described above.

Computation time for the optimization procedure could be reduced by using the appropriate optimization results from the previous calculation time interval as the initial values for the first part of the control history for the optimization procedure during the current calculation time interval. Initial values for the latest time periods for the control history could be estimated by extrapolation or some other procedure. This should reduce the number of iterations required to obtain the optimal solution, especially if t_{cal} is small relative to t_{opt}.

The ERH optimization results indicated that the effect of changes in weather conditions had a relatively small effect on the optimal system output. Therefore, a simple weather prediction algorithm, that assumes the present conditions will not change during the future optimization time interval, may provide sufficient accuracy for the control strategy implementation. Other systems may require more sophisticated weather prediction algorithms.

The desired level of indoor environmental quality (z) was defined as the desired standard temperature (T_{ds}) for the ERH scenarios. The calculation of this parameter requires knowledge of the occupants' future clothing and

activity levels. Although it would be technically possible to "train" the occupants to estimate their future clothing and activity levels, and to somehow input these estimates into the control system, significant errors in predicting the desired temperature could still occur due to individual comfort preferences and errors in the assumed comfort model. Better results might be obtained by having the control strategy use an assumption for an initial desired temperature. The occupant could then periodically input a perceived thermal sensation to the control system which, in turn, would compare the occupant's thermal sensation to the thermal sensation predicted by the control system. Adjustments to the desired temperature could then be made in terms of the differences between the predicted and perceived thermal sensations. As an example, if the occupant input a slightly cool thermal sensation to the control system when the control system predicted a slightly cool sensation should have existed, no changes would be made to the assumed desired temperature. However, if the occupant input a slightly warm sensation when the control system predicted a slightly cool sensation should have existed, the desired temperature would be adjusted downward. Certain other indoor environmental factors such as lighting could be treated in a similar manner, however some indoor environmental factors (e.g., carbon dioxide levels) may not

be perceivable by the occupants. However, the desired levels of such factors are usually zero.

Values for the weighting factors for energy (r) at each time step could easily be input to the control system in terms of the actual utility rates. Occupancy schedules could also be easily input to the control strategy to indicate when the environmental weighting factors (q) should be zero. A value for q during occupied periods could be initially assumed by the control strategy. A simple input device such as a rotatable knob could then be used by the occupants to indicate when they might desire to alter their relative weighting on discomfort for the purpose of reducing their energy costs.

There is, perhaps, a subtle difference between the reduction of the desired temperature and the reduction of the discomfort weighting factor. For the case of the ERH, if an occupant desired to reduce energy costs during the heating season by increasing clothing level, the impact of this decision on the control system should be in terms of the occupant indicating a slightly warm sensation, thus causing the control system to reduce its assumed desired temperature, which in turn should cause the optimization strategy to predict a lower optimal effective temperature. However, if the occupant wants to reduce energy costs without changing his lifestyle, the control input for the

weighting on discomfort relative to energy costs should be decreased, thus resulting in slightly cooler conditions, especially at the beginning and end of occupied periods as indicated in Fig. 13.

As indicated above, the actual implementation of this control strategy requires modification of the algorithms for the system model and optimization procedure, and the development of additional algorithms for weather prediction and several other practical considerations. The hardware required for this optimal control strategy may be considerably more complex than the hardware used by existing residential control systems. However, the improvements in system performance that could be feasibly obtained with this optimal control strategy require further testing in actual occupied buildings.

Further Applications

General procedures, which have been developed for determining the optimal performance of a building, were validated for the specific case of a single-family residence with an electric-resistance, forced-air heating system. These procedures also may have possible application for determining the optimal performance of more complex building environments. Although the ERH application was limited to a linear, time-invariant system, the system modeling and optimization procedures used can be applied to nonlinear,

time varying systems as well. Some possible future applications are described below.

Heat pump systems

The optimization of a residence which uses a typical vapor-compression heat pump for heating, with an outdoor air source, would require a system model that includes the effect of the outdoor temperature on both the capacity and "coefficient of performance" of the heat pump. Although these effects would cause the system model to be nonlinear and time-varying, these changes could possibly be handled by the linear modeling procedure in Appendix A by using manufacturer's data for the heat pump performance characteristics in the model development. The sensitivity of the heat pump to outdoor conditions may affect the requirements for weather predictions as compared to other heating systems. The relatively slow transient performance of a heat pump compared to an electric furnace may require a better short term transient response of the system model.

Cooling systems

The optimization of residential cooling systems in humid climates would require a system model and performance index that could predict the interactive effects of humidity levels and temperatures on energy consumption and thermal

acceptability. The required system model would be nonlinear and perhaps difficult to derive.

Ventilation systems

Controlled ventilation systems for residences are being implemented, to a limited degree, in residences which have real or potential indoor mass air quality problems due to construction techniques that reduce the infiltration rate to possible unsafe levels. Although the modeling of indoor mass air quality is often analogous to the modeling of the building's thermal performance, the required model may be more or less complex than the model required for the prediction of thermal conditions in the same building. Linear models have been found to be applicable for modeling indoor mass air quality, however these models tend to be more time-varying than building thermal models due to the increased sensitivity of infiltration on the model behavior.

Although the effects of thermal conditions on building occupants are fairly well known, the effects of many potential indoor air contaminants on building occupants are less understood due to the long time period that may be required for a noticeable occupant response. Since occupants cannot perceive many indoor air contaminants until they are significantly higher than levels allowed by health standards, adaptive methods for predicting occupant preferences are not feasible. Thus, the formulation of the

performance index requires a priori knowledge of the effects of indoor air contaminants at various levels.

Commercial buildings

The optimization of commercial buildings would involve many of the same principles as applied to residences. However, commercial buildings are generally more complex and include many controllable inputs for mechanical systems which often require nonlinear system models. A more complex building model may be required to predict the effects of the increased thermal capacity resulting from the general use of masonry construction. Internal loads such as lighting and occupants usually have a greater impact on energy requirements than in residences and thus require prediction by the control strategy.

The assessment of indoor environmental quality in commercial buildings would generally require the inclusion of thermal factors, mass air quality, and lighting factors as controlled variables. A dilemma may exist in determining the proper form of the performance index since the people who experience the "cost" of energy consumption and the people who experience the "cost" of suboptimal indoor environmental quality are usually not the same.

Conclusions

The conclusions which have resulted from the development of the general optimization procedure are:

1. The optimization of the operating performance of a building requires consideration of energy consumption costs and their resulting impact on indoor environmental quality.

2. Building performance models can be developed using data obtained during the actual building performance.

3. Optimization techniques exist that can be adapted for use in optimizing the performance of buildings.

Specific conclusions which resulted from the application of the above procedures to the ERH are:

1. Accurate dynamic system models can be developed for predicting the transient thermal response of wood-frame single-family residences with electric-resistance forced-air heating systems.

2. The optimal control for these types of structures can compensate for the effect of the lag of indoor mean radiant temperature on conditions of thermal acceptability.

3. The thermal capacitance of a residence can be used to shift electrical loads for the reduction of electrical costs governed by time-of-day utility rate structures. These cost savings can be obtained with a relatively small sacrifice in thermal comfort conditions.

4. During conditions of intermittent occupancy, greater energy savings can be obtained by sacrificing comfort at the beginning and the end of occupied periods than during the interim.

5. Although diurnal outdoor weather variations do affect the optimal heat input, they have a minor effect on the optimal temperature profiles. Thus, the level of accuracy of the system model in predicting the transient effects of ambient weather conditions is not as important as the accuracy of the model in predicting the transient effects associated with the operation of the heating system.

Recommendations

The results of this study have indicated the need for future research in several areas related to the optimization of building performance.

1. The accuracy of the procedure used to optimize a building depends on the validity of the performance index in describing the optimal performance of the building. Thus, additional research is needed to validate the performance index proposed in this study as a measure of an occupant's subjective response to indoor environmental conditions relative to energy consumption costs.

2. Although the optimization results for the ERH scenarios serve as a "yardstick" for the comparison of other control strategies in similar structures, additional

research is necessary to determine the practical aspects of implementing the optimization procedure into an actual optimal control system.

3. The procedures derived in this study were applied to a limited class of building systems. These procedures may have a greater potential for improving the performance of more complex building systems. Thus, future studies should be directed towards the application of these procedures to other types of systems to determine their effectiveness in reducing energy consumption and improving indoor environmental quality.

REFERENCES

1. Billington, N. S.; and Roberts, B. M. Building Services Engineering: A Review of Its Development. New York: Pergamon Press, 1982.

2. Department of Energy. Final Report. "Emergency Building Temperature Restrictions." Federal Register 44, no. 130, 5 July 1979, 39354-39368.

3. Woods, J. E. "Do Buildings Make You Sick?" Presented at the Third Canadian Building Congress, Victoria, British Columbia, Canada, October 18-20, 1982.

4. ANSI/ASHRAE Standard 55-1981: Thermal Environmental Conditions for Human Occupancy. Atlanta: American Society of Heating, Refrigerating, and Air-Conditioning Engineers, 1981.

5. Houghten, F. C.; and Yagloglou, C. P. "Determining Lines of Equal Comfort." ASHVE Transactions 29 (1923): 163-176.

6. Bedford, T.; and Warner, C. G. "The Globe Thermometer in Studies of Heating and Ventilating." Journal of Hygiene 34 (1934): 458-473.

7. American Society of Heating, Refrigerating and Air-Conditioning Engineers. ASHRAE Handbook: 1981 Fundamentals. Atlanta: American Society of Heating, Refrigerating and Air-Conditioning Engineers, 1981.

8. Belding, H. S.; and Hatch, T. F. "Index for Evaluating Heat Stress in Terms of Resulting Physiological Strains." Heating, Piping and Air Conditioning 27 (August 1955): 129-136.

9. Yaglou, C. P.; and Minard, D. "Control of Heat Casualties at Military Centers." AMA Archives of Industrial Health 16 (October 1957): 302-316.

10. Siple, P. A.; and Passel, C. F. "Measurements of Dry Atmospheric Cooling in Subfreezing Temperatures." Proceedings of the American Philosphical Society 89 (1945): 177-199.

11. Yaglou, C. P. "A Method for Improving the Effective Temperature Indices." ASHVE Transactions 53 (1947): 307-326.

12. Rohles, F. H.; and Nevins, R. G. "The Nature of Thermal Comfort for Sedentary Man." ASHRAE Transactions 77 (part 1)(1971): 239-246.

13. Fanger, P. O. Thermal Comfort: Analysis and Applications in Environmental Engineering. New York: McGraw-Hill Book Company, 1970.

14. Gagge, A. P.; Stolwijk, J. A. J.; and Nishi, Y. "An Effective Temperature Scale Based on a Simple Model of Human Physiological Regulatory Response." ASHRAE Transactions 77 (part 1)(1971): 247-262.

15. Sprague, C. H.; Jai, R. B.; Nevins, R. G.; and Azer, N. Z. "The Prediction of Thermal Sensation for Man in Moderate Thermal Environments via a Simple Thermoregulatory Model." ASHRAE Transactions 80 (part 1)(1974): 130-146.

16. Azer, N. Z.; and Hsu, S. "The Prediction of Thermal Sensation from a Simple Model of Human Physiological Regulatory Response." ASHRAE Transactions 83 (part 1)(1977): 88-102.

17. Berglund, L. "Mathematical Models for Predicting the Thermal Comfort Response of Building Occupants." ASHRAE Transactions 84 (part 1)(1978): 735-749.

18. Gagge, A. P.; Nishi, Y,; and Gonzalez, R. R. "Standard Effective Temperature." Proceedings of the Symposium on Thermal Comfort and Moderate Heat Stress. International Council for Build Research, Studies and Documentation (CIB) Commission W45 (Human requirements). London: Great Britain Building Research Establishment. Department of the Environment, 1972.

19. McIntyre, D. A. "The Effect of Air Movement on Thermal Comfort and Sensation." In Indoor Climate, pp. 541-560. Edited by P. O. Fanger and O. Valbjorn. Horsholm, Denmark: Danish Building Research Institute, 1978.

20. Fanger, P. O.; Banhidi, L.; Olesen, B. W.; and Langkilde, G. "Comfort Limits for Heated Ceilings." ASHRAE Transactions 86 (part 2)(1980): 141-156.

21. Nevins, R. G.; Gonzalez, R. R.; Nishi, Y.; and Gagge, A. P. "Effect of Changes in Ambient Temperature and Level of Humidity on Comfort and Thermal Sensations." ASHRAE Transactions 81 (part 2)(1975): 169-181.

22. Rohles, F. H.; Bennett, C. A.; and Milliken, G. A. "The Effects of Lighting, Color, and Room Decor on Thermal Comfort." ASHRAE Transactions 87 (part 2)(1981): 511-527.

23. Carlton-Foss, J. A.; and Rohles, F. H. "Personality Factors in Thermal Acceptability and Comfort." ASHRAE Transactions 88 (part 2)(1982): 776-790.

24. Woods, J. E.; Winakor, G.; Maldonado, E.; and Kipp, S. "Subjective and Objective Evaluation of a CO_2-Control Variable Ventilation System." ASHRAE Transactions 88 (part 1)(1982): 1385-1408.

25. Hayter, R. B. "Defining Thermal Acceptability in Structures Passively Heated by Solar Energy." ASHRAE Transactions 88 (part 1)(1982): 1043-1047.

26. Carroll, J. A. "An Index to Quantify Thermal Comfort in Residential Buildings." ASHRAE Transactions 87 (part 1)(1981): 566-576.

27. ASHRAE Standard 62-1981: Ventilation for Acceptable Indoor Air Quality. Atlanta: American Society of Heating, Refrigerating and Air-Conditioning Engineers, 1981.

28. Szokolay, S. V. "Energy, Building and the User." In Building Energy Management: Transitions in Technologies and Policies, pp. 1-11. Edited by J. E. Woods, R. E. Welch, A. P. Faist, and E. O. Fernandes. Ames, Iowa: Iowa State University Research Foundation, Inc., 1983.

29. Nuckolls, J. L. Interior Lighting for Environmental Designers. New York: John Wiley & Sons, 1976.

30. Stephenson, D. G.; and Mitalas, G. P. "Calculation of Heat Conduction Transfer Functions for Multi-Layer Slabs." ASHRAE Transactions 77 (part 2)(1971): 117-126.

31. Kusuda, T. "Thermal Response Factors for Multi-Layer Structures of Various Heat Conduction Systems." ASHRAE Transactions 75 (part 1)(1969): 246-271.

32. Kuehn, T. H.; and Maldonado, E. A. B. "A Finite Difference Transient Heat Conduction Program for Studying the Thermal Performance of Composite Building Envelopes." In Building Energy Management: Conventional and Solar Approaches, pp. 265-276. Edited by E. O. Fernandes, J. E. Woods, and A. P. Faist. New York: Pergamon Press, 1981.

33. Mehta, D. P.; and Woods, J. E. "An Experimental Validation of a Rational Model for Dynamic Responses of Buildings." ASHRAE Transactions 86 (part 2)(1980): 497-520.

34. Yi, J. "State-Space Method for the Calculation of Air-Conditioning Loads and the Simulation of Thermal Behavior of the Room." ASHRAE Transactions 88 (part 2)(1982): 122-141.

35. Sinden, F. W. "Multi-Chamber Theory of Air Infiltration." Building and Environment 13 (1978): 21-28.

36. Janssen, J. E. "Application of Building Thermal-Resistance Measurement." ASHRAE Transactions 88 (part 1)(1982): 713-731.

37. Schumann, R. "Digital Parameter-Adaptive Control of an Air-conditioning Plant." Automatica 18 (September 1982): 569-575.

38. Strejc, Vladimir. "Trends in Identification." Automatica 17 (1981): 7-21.

39. Sage, A. P.; and Melsa, J. L. System Identification. New York: Academic Press, 1971.

40. Strejc, V. "Least Squares Parameter Estimation." Automatica 16 (September 1980): 535-550.

41. Anderson, T. W. An Introduction to Multivariate Statistical Analysis. New York: John Wiley & Sons, 1958.

42. Deutsch, R. Estimation Theory. Englewood Cliffs, N. J.: Prentice-Hall, 1965.

43. Eykhoff, P. "Process Parameter and State Estimation." Automatica 4 (1968): 205-233.

44. Young, P. C. "An Instrumental Variable Method for Real Time Identification of a Noisy Process." Automatica 6, (1970): 271-287.

45. Davies, W. D. T. System Identification for Self-Adaptive Control. London: Wiley-Interscience, 1970.

46. Eykhoff, P. System Identification: Parameter and State Estimation. London: John Wiley & Sons, 1974.

47. Graupe, D. Identification of Systems. New York: Van Nostrand, 1972.

48. Mendel, J. M. Discrete Techniques of Parameter Estimation. New York: Marcel Dekker, 1973.

49. Benton, R. "The Impact of Thermostat Performance on Energy Consumption and Occupant Comfort in Residential Electric Heating Systems." ASHRAE Transactions 88 (part 1)(1982): 1029-1041.

50. Stoecker, W. F.; Crawford, R. R.; Ikeda, S.; Dolan, W. H.; and Leverenz, D. J. "Reducing the Peaks of Internal Air-Conditioning Loads by Use of Temperature Swings." ASHRAE Transactions 87 (part 2)(1981): 599-608.

51. Bloomfield, D. P.; and Fisk, D. J. "The Optimisation of Intermittent Heating." Building and Environment 12 (1977): 43-55.

52. Backus, A. O. "Energy Savings through Improved Control of Heat Pump Setback." ASHRAE Transactions 88 (part 1)(1982): 467-478.

53. Benton, R. "Heat Pump Setback: Computer Prediction and Field Test Verification of Energy Savings with Improved Controls." ASHRAE Journal 24 (December 1982): 23-29.

54. Kaya, A. "Optimum Control of HVAC System to Save Energy." In Vol. 6: Electrical Power Systems, pp. 3231-3240. In Control Science and Technology for the Progress of Society. 7 vols. Edited by H. Akashi. Oxford: Pergamon Press, 1982.

55. Kaya, A. "Modeling of an Environmental Space for Optimum Control of Energy Use." In Vol. 1, pp. 327-334. In A Link between Science and Applications of Automatic Control. 4 vols. Edited by A. Niemi. Oxford: Pergamon Press, 1979.

56. Kaya, A.; Chen, C. S.; Raina, S.; and Alexander, S. J. "Optimum Control Policies to Minimize Energy Use in HVAC Systems." ASHRAE Transactions 88 (part 2)(1982): 235-248.

57. Crawford, R. R.; and Woods, J. E. "Optimal Control of Residential Heating Systems." In Building Energy Management: Transitions in Technologies and Policies, pp. 4.35.1-4.35.12. Edited by J. E. Woods, R. E. Welch, A. P. Faist, and E. O. Fernandes. Ames, Iowa: Iowa State University Research Foundation, Inc., 1983.

58. Stoecker, W. F. Design of Thermal Systems. New York: McGraw-Hill Book Company, 1971.

59. Ozisik, M. N. Heat Conduction. New York: John Wiley & Sons, 1980.

60. Woods, J. E. "Climatological Effects on Thermal Comfort and Energy Utilization in Residences and Offices." In Proceedings of the 7th International Biometeorological Congress, pp. 95-105. College Park, Maryland, 1975.

61. Wyon, D. P.; Kok, R,; Lewis, M. T.; and Meese, G. B. "Combined Noise and Heat Stress Effects on Human Performance." In Indoor Climate, pp. 857-881. Edited by P. O. Fanger and O. Valbjorn. Horsholm, Denmark: Danish Building Research Institute, 1978.

62. Franklin, G. F.; and Powell, J. D. Digital Control of Dynamic Systems. Reading, Mass.: Addison-Wesley Publishing Company, 1980.

63. Sage, A. P.; and White, C. C. Optimum Systems Control. 2nd ed. Englewood Cliffs, N. J.: Prentice-Hall, Inc., 1977.

64. Stuck, J. E.; and Woods, J. E. "The Heating to Cooling Load Ratio: An Objective Function for Optimizing Heat Pump Performance." Presented at the 5th Annual Heat Pump Technology Conference, Oklahoma State University, Stillwater, Oklahoma, April 14-15, 1980.

65. Maldonado, E. A. B. "A Method to Characterize Air Exchange in Residences for Evaluation of Indoor Air Quality." Unpublished Ph.D. dissertation, Iowa State University, 1982.

66. Ott, L. An Introduction to Statistical Methods and Data Analysis. North Scituate, Mass.: Duxbury Press, 1977.

67. Chatfield, C. Statistics for Technology: A Course in Applied Statistics. 2nd. ed. London: Chapman and Hall, 1978.

68. Kirk, D. E. Optimal Control Theory: An Introduction. Englewood Cliffs, N. J.: Prentice-Hall, Inc., 1970.

APPENDIX A

Stepwise Procedure Used for the System Model Derivation

The details of the procedure used to derive the system model are described in this section. This procedure starts with one independent variable and sequentially adds additional variables after testing them for significance in reducing the model error.

A general linear model for predicting one dependent variable as a function of n independent variables can be expressed as follows.

$$y(k) = \mathbf{b}'\mathbf{x}_n(k) + e_n(k) \tag{90}$$

In this equation, y(k) is the variable which is to be predicted by the model. The vector $\mathbf{x}_n(k)$ contains as its elements, the n independent variables used in the model. These elements can be any arbitrary combinations of the independent variables used in the general system model equation (28), i.e., y(k-i), u(k-i), $w_j(k-i)$. Note that the time step associated with $\mathbf{x}(k)$ corresponds with the time step associated with the independent variable, y(k), rather than the independent variables' time steps. The vector $\mathbf{b}_n$ contains as its elements, the n parameters, a_i, b_i, and d_{ij} from equation (28), which correspond to the n independent variables in the vector $\mathbf{x}_n$. The final variable in equation

(90), $e_n(k)$, is the error resulting from the model prediction of y at the kth time step. The nomenclature for the equations used in this appendix does not necessarily correspond to the nomenclature used for the main part of this study.

A least squares regression procedure [46] can be used to calculate the model parameters, b_n, in terms of actual data values for y(k) and $x_n(k)$ over a time interval from k_i (assumed to be 1) to k_f by minimizing the sum of the squared error over the same time interval. This results in an equation for calculating b_n given by

$$b_r = W_n^{-1} z_n \tag{91}$$

where W_n and z_n are nxn and nx1 matrices, respectively, which can be calculated from the following equations.

$$W_n = \sum_{k=1}^{k_f} x_n(k) x_n'(k) \tag{92}$$

$$z_n = \sum_{k=1}^{k_f} y(k) x_n(k) \tag{93}$$

The above equations for calculating the model parameters requires that the inversion of the nxn matrix, W_n, which can be difficult and time consuming on a digital computer for

the larger values of n that may occur as more independent variable terms are added during the model development.

The model described by equations (91-93) can be rewritten to include one additional independent variable defined as x_{n+1} in the following manner.

$$\mathbf{b}_{n+1} = \mathbf{W}_{n+1}^{-1}\mathbf{z}_{n+1} \tag{94}$$

$$\mathbf{W}_{n+1} = \sum_{k=1}^{k_f} \mathbf{x}_{n+1}(k)\mathbf{x}'_{n+1}(k)$$

$$= \sum_{k=1}^{k_f} \left[\begin{array}{c|c} \mathbf{x}_n(k)\mathbf{x}'_n(k) & \mathbf{x}_n(k)x_{n+1}(k) \\ \hline \mathbf{x}_n'(k)x_{n+1}(k) & x_{n+1}(k)^2 \end{array}\right] \tag{95}$$

$$\mathbf{z}_{n+1} = \sum_{k=1}^{k_f} y(k)\mathbf{x}_{n+1}(k) = \sum_{k=1}^{k_f} \left[\begin{array}{c} y(k)\mathbf{x}_n(k) \\ \hline y(k)x_{n+1}(k) \end{array}\right] \tag{96}$$

The matrix, $\mathbf{W}_{n+1}$, can be rewritten as

$$\mathbf{W}_{n+1} = \left[\begin{array}{c|c} \mathbf{W}_n & \mathbf{g} \\ \hline \mathbf{g}' & h \end{array}\right] \tag{97}$$

where

$$g = \sum_{k=1}^{k_f} \mathbf{x}_n(k) x_{n+1}(k) \tag{98}$$

$$h = \sum_{k=1}^{k_f} x_{n+1}^2(k) \tag{99}$$

The inverse of this matrix can be written in a similar form as

$$W_{n+1}^{-1} = \left[\begin{array}{c|c} \mathbf{A} & \mathbf{d} \\ \hline \mathbf{d}' & c \end{array}\right] \tag{100}$$

Matrix algebra can be used to calculate **A**, **d**, and c as a function of W_n, g, and h as shown below.

$$c = (h - g'W_n^{-1}g)^{-1} \tag{101}$$

$$\mathbf{d} = - cW_n^{-1}g \tag{102}$$

$$\mathbf{A} = \mathbf{d}\mathbf{d}'c^{-1} + W_n^{-1} \tag{103}$$

The use of equations (100-103) to calculate the inverse of W_{n+1} eliminates the need for a matrix inversion algorithm if the inverse of W_n is known. Since this modeling process begins with only one independent variable (n = 1), matrix inversion procedures will not be required during the entire

modeling procedure. This feature is especially advantageous if the model is to be incorporated in a microprocessor-based, optimal control system.

The quantity used to test the significance of the added independent variable (x_{n+1}) is the "F-statistic" [66] defined as

$$F = \frac{SSE_n - SSE_{n+1}}{SSE_{n+1}/(k_f - n - 1)} \tag{104}$$

where

$$SSE_n = \sum_{k=1}^{k_f} y(k)^2 - b_n' z_n \tag{105}$$

and

$$SSE_{n+1} = \sum_{k=1}^{k_f} y(k)^2 - b_{n+1}' z_n \tag{106}$$

The null hypothesis used in this case is b_{n+1} is zero. If the calculated value of F from equation (104) is greater than the value of F given by the F-distribution for 1 and k_f-n-1 degrees of freedom and a predetermined significance level (p), the null hypothesis is rejected and x_{n+1} is added to the model. Otherwise the new independent variable is

omitted from the model. Each independent variable's statistical significance can be tested at any stage of the model development using the "t-statistic" [66]. This test may be useful since an independent variable that is significant when it is added to the model may not be significant when other variables are subsequently added. The t-statistic at any stage of the model development is defined for the ith independent variable as

$$t = \frac{b_{ni}(k_f-n)}{SSE_n W_n^{-1}(i,i)} \qquad (107)$$

If the absolute value of the calculated value for t is less than the tabulated value for t at a given significance level (p), then b_{ni} is not significantly different from zero and the ith independent variable is not statistically significant in the model development.

APPENDIX B

ERH System Model Results

The following figures compare the ERH system model, using the parameters from the 29-day model development, to the actual measured performance of the ERH for each of the contiguous days of data collection from January 21, 1983 (day 1) to February 18, 1983 (day 29). These graphs compare the measured and predicted system output variables and show the measured variables used as inputs for the model predictions. These variables are defined below.

outputs: T_a = indoor dry-bulb temperature (C)

T_g = indoor globe temperature (C)

inputs: T_o = outdoor dry-bulb temperature (C)

T_s = solar radiation (1 C = 20 W/m^2)

Q_h = electric furnace consumption (kW)

Q_l = electrical internal load (kW)

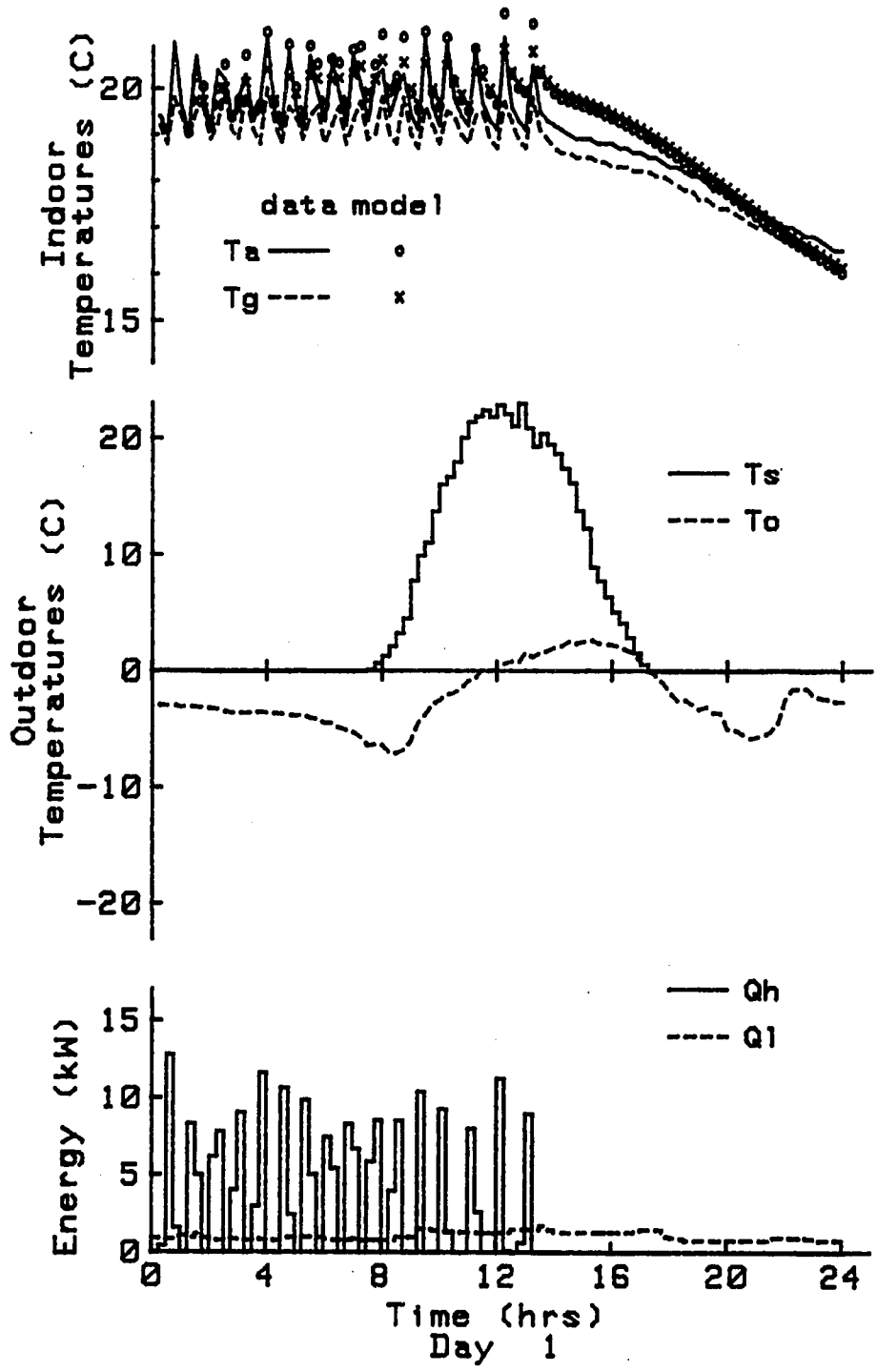
Indoor Temperatures (C)
20
15
data model
Ta
Tg
Outdoor Temperatures (C)
20
10
0
-10
-20
Ts
To
Energy (kW)
15
10
5
0
Qh
Ql
0
4
8
12
16
20
24
Time (hrs)
Day 1

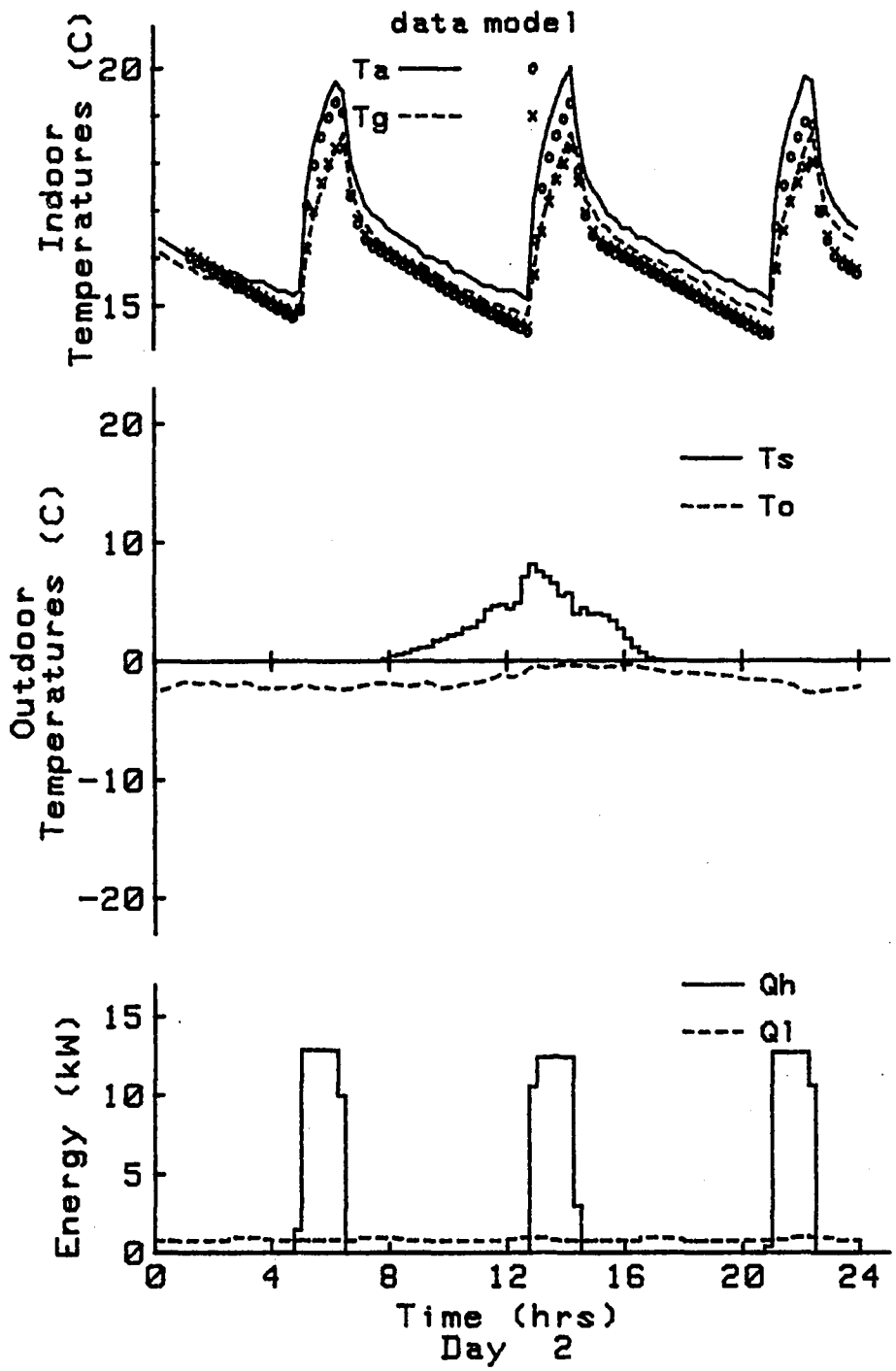
data model
Ta
Tg
Indoor Temperatures (C)
20
15
Ts
To
Outdoor Temperatures (C)
20
10
0
-10
-20
Qh
Ql
Energy (kW)
15
10
5
0
0
4
8
12
16
20
24
Time (hrs)
Day 2

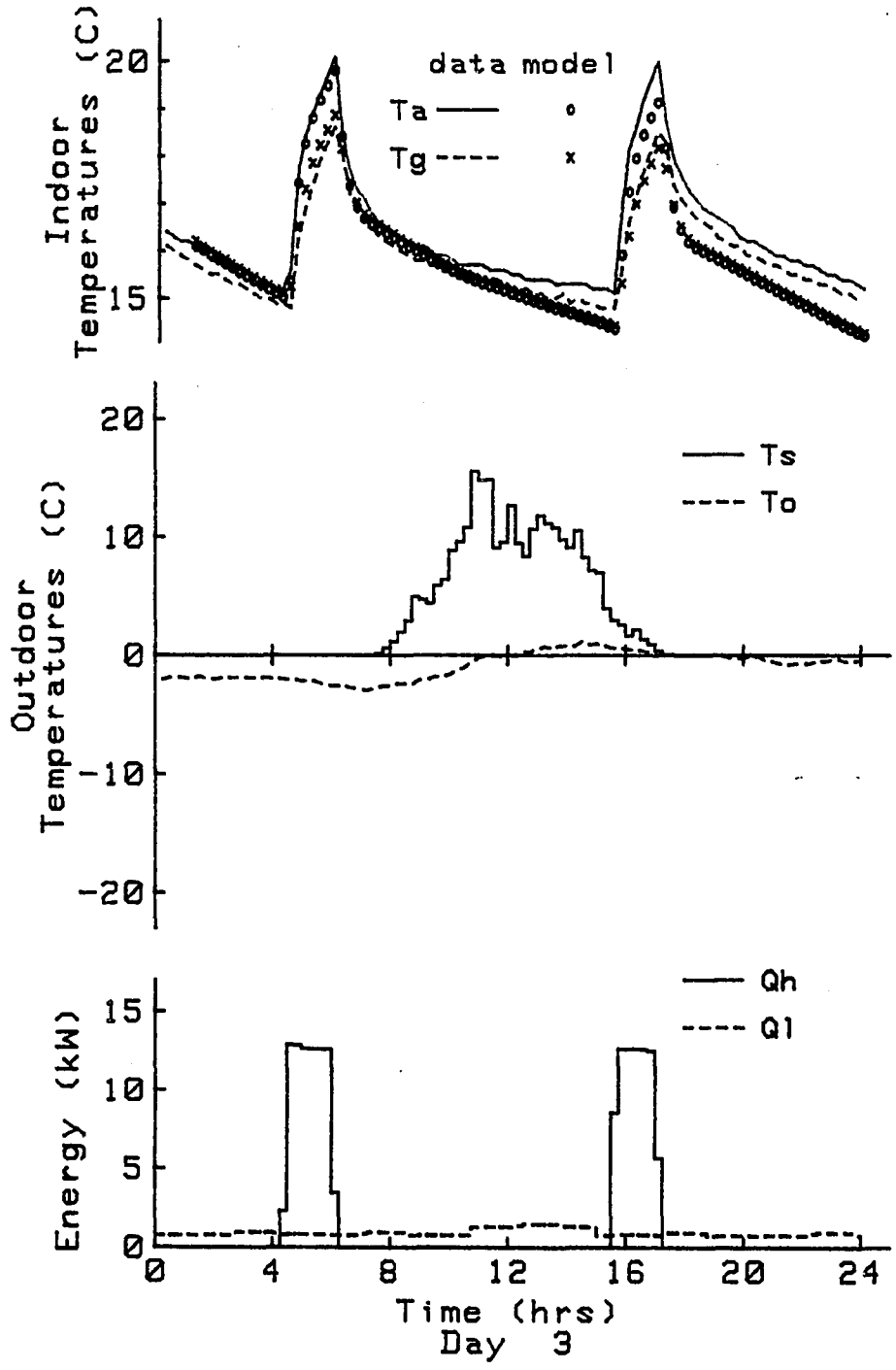
Indoor Temperatures (C)
20
15
data model
Ta
Tg
o
x
Outdoor Temperatures (C)
20
10
0
-10
-20
Ts
To
Energy (kW)
15
10
5
0
Qh
Ql
0
4
8
12
16
20
24
Time (hrs)
Day 3

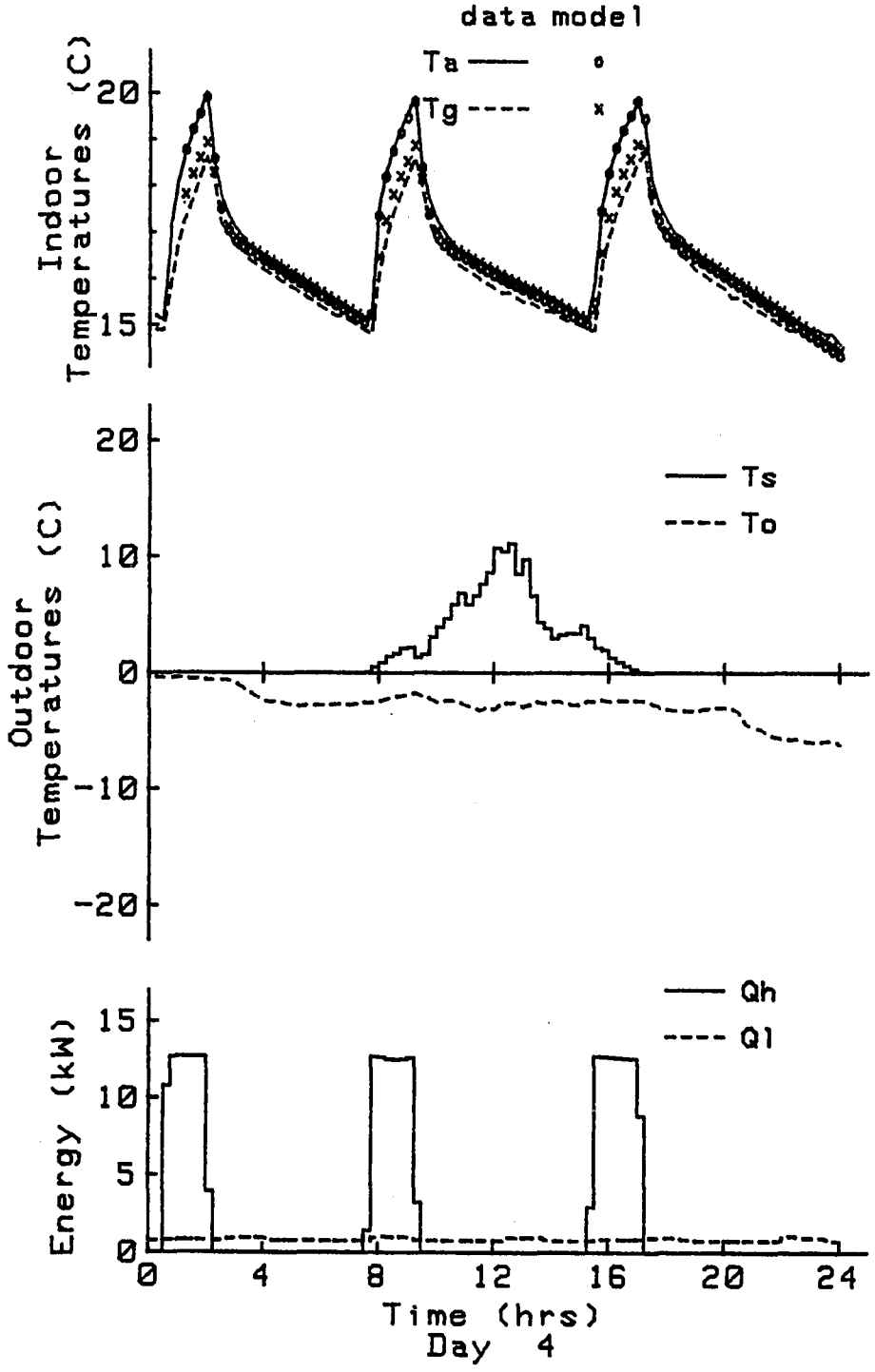
data model
Ta
Tg
Indoor Temperatures (C)
20
15
Ts
To
Outdoor Temperatures (C)
20
10
0
-10
-20
Qh
Ql
Energy (kW)
15
10
5
0
0
4
8
12
16
20
24
Time (hrs)
Day 4

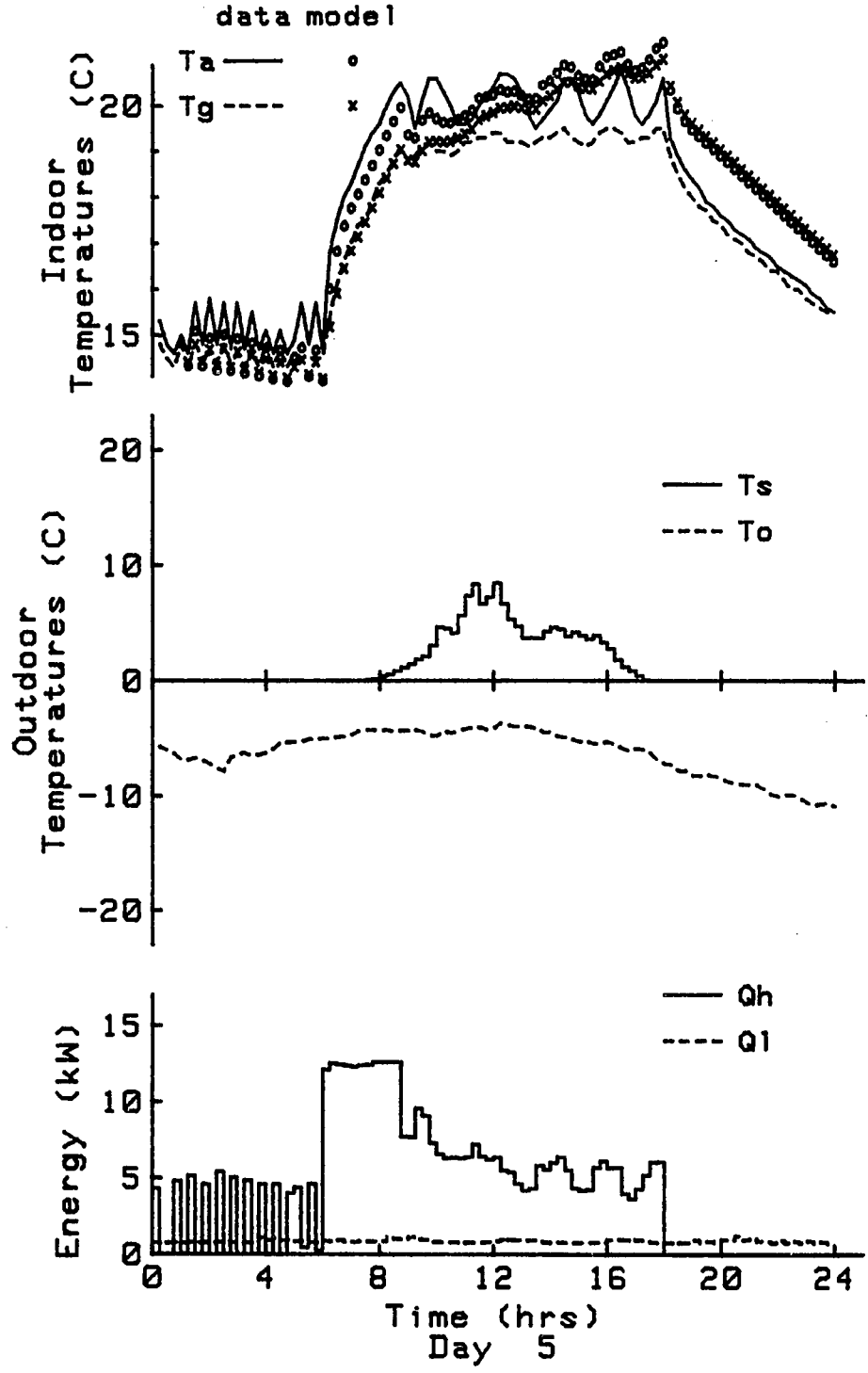
data model
Ta
Tg
Indoor Temperatures (C)
20
15
Ts
To
Outdoor Temperatures (C)
20
10
0
-10
-20
Qh
Ql
Energy (kW)
15
10
5
0
0
4
8
12
16
20
24
Time (hrs)
Day 5

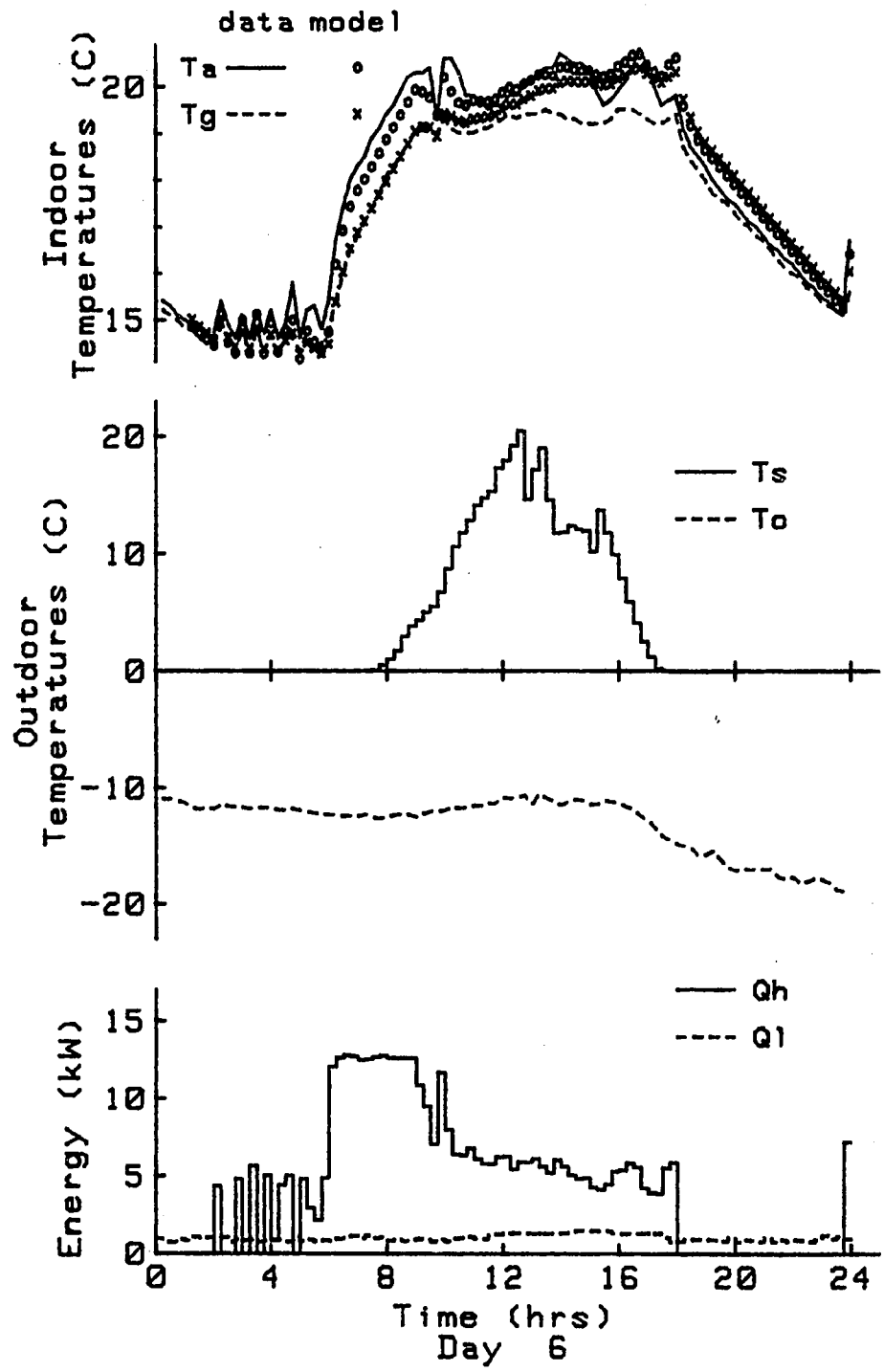
data model
Ta
Tg
Indoor Temperatures (C)
20
15
Ts
To
Outdoor Temperatures (C)
20
10
0
-10
-20
Qh
Ql
Energy (kW)
15
10
5
0
0
4
8
12
16
20
24
Time (hrs)
Day 6

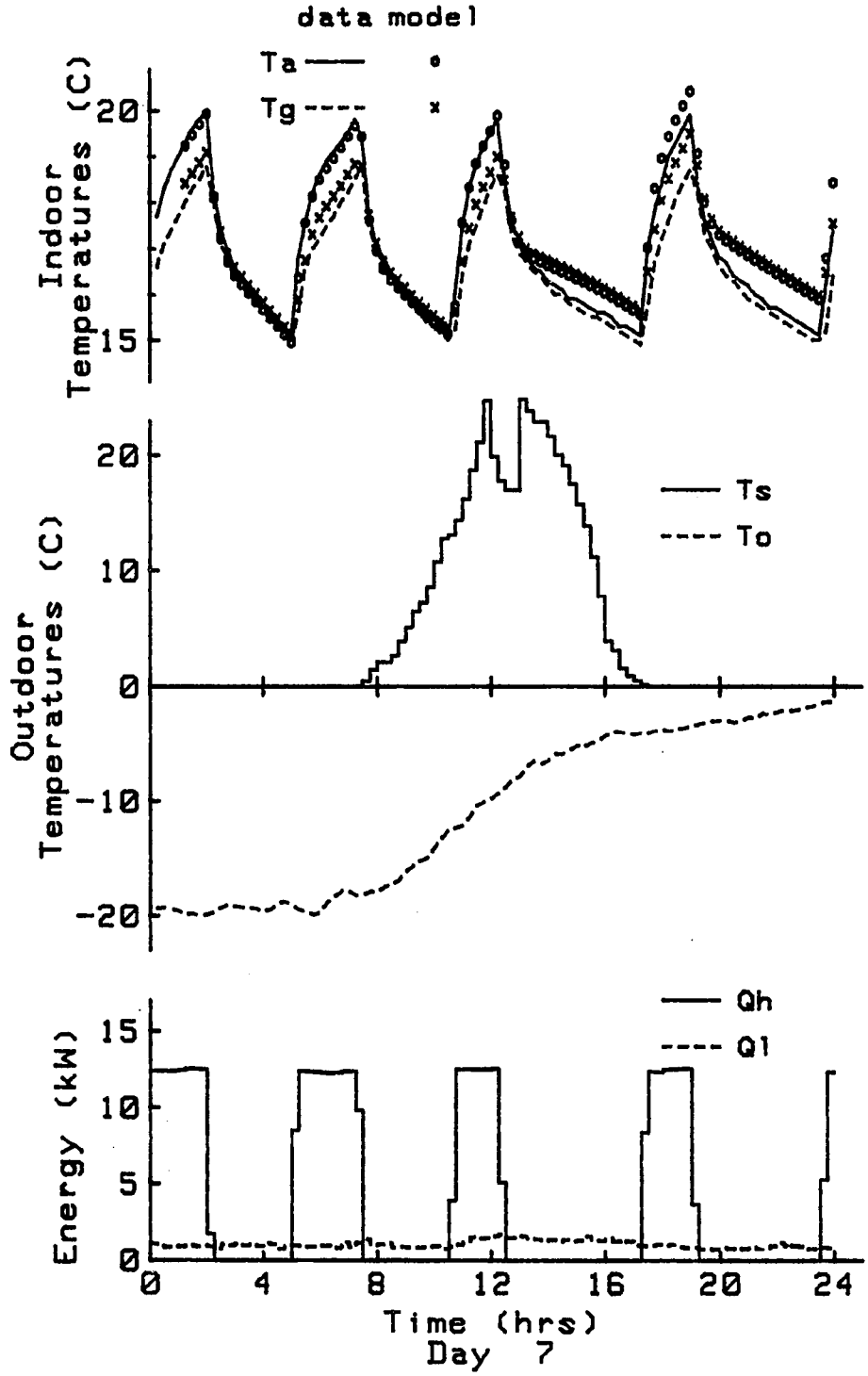
data model
Ta
Tg
Indoor Temperatures (C)
20
15
Ts
To
Outdoor Temperatures (C)
20
10
0
-10
-20
Qh
Ql
Energy (kW)
15
10
5
0
0
4
8
12
16
20
24
Time (hrs)
Day 7

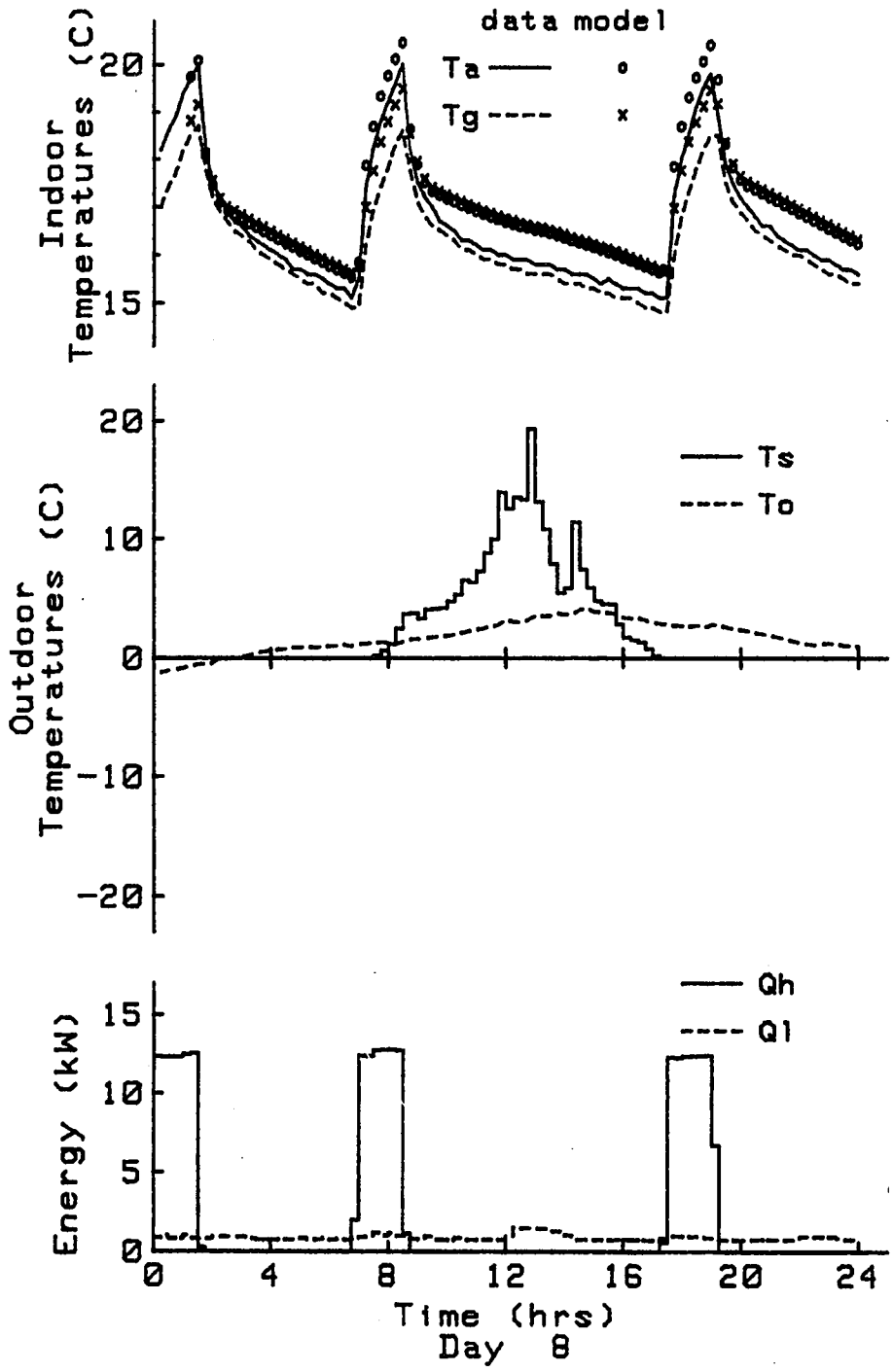
data model
Ta
Tg
Indoor Temperatures (C)
20
15
Ts
To
Outdoor Temperatures (C)
20
10
0
-10
-20
Qh
Ql
Energy (kW)
15
10
5
0
0
4
8
12
16
20
24
Time (hrs)
Day 8

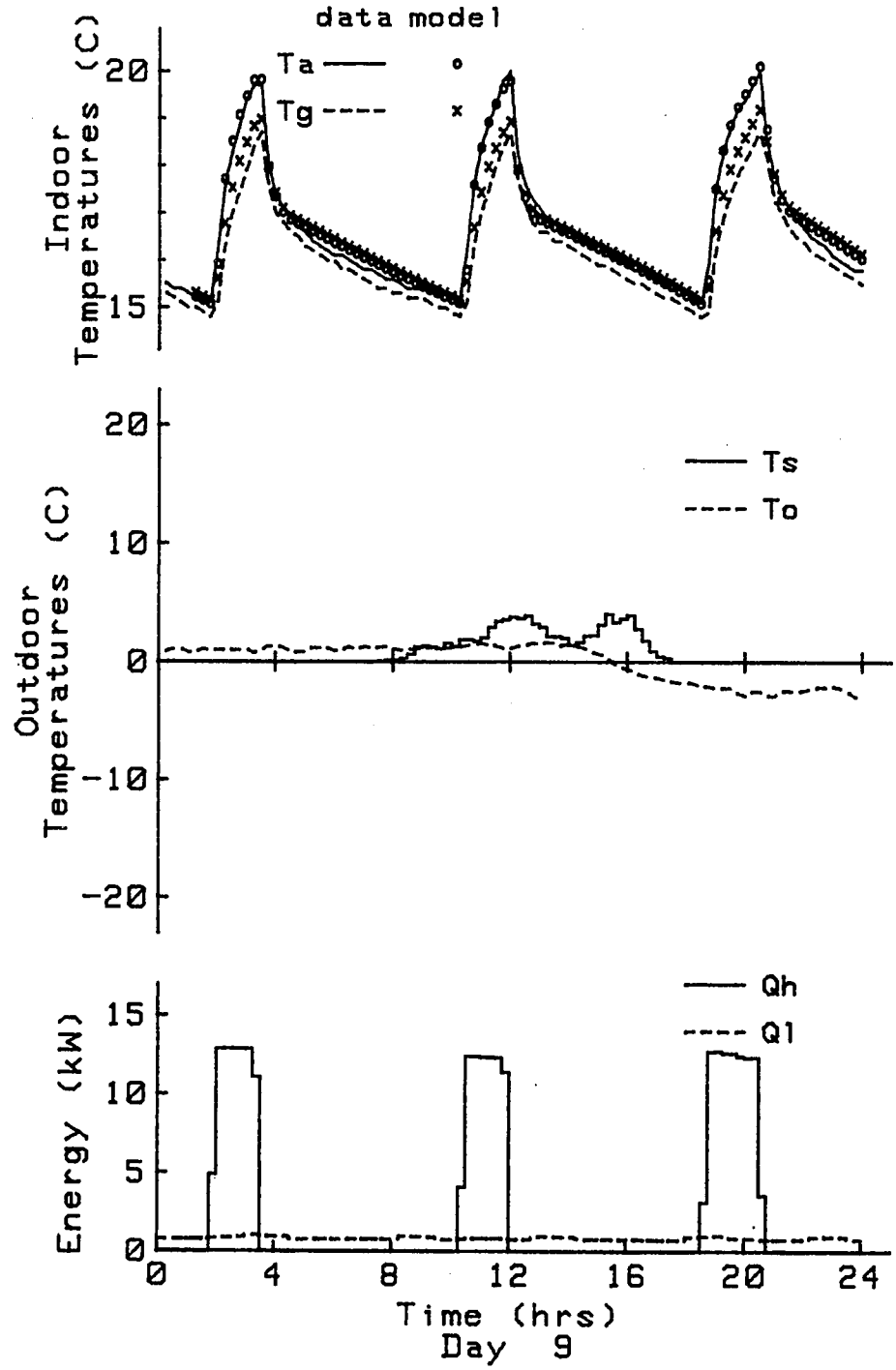
data model
Ta
Tg
Indoor Temperatures (C)
20
15
Ts
To
Outdoor Temperatures (C)
20
10
0
-10
-20
Qh
Q1
Energy (kW)
15
10
5
0
0
4
8
12
16
20
24
Time (hrs)
Day 9

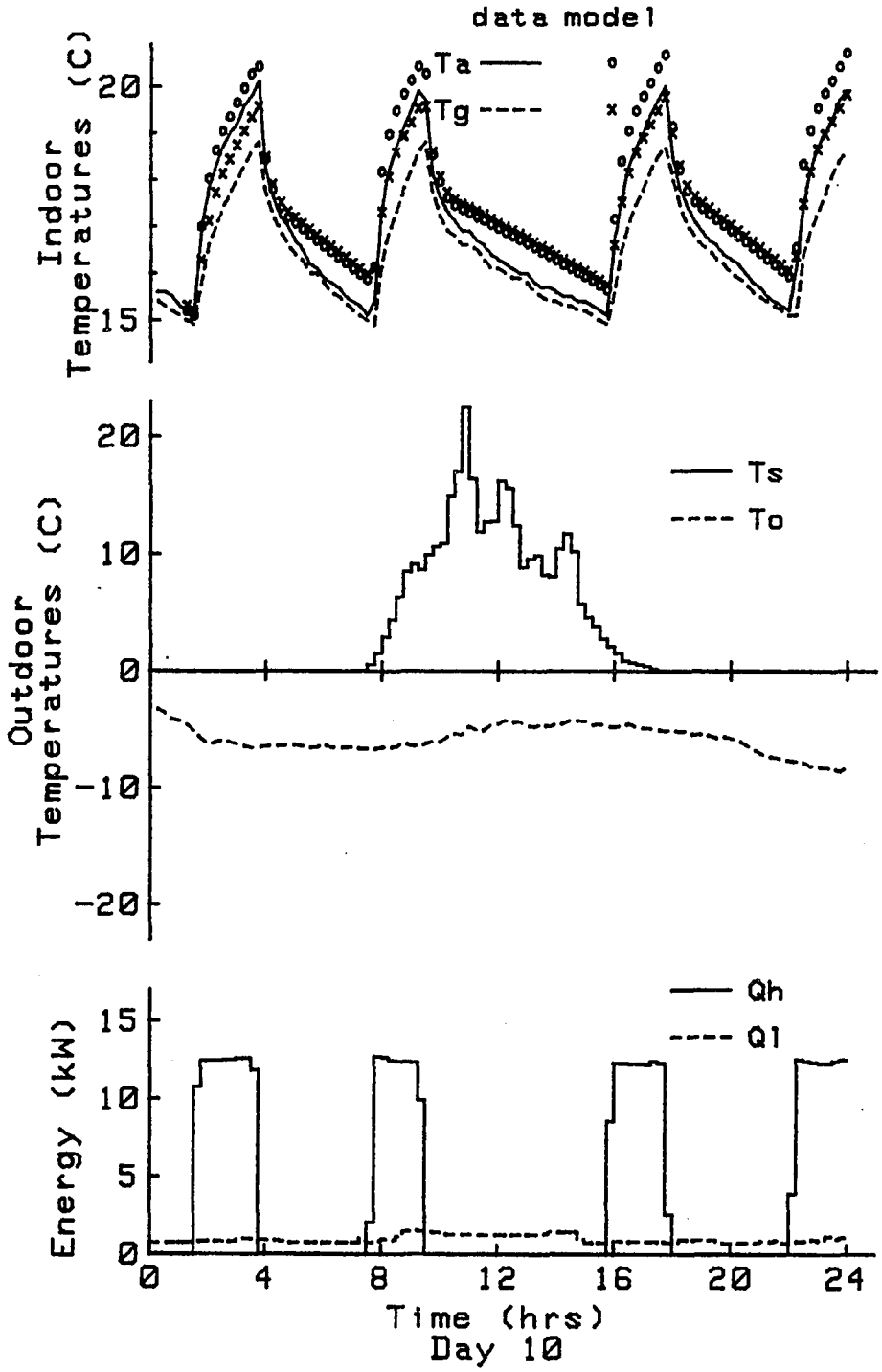
data model
Ta
Tg
Indoor Temperatures (C)
20
15
Ts
To
Outdoor Temperatures (C)
20
10
0
-10
-20
Qh
Ql
Energy (kW)
15
10
5
0
0
4
8
12
16
20
24
Time (hrs)
Day 10

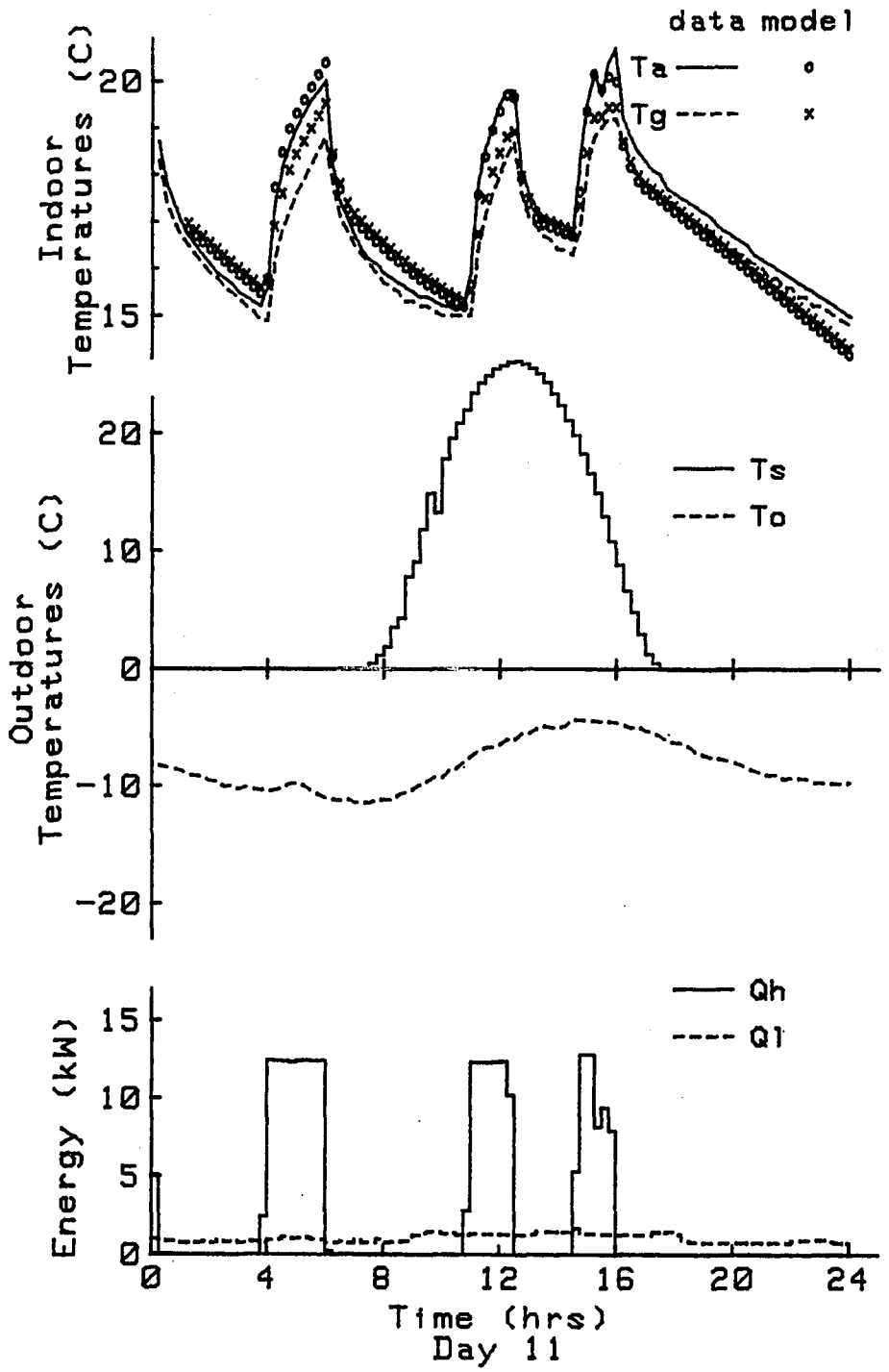
data model
Ta
Tg
Indoor Temperatures (C)
20
15
Ts
To
Outdoor Temperatures (C)
20
10
0
-10
-20
Qh
Ql
Energy (kW)
15
10
5
0
0
4
8
12
16
20
24
Time (hrs)
Day 11

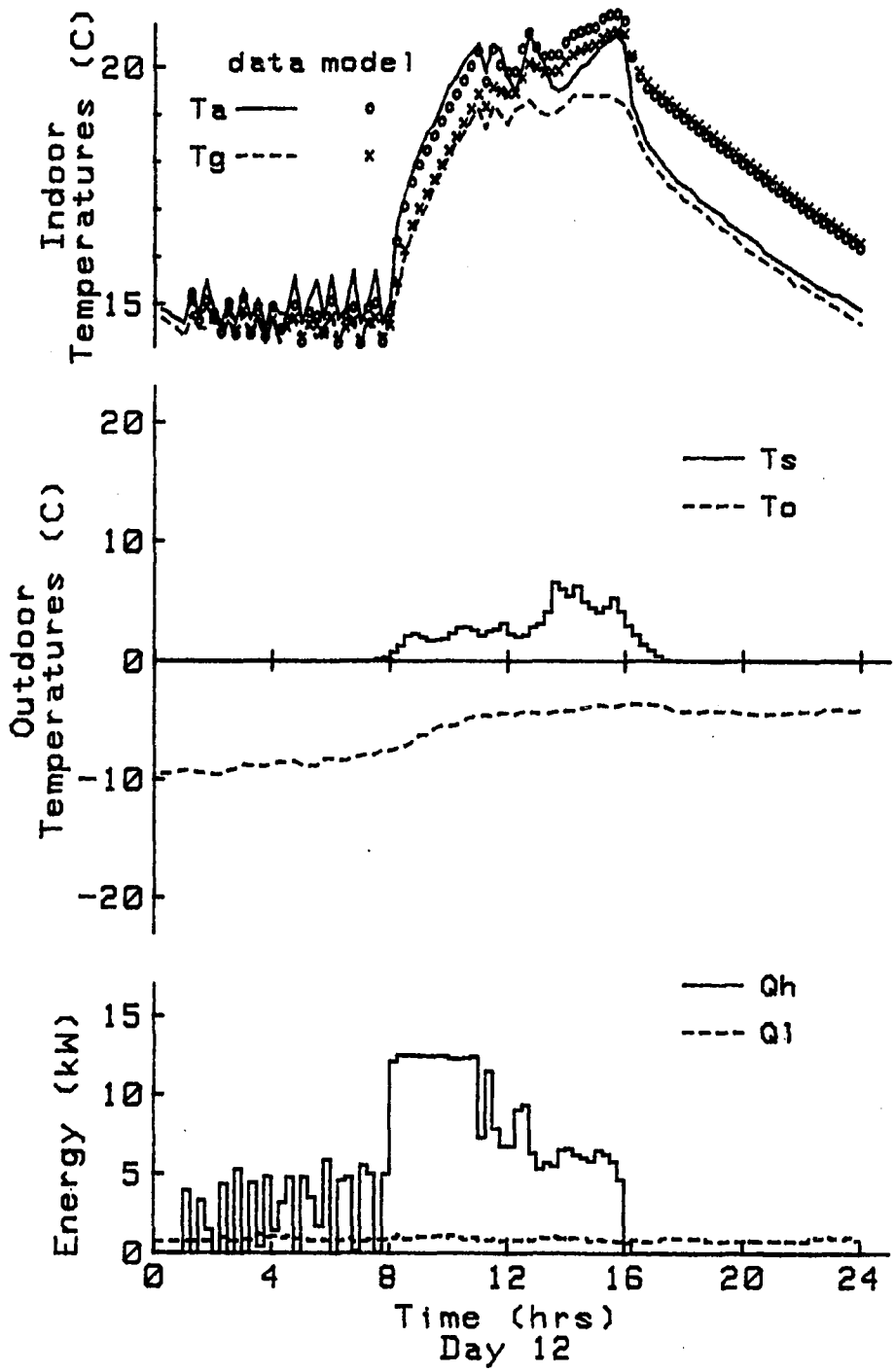
Indoor Temperatures (C)
20
15
data model
Ta
Tg
Outdoor Temperatures (C)
20
10
0
-10
-20
Ts
To
Energy (kW)
15
10
5
0
Qh
Ql
0
4
8
12
16
20
24
Time (hrs)
Day 12

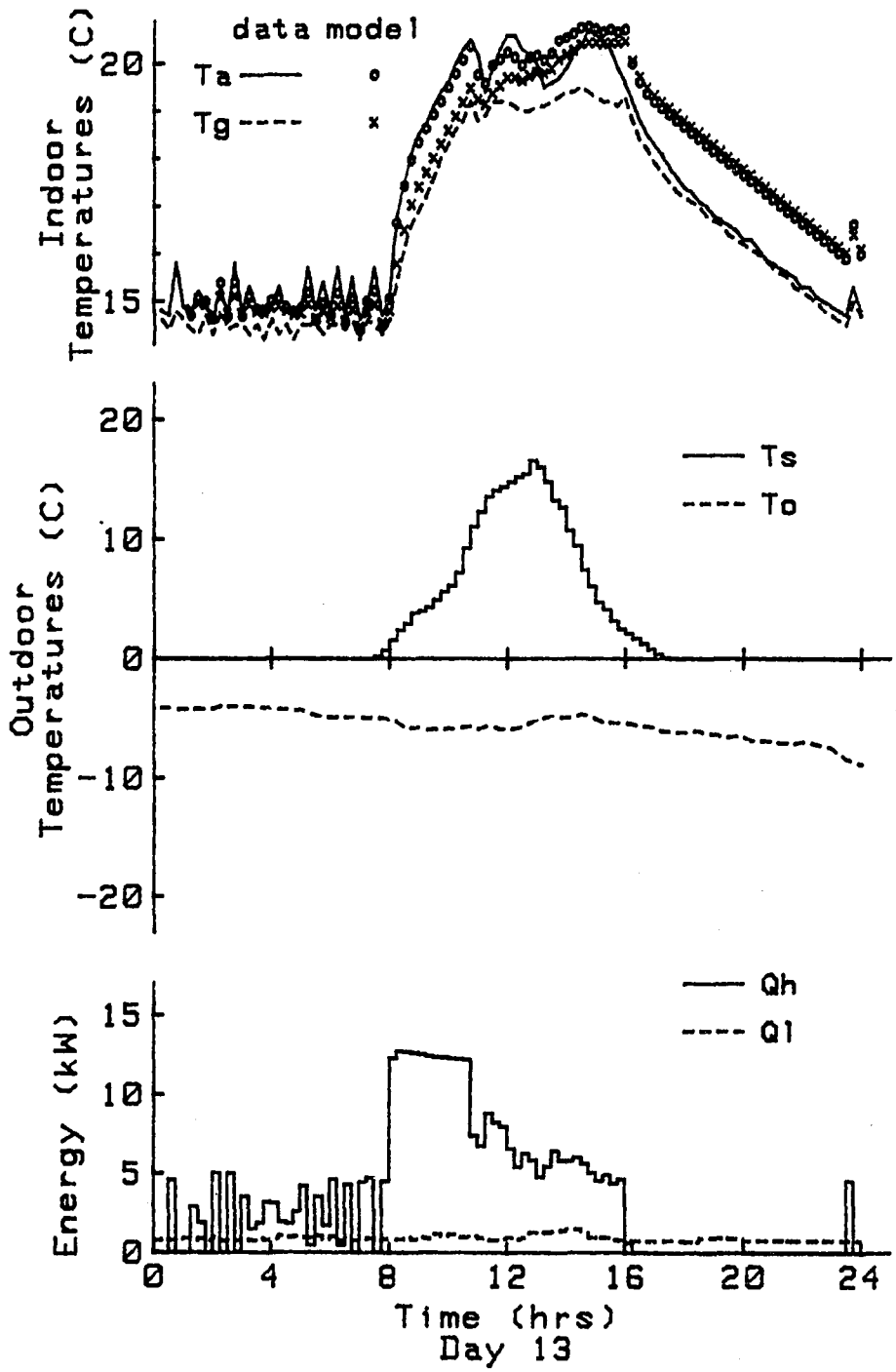
data model
Ta
Tg
Indoor Temperatures (C)
20
15
Ts
To
Outdoor Temperatures (C)
20
10
0
-10
-20
Qh
Ql
Energy (kW)
15
10
5
0
0
4
8
12
16
20
24
Time (hrs)
Day 13

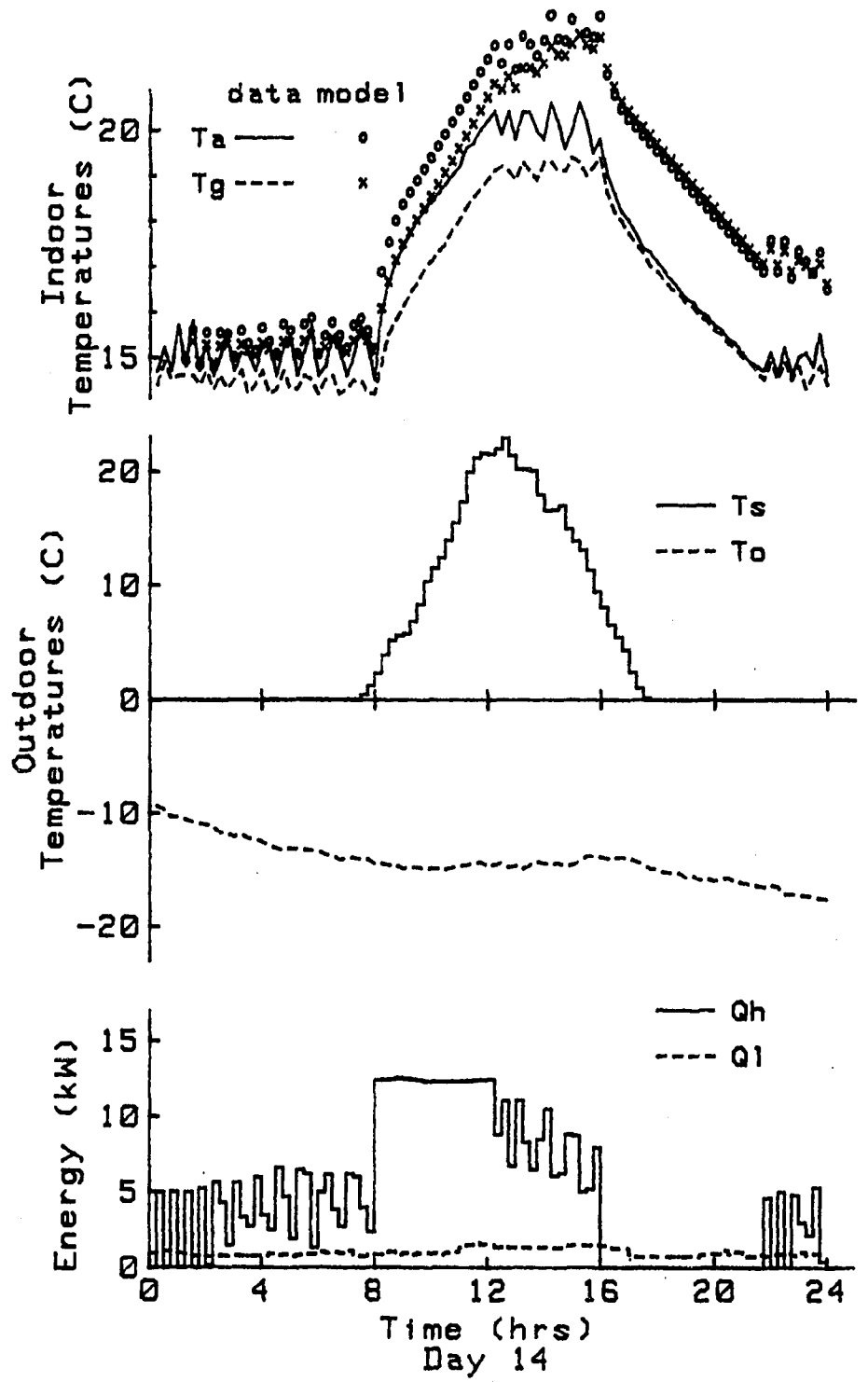
data model
Ta
Tg
Indoor Temperatures (C)
20
15
Ts
To
Outdoor Temperatures (C)
20
10
0
-10
-20
Qh
Q1
Energy (kW)
15
10
5
0
0
4
8
12
16
20
24
Time (hrs)
Day 14

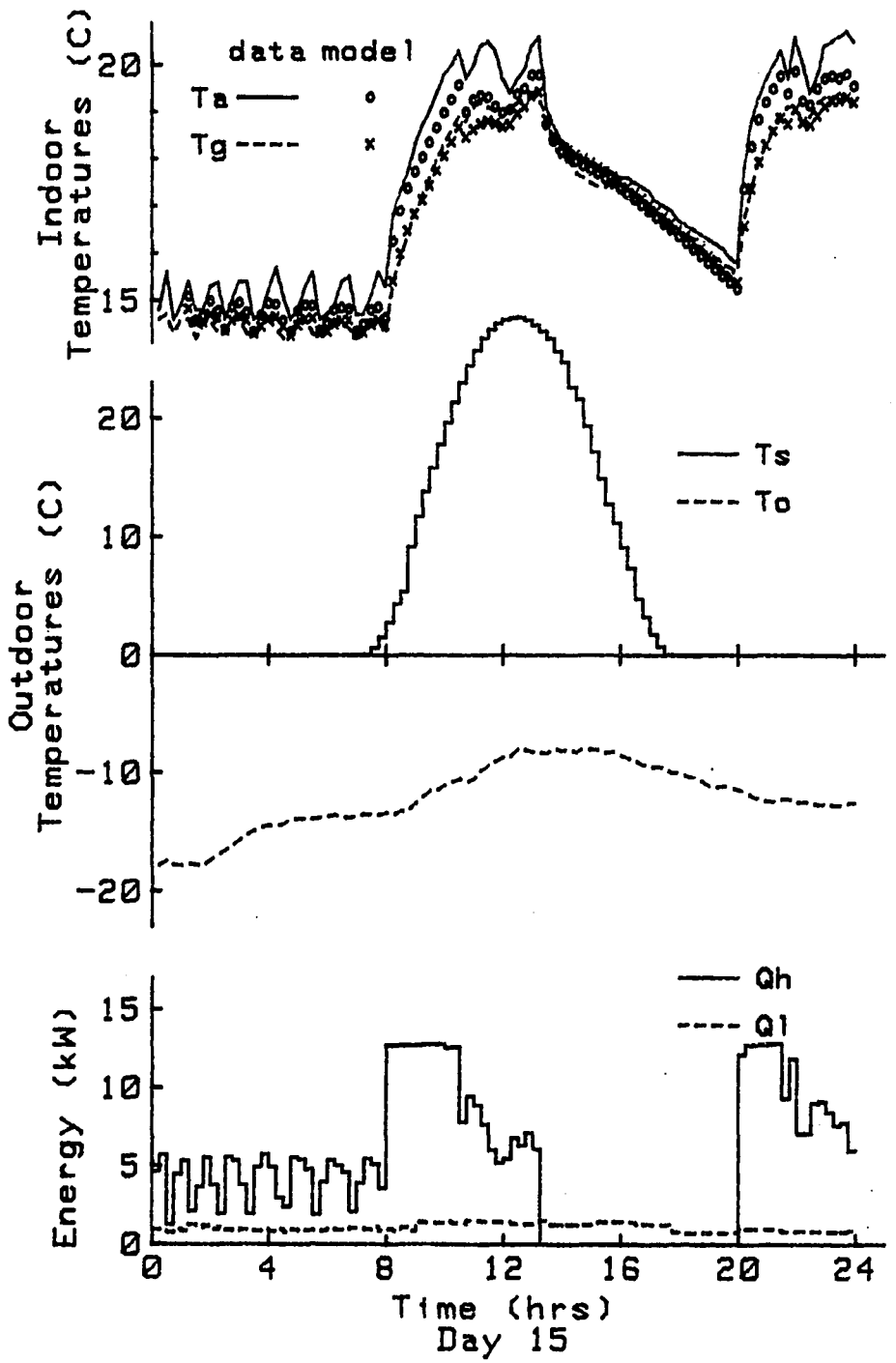
Indoor Temperatures (C)
data model
Ta
Tg
20
15
Outdoor Temperatures (C)
Ts
To
20
10
0
-10
-20
Energy (kW)
Qh
Ql
15
10
5
0
0
4
8
12
16
20
24
Time (hrs)
Day 15

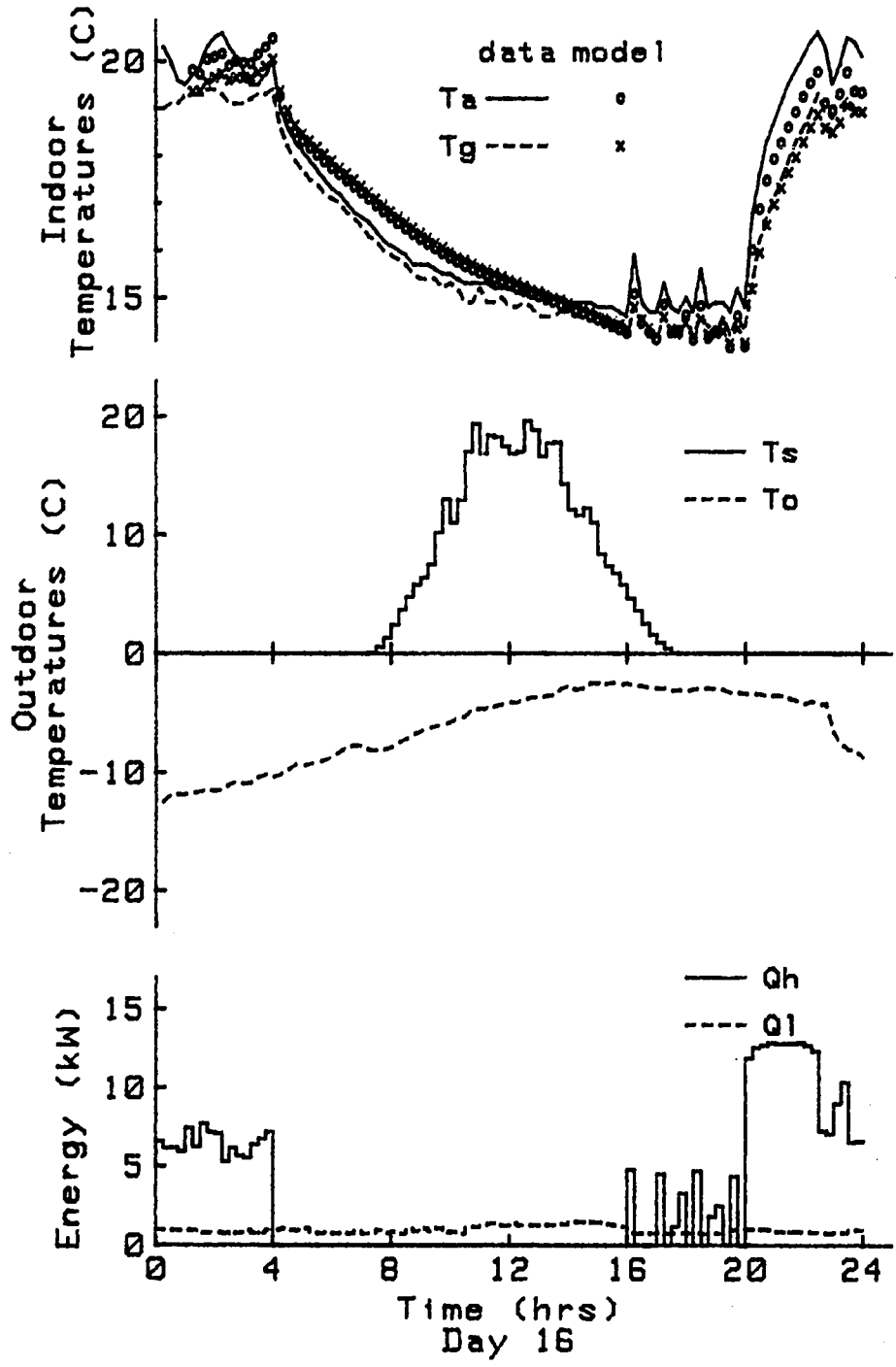
Indoor Temperatures (C)
20
15
data model
Ta
Tg
Outdoor Temperatures (C)
20
10
0
-10
-20
Ts
To
Energy (kW)
15
10
5
0
Qh
Ql
0
4
8
12
16
20
24
Time (hrs)
Day 16

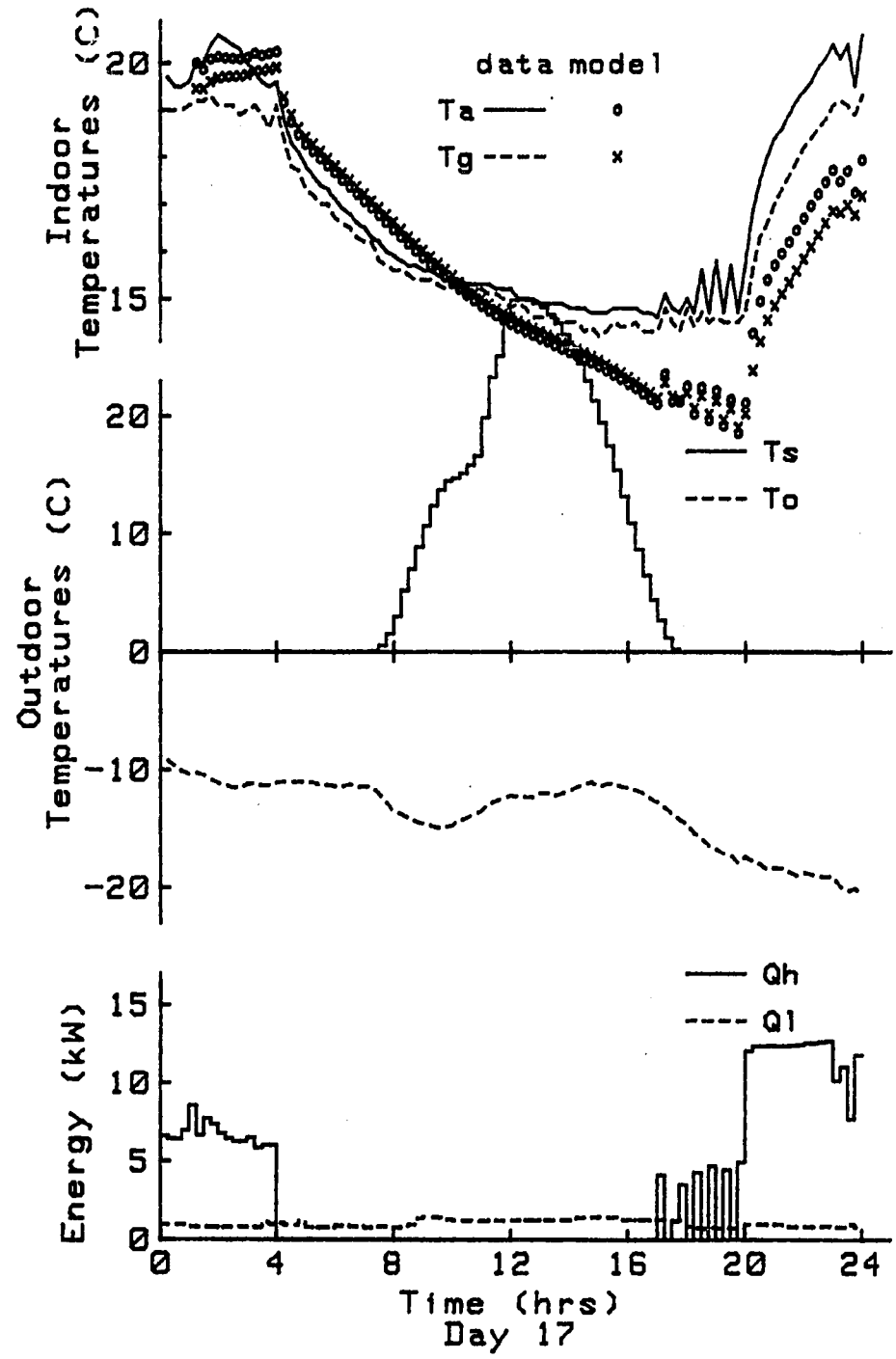
Indoor Temperatures (C)
20
15
data model
Ta
Tg
Outdoor Temperatures (C)
20
10
0
-10
-20
Ts
To
Energy (kW)
15
10
5
0
Qh
Ql
0
4
8
12
16
20
24
Time (hrs)
Day 17

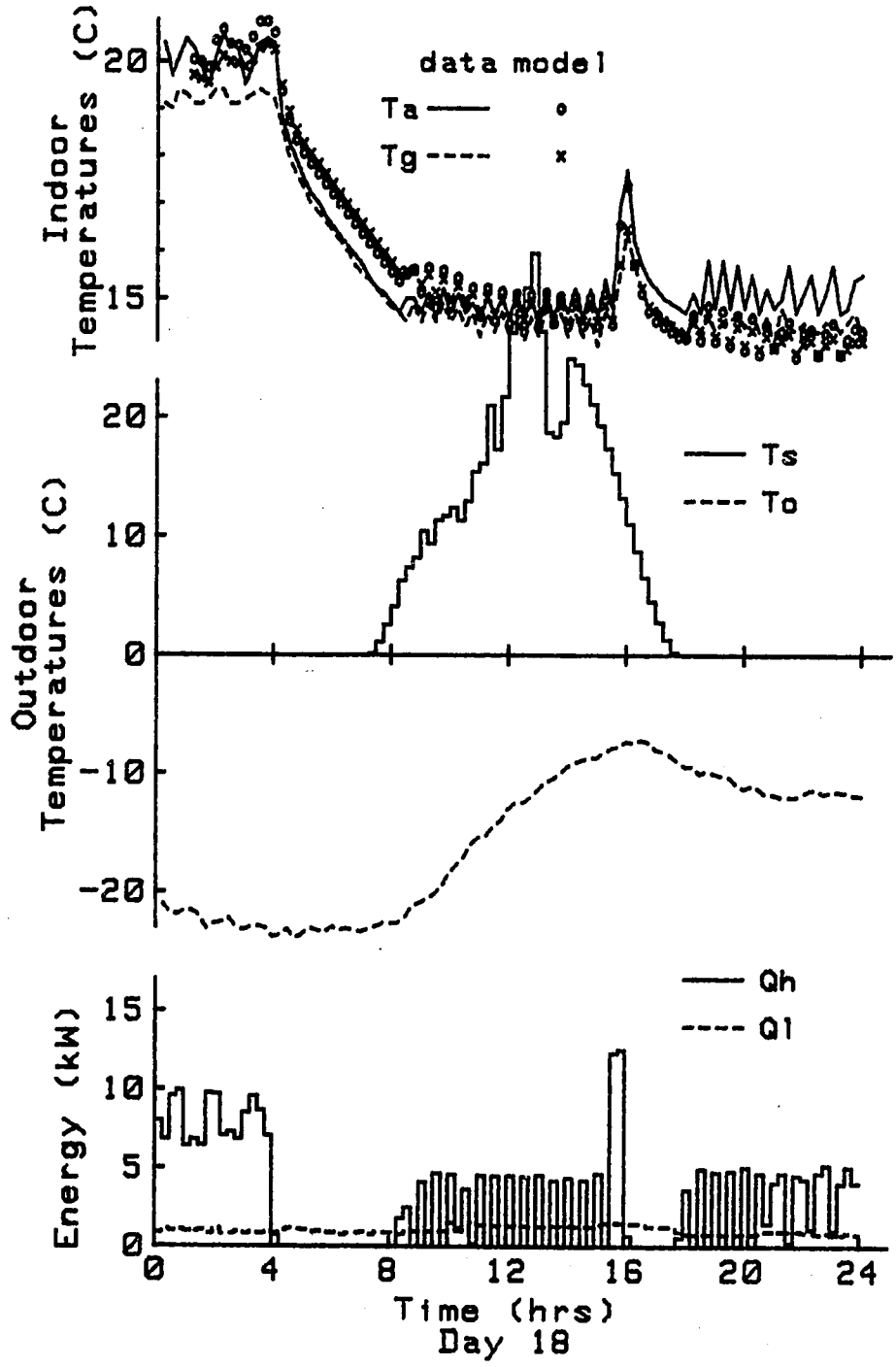
Indoor Temperatures (C)
20
15
data model
Ta
Tg
o
x
Outdoor Temperatures (C)
20
10
0
-10
-20
Ts
To
Energy (kW)
15
10
5
0
Qh
Ql
0
4
8
12
16
20
24
Time (hrs)
Day 18

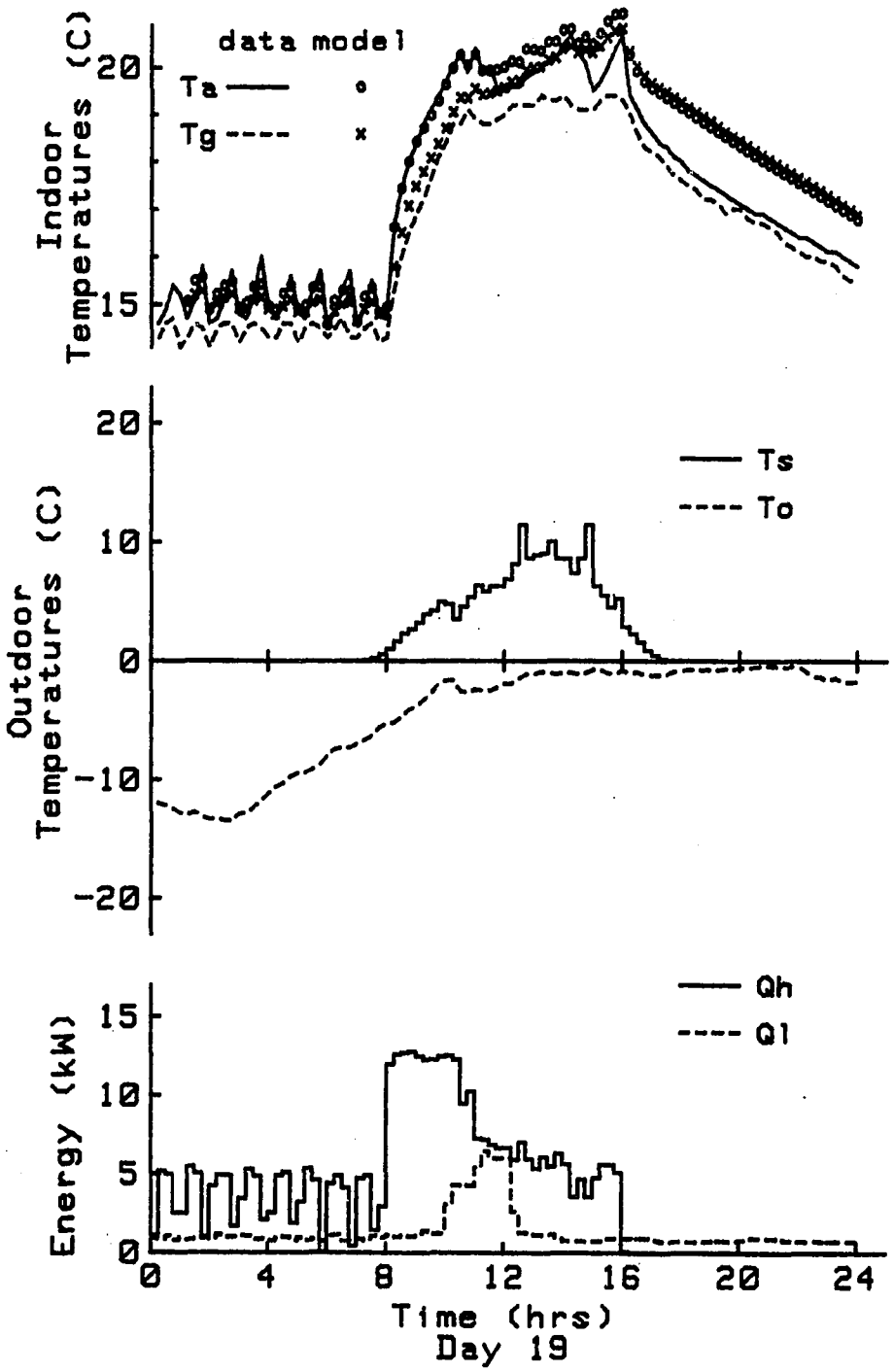
data model
Ta
Tg
Indoor Temperatures (C)
20
15
Ts
To
Outdoor Temperatures (C)
20
10
0
-10
-20
Qh
Ql
Energy (kW)
15
10
5
0
0
4
8
12
16
20
24
Time (hrs)
Day 19

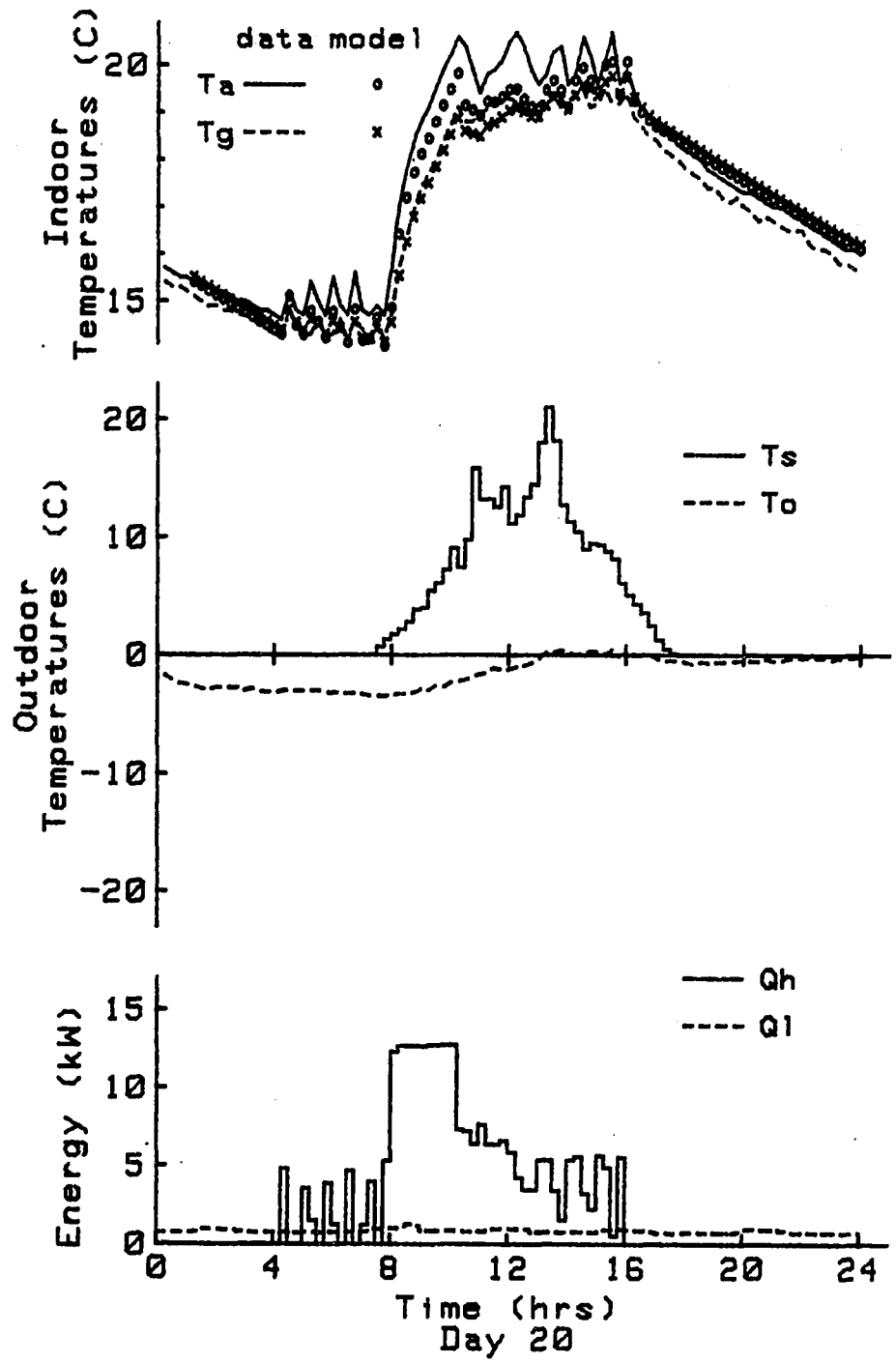
data model
Ta
Tg
Indoor Temperatures (C)
20
15
Ts
To
Outdoor Temperatures (C)
20
10
0
-10
-20
Qh
Ql
Energy (kW)
15
10
5
0
0
4
8
12
16
20
24
Time (hrs)
Day 20

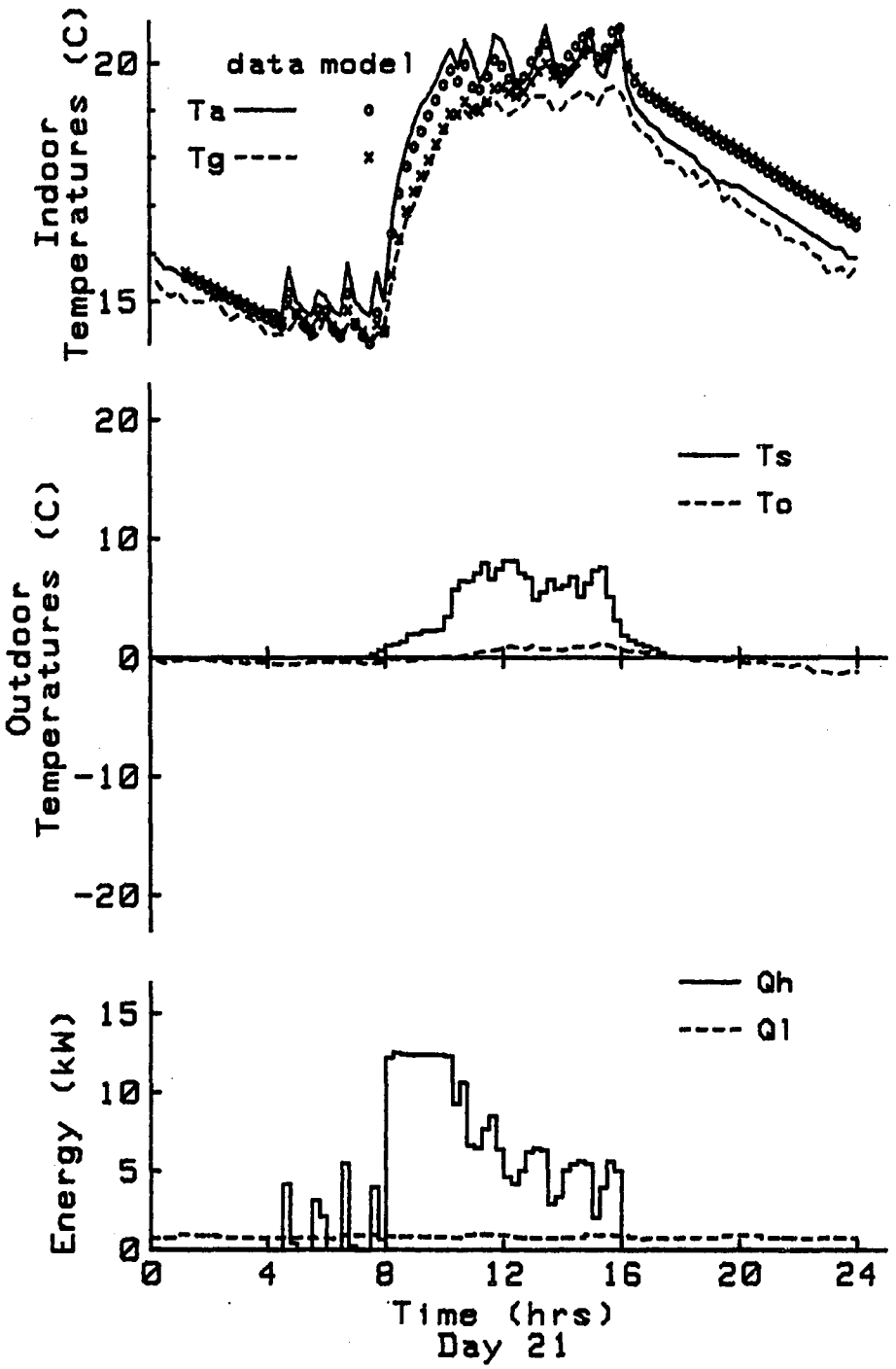
Indoor Temperatures (C)
20
15
data model
Ta
Tg
Outdoor Temperatures (C)
20
10
0
-10
-20
Ts
To
Energy (kW)
15
10
5
0
Qh
Ql
0
4
8
12
16
20
24
Time (hrs)
Day 21

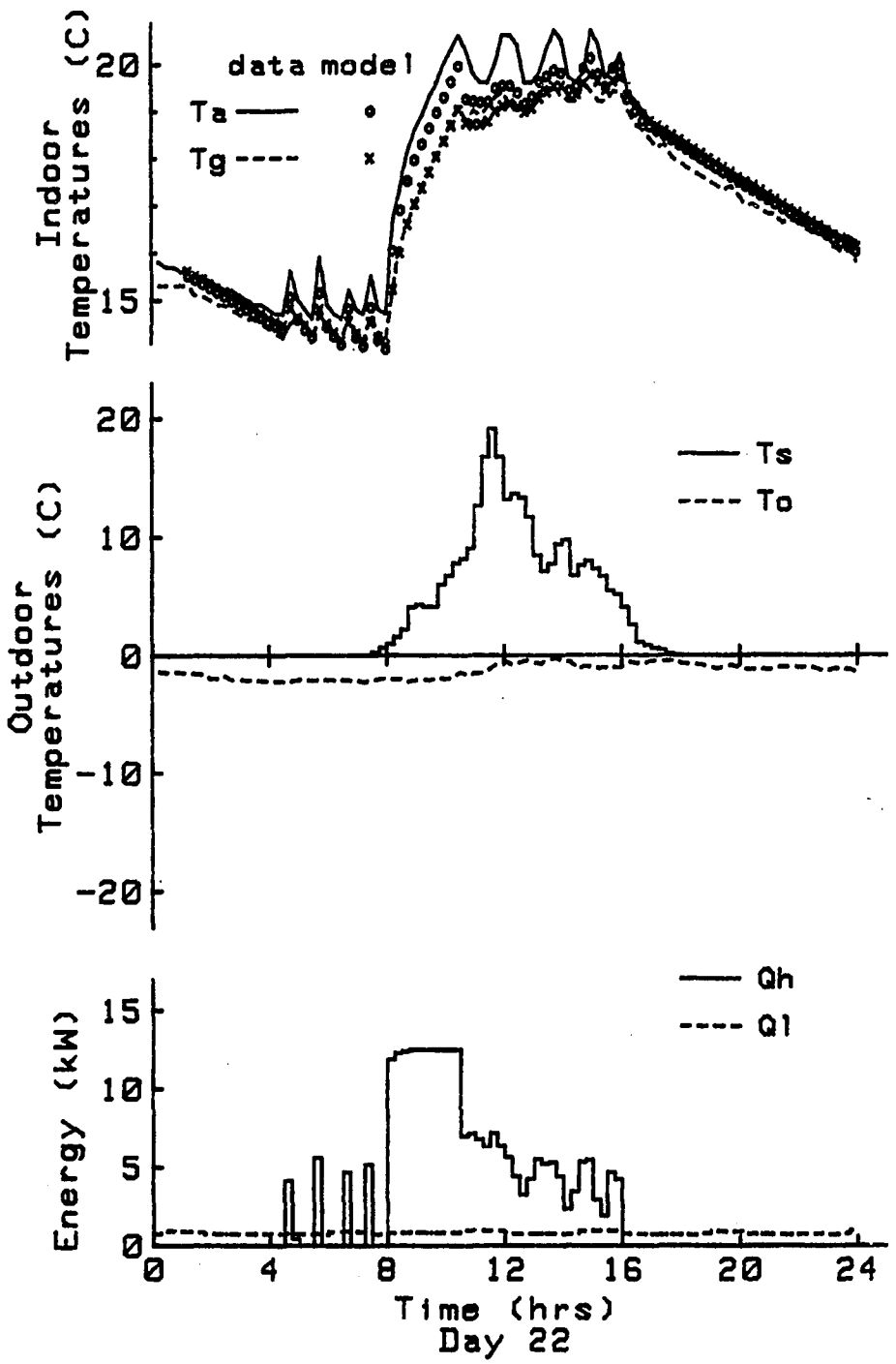
Indoor Temperatures (C)
20
15
data model
Ta
Tg
Outdoor Temperatures (C)
20
10
0
-10
-20
Ts
To
Energy (kW)
15
10
5
0
Qh
Ql
0
4
8
12
16
20
24
Time (hrs)
Day 22

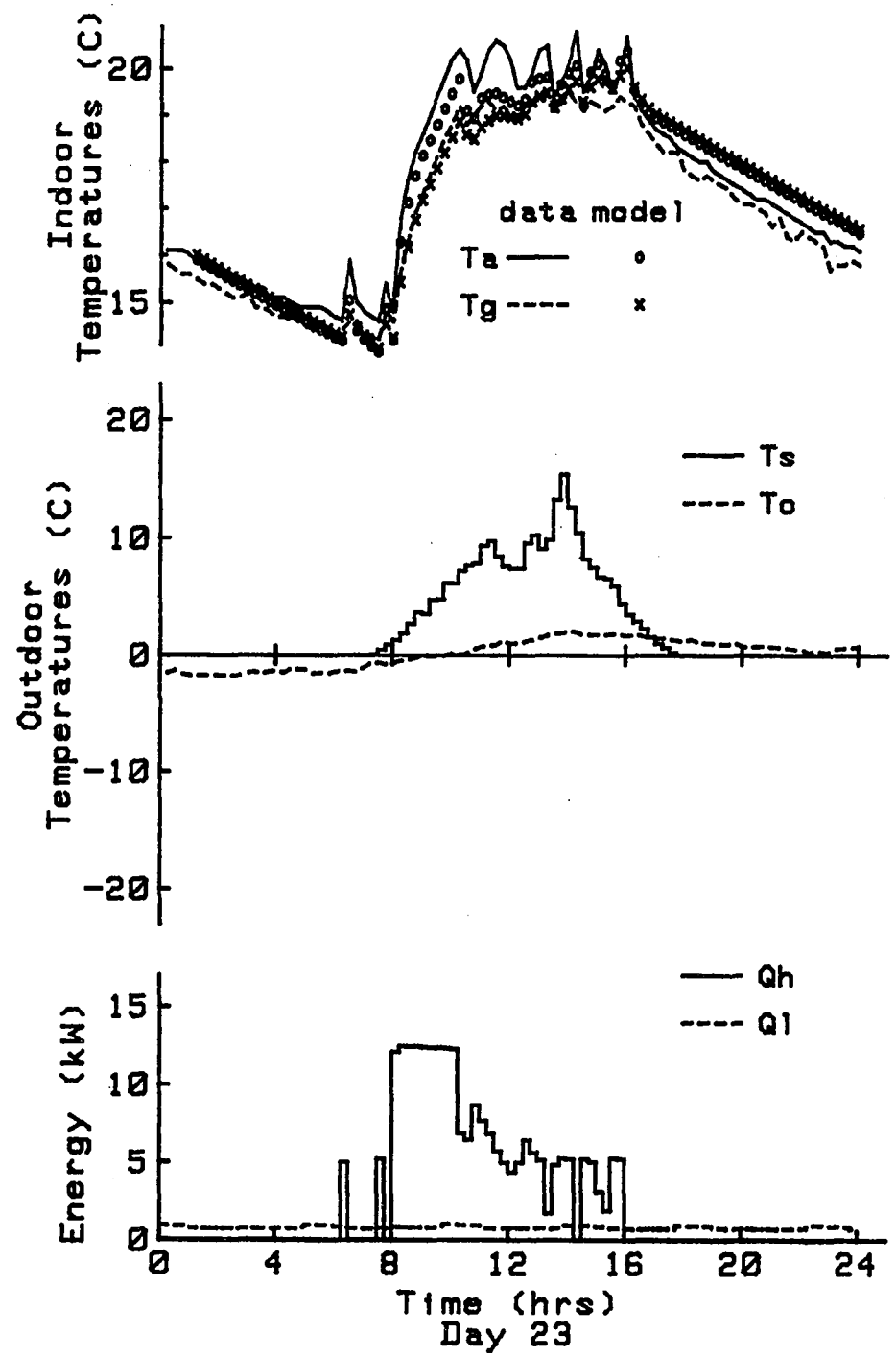
Indoor Temperatures (C)
20
15
data model
Ta
Tg
o
x
Outdoor Temperatures (C)
20
10
0
-10
-20
Ts
To
Energy (kW)
15
10
5
0
Qh
Ql
0
4
8
12
16
20
24
Time (hrs)
Day 23

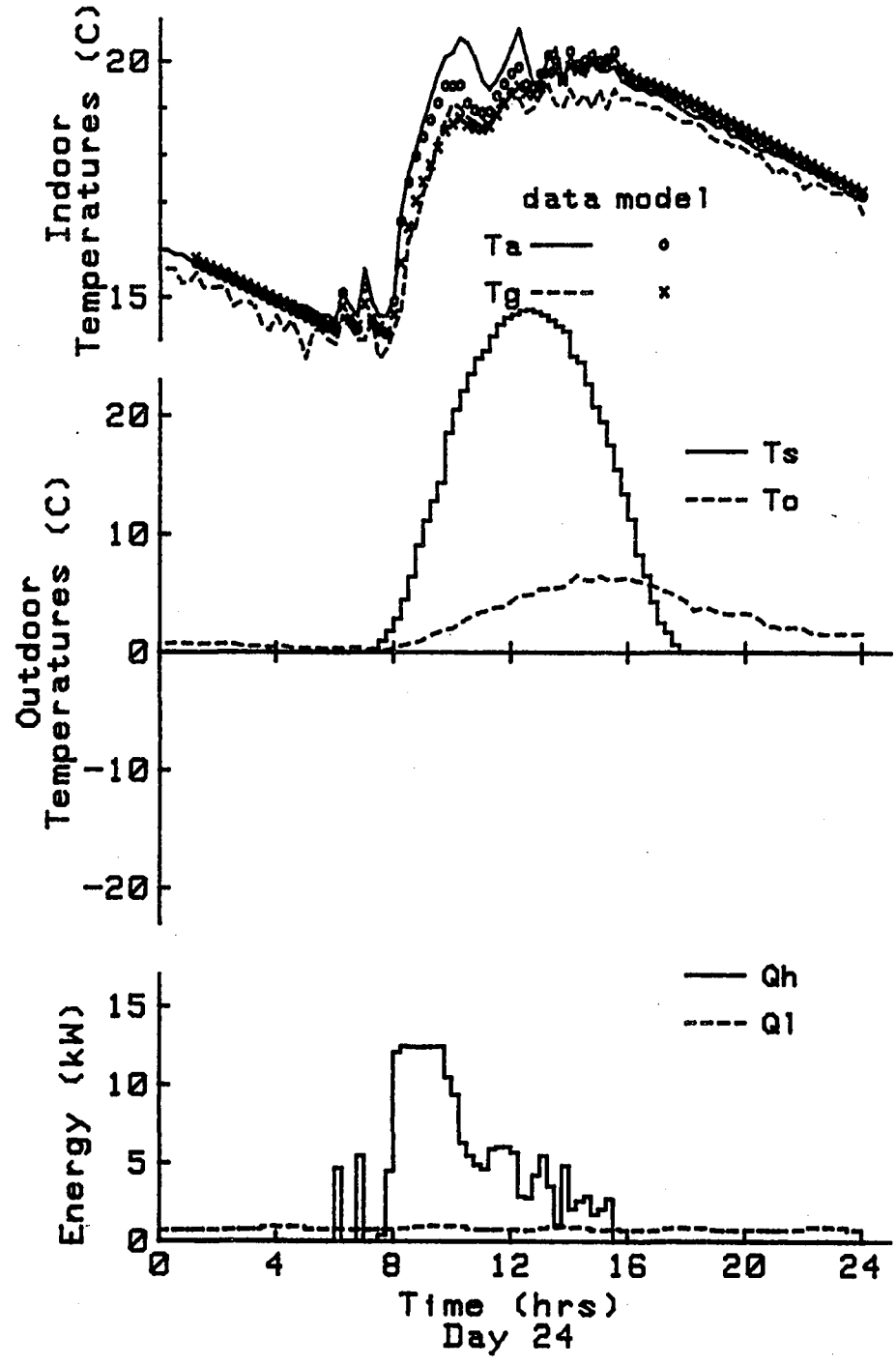
Indoor Temperatures (C)
20
15
data model
Ta
Tg
o
x
Outdoor Temperatures (C)
20
10
0
-10
-20
Ts
To
Energy (kW)
15
10
5
0
Qh
Ql
0
4
8
12
16
20
24
Time (hrs)
Day 24

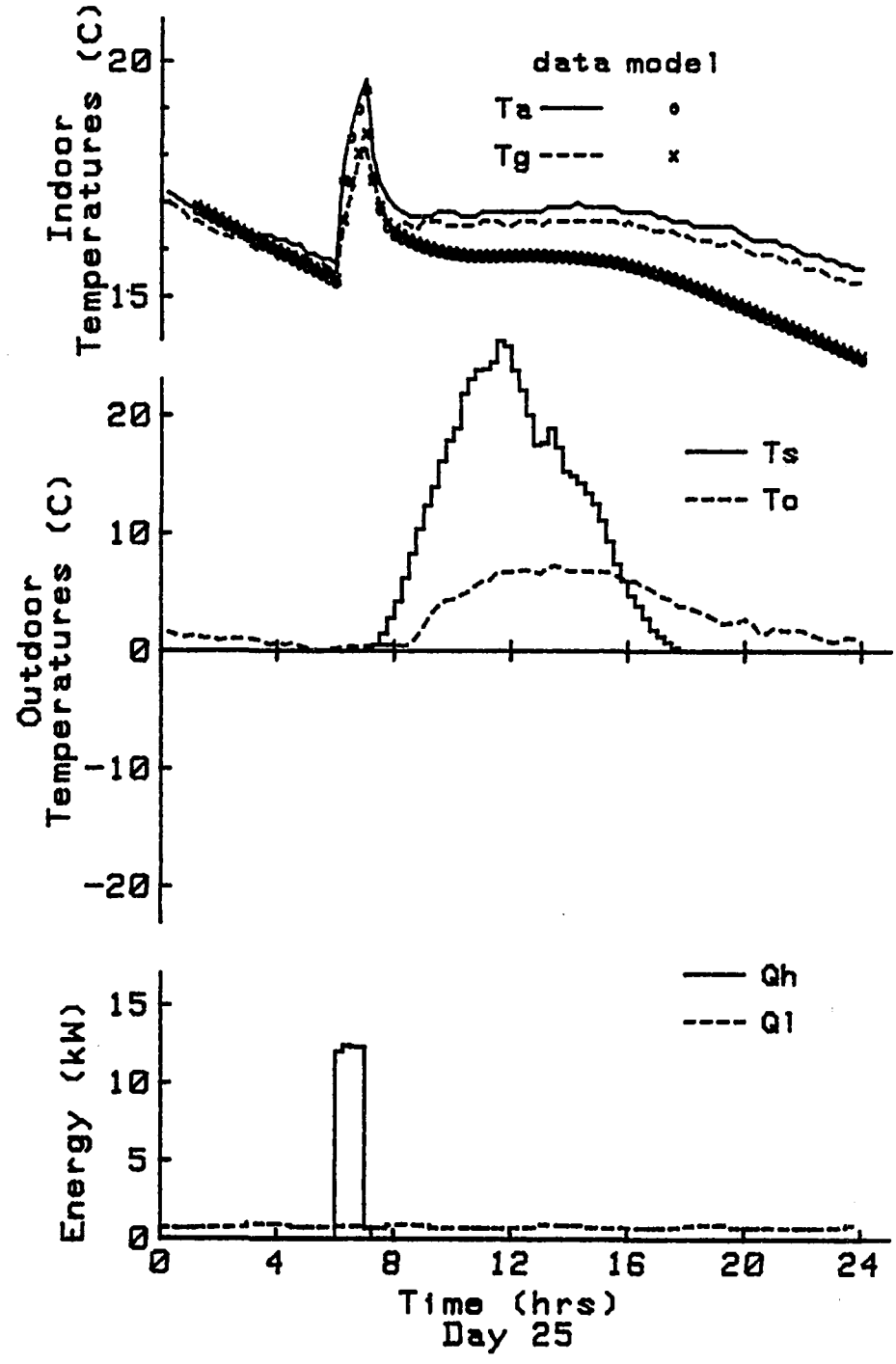
Indoor Temperatures (C)
20
15
data model
Ta
Tg
Outdoor Temperatures (C)
20
10
0
-10
-20
Ts
To
Energy (kW)
15
10
5
0
Qh
Ql
0
4
8
12
16
20
24
Time (hrs)
Day 25

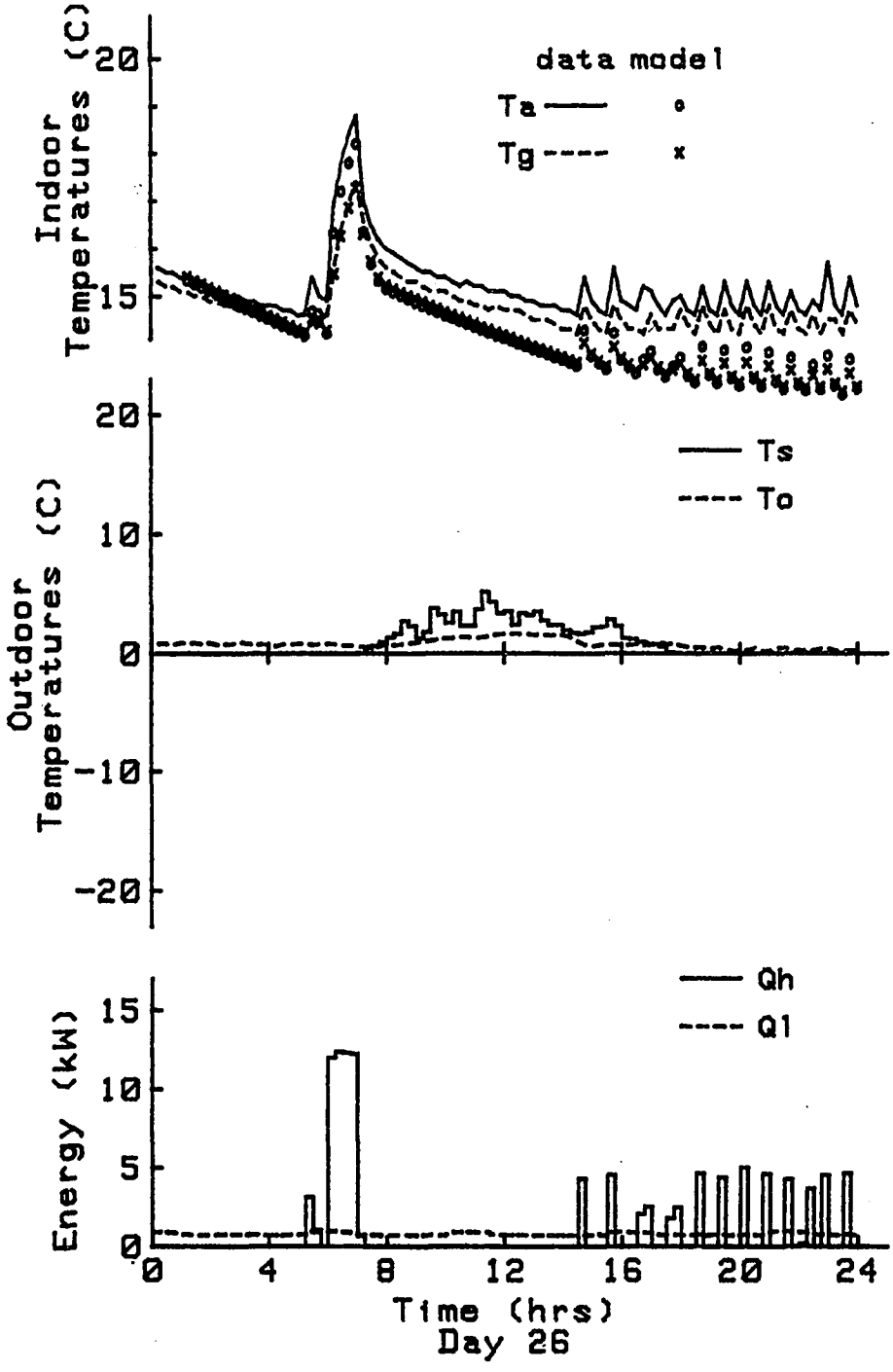
Indoor Temperatures (C)
20
15
data model
Ta
Tg
Outdoor Temperatures (C)
20
10
0
-10
-20
Ts
To
Energy (kW)
15
10
5
0
Qh
Ql
0
4
8
12
16
20
24
Time (hrs)
Day 26

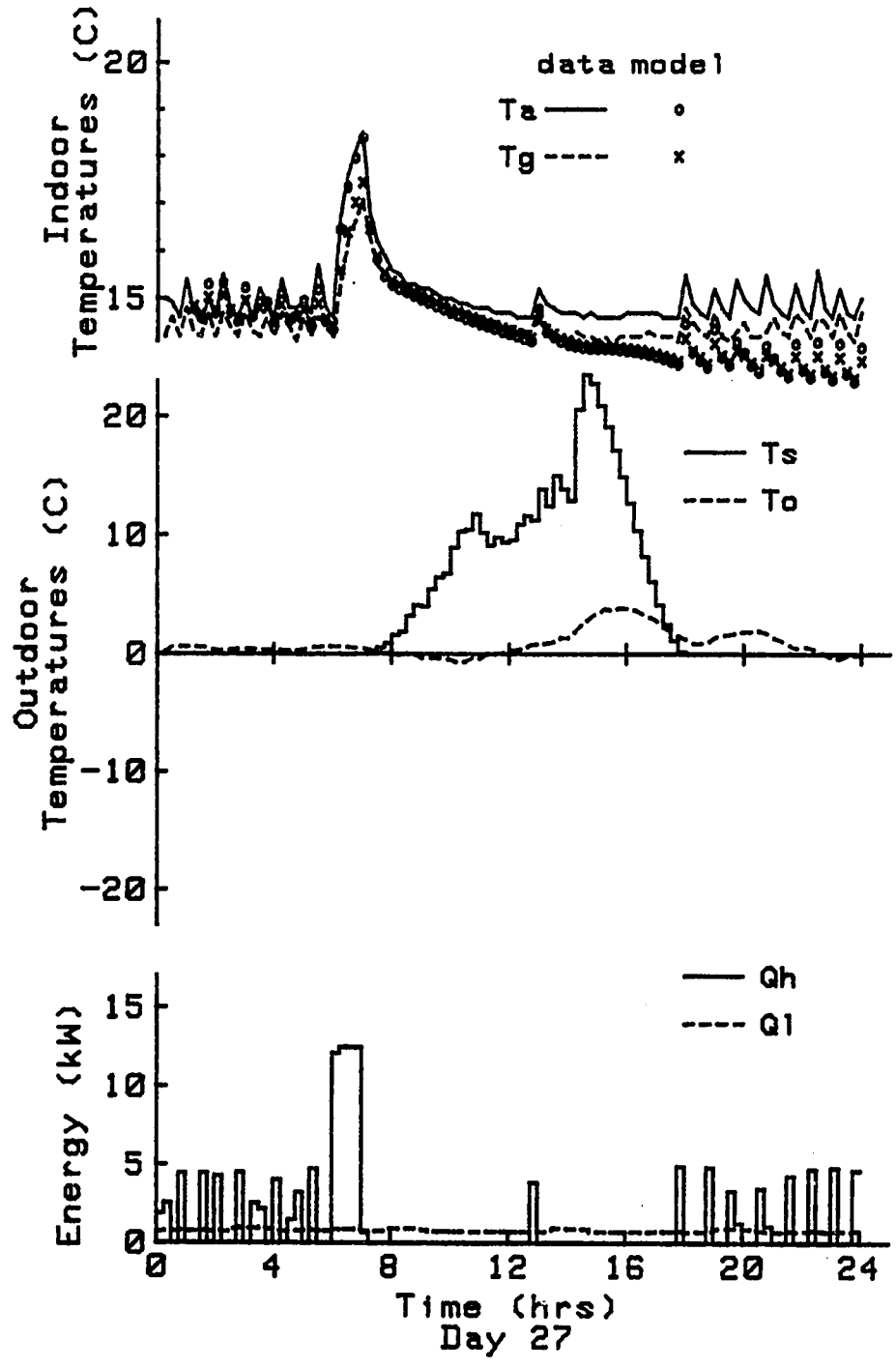
Indoor Temperatures (C)
20
15
data model
Ta
Tg
Outdoor Temperatures (C)
20
10
0
-10
-20
Ts
To
Energy (kW)
15
10
5
0
Qh
Q1
0
4
8
12
16
20
24
Time (hrs)
Day 27

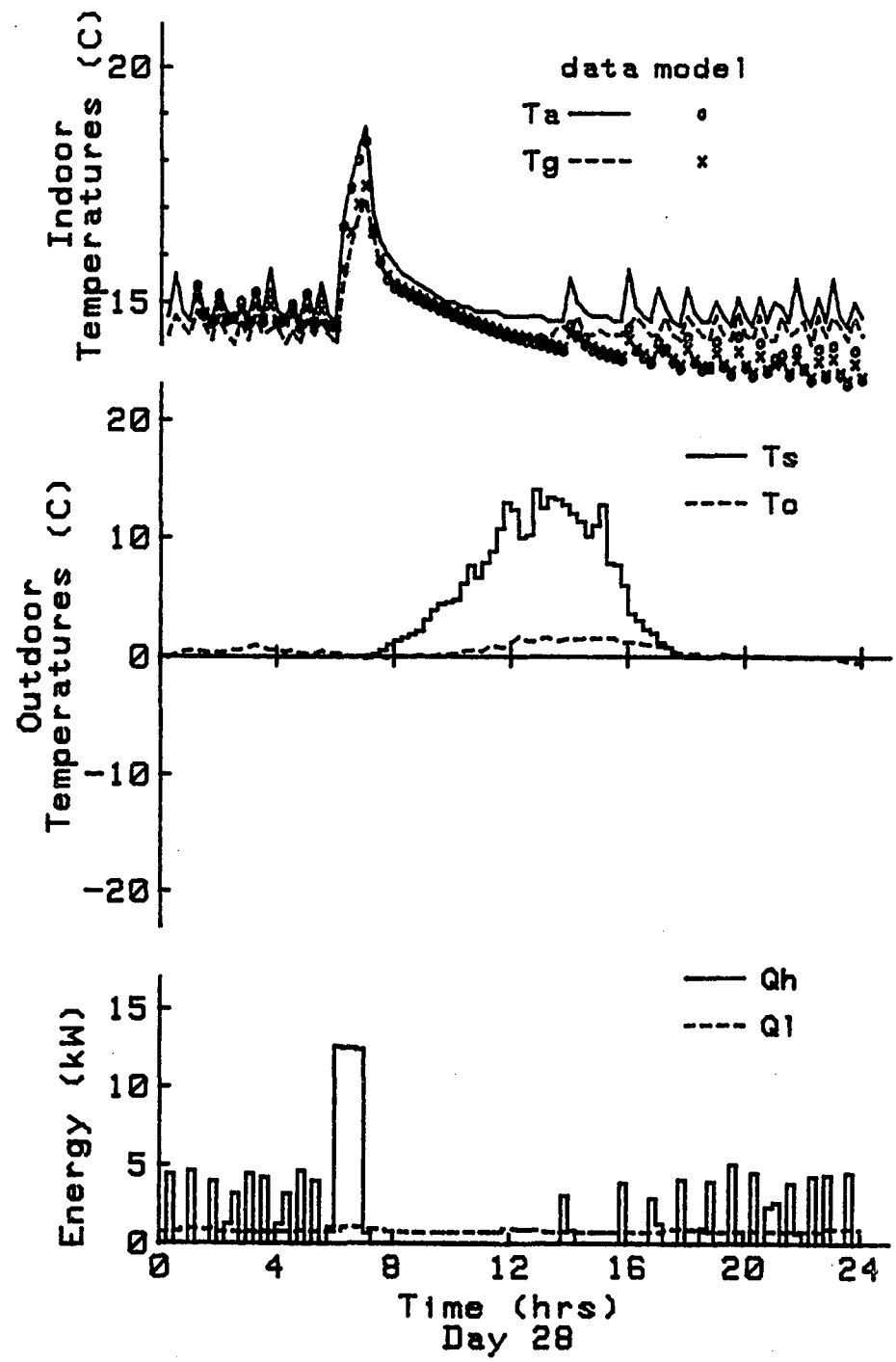
Indoor Temperatures (C)
20
15
data model
Ta
Tg
Outdoor Temperatures (C)
20
10
0
-10
-20
Ts
To
Energy (kW)
15
10
5
0
Qh
Ql
0
4
8
12
16
20
24
Time (hrs)
Day 28

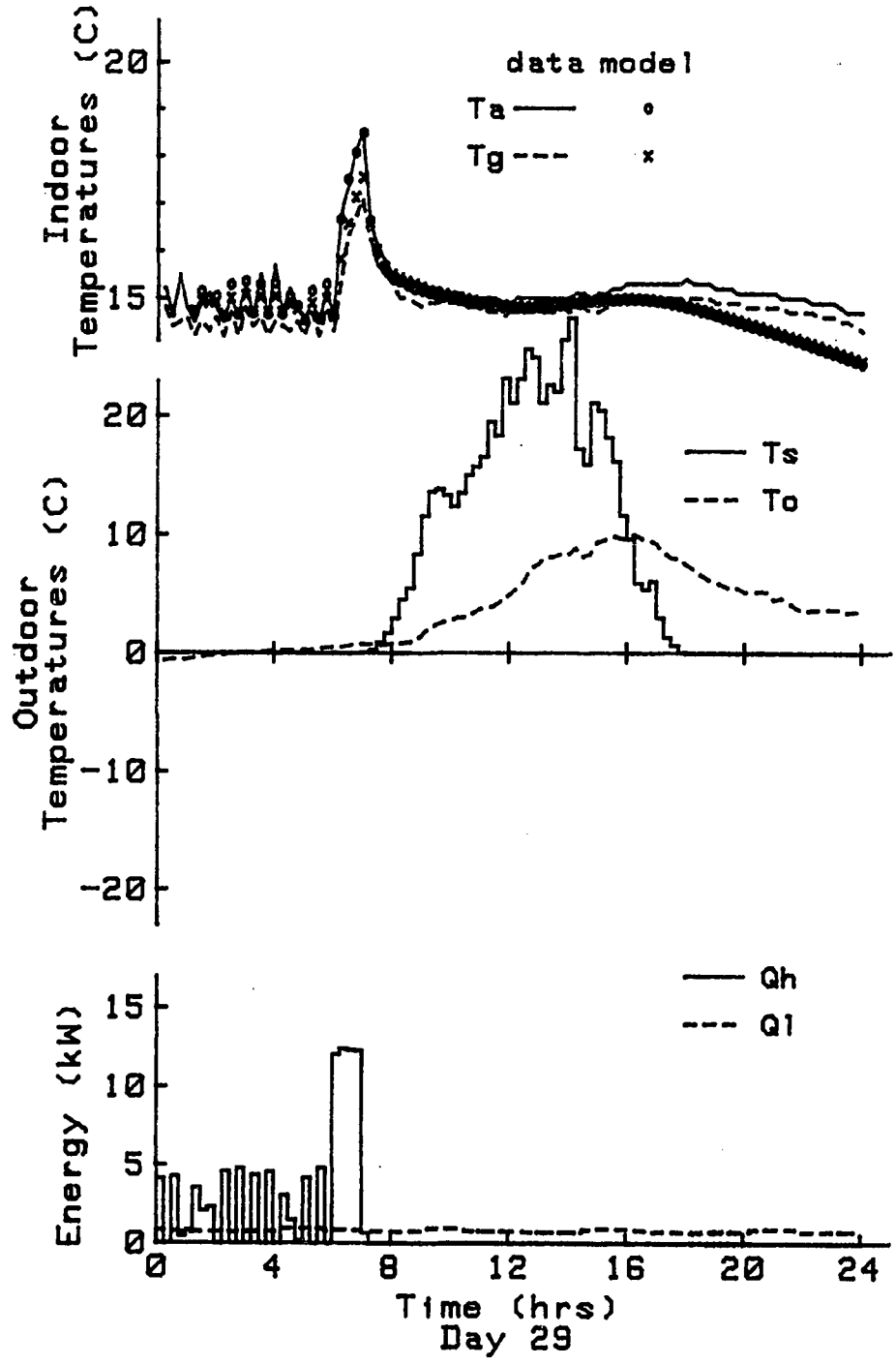
Indoor Temperatures (C)
20
15
data model
Ta
Tg
Outdoor Temperatures (C)
20
10
0
-10
-20
Ts
To
Energy (kW)
15
10
5
0
Qh
Ql
0
4
8
12
16
20
24
Time (hrs)
Day 29

APPENDIX C

Optimization Computer Program

The listing of the computer program developed in this study for calculating the optimal performance of the ERH is shown below. This program was written in an enhanced form of BASIC for a Hewlett-Packard System 35 (model number HP9835A) desktop computer.

```
10    OPTION BASE 1
20    RAD
30    DIM A(6,6),B(6,1),D(6,2),X(6,1),Wo(2,1),Ax(6,1),Bu(6,1)
,W(6,1)
40    DIM C(6,1),Y(1,1),Xi(6,1)
50    DIM Q(192),R(0:191),To(0:191),Ts(0:191),Z(192),U(0:191)
,S(0:191),Ys(192)
60    DIM P(6,1),At(6,6),Atp(6,1),Ct(1,6),Bt(1,6),Ptb(1,1),Un
(0:191),Ysn(192)
70    DIM I(6,6),Ima(6,6),Imai(6,6),Ca(1,6),Cab(1,1),Caw(1,1)
,Unl(0:191),Ysnl(192)
80    DIM Xls(192),Xlsn(192),Xlsnl(192)
90    SHORT S1,S2,S5,S6,S7,S8,S9
100 REM ----- DEFINE SPECIAL FUNCTIONS -----
110   Pr=0
120   Pl=0
130   St=0
140   ON KEY #0 GOSUB Pr
150   ON KEY #1 GOSUB Pl
160   ON KEY #2 GOSUB St
170   GOTO 240
180 Pr:    Pr=NOT Pr
190        RETURN
200 Pl:    Pl=1
210        RETURN
220 St:    St=1
230        RETURN
240 REM ----- SET-UP SYSTEM MATRICES -----
250   DATA 5.18550875820E-3,.187025430070,-.110257096866,-.02
08255279063,-1.48510344133E-2,-6.89275755656E-3,2.1142922477
9E-3
260   DATA -.025641332230,-.081773299634,-4.84137206800E-3,-.
00548015392200
270   READ Bn11,Bn12,Bn13,Bn14,Bn15,Bn16,Bn17
280   READ Bn21,Bn22,Bn23,Bn24
290   MAT A=(0)
300   MAT B=(0)
310   MAT D=(0)
320   A(1,1)=1-Bn11
330   A(2,2)=Bn21
340   Gam=1-Bn21-Bn24
350   A(2,1)=Gam*Bn21
360   A(2,3)=Bn23
370   D(1,1)=Bn11
380   D(1,2)=Bn17
390   D(2,1)=Bn24
400   A(1,3)=Bn13
410   A(1,4)=Bn14
420   A(1,5)=Bn15
```

```
430  A(1,6)=Bn16
440  A(4,3)=A(5,4)=A(6,5)=1
450  B(1,1)=Bn12
460  B(2,1)=Bn22
470  B(3,1)=1
480  C(2,1)=1
490  C(1,1)=Gam
500  MAT Ct=TRN(C)
510  MAT At=TRN(A)
520  MAT Bt=TRN(B)
530 REM ----- CONTINUE PREVIOUS OPTIMIZATION -----
540  Q$="N"
550  INPUT "CONTINUE PREVIOUS OPTIMIZATION? Y or N",Q$
560  IF Q$="N" THEN GOTO 680
570    CAT
580    INPUT "NAME OF FILE?",F$
590    ASSIGN #1 TO F$
600    READ #1,1;Xi(1,1),Ys,Us,Um,Juo,Jyo,Dj,Itau,Niter
610    Jo=Juo+Jyo
620    Xi(2,1)=Ys-Gam*Xi(1,1)
630    Xi(3,1)=Xi(4,1)=Xi(5,1)=Xi(6,1)=Us
640    FOR K=1 TO 192
650      READ #1,K+1;Xls(K),Ys(K),U(K-1),S(K-1),R(K-1),Q(K),
Z(K),To(K-1),Ts(K-1)
660    NEXT K
670  GOTO Costate
680 REM ----- INITIALIZE OPTIMIZATION PARAMETERS -----
690  DATA 6,19,36,57,89,128,181,223,256,287,371,410,441,470,
496,509,534,554,565,571,577,579
700  DATA 575,570,561,551,542,500,490,453,415,390,351,310,26
9,226,166,130,85,50,34,13,1
710  FOR K=0 TO 95
720    Qc=1
730    Rc=.5
740    Q(K+1)=Q(K+97)=Qc
750    REM IF (K+1>24) AND (K+1<72) THEN Q(K+1)=Q(K+97)=0
760    REM IF (K+1=24) OR (K+1=72) THEN Q(K+1)=Q(K+97)=Qc/2
770    R(K)=R(K+96)=Rc
780        IF (K>23) AND (K<72) THEN R(K)=R(K+96)=2*Rc
790    Z(K+1)=Z(K+97)=20
800    To(K)=To(K+96)=0
810 REM To(K)=To(K+96)=5*SIN((K/4-9)*PI/12)
820    Qs=0
830    REM IF (K>=29) AND (K<=71) THEN READ Qs
840    Ts(K)=Ts(K+96)=Qs/20
850  NEXT K
860  Q(192)=Qc/2
870  Um=12
880  Itau=-1
```

```
890  Niter=0
900 REM ----- CALCULATE OPTIMAL STEADY STATE PERFORMANCE ---
--
910  Zs=Z(1)
920  Q=Q(1)
930  R=R(0)
940  Wo(1,1)=To(0)
950  Wo(2,1)=Ts(191)
960  MAT I=IDN
970  MAT Ima=I-A
980  MAT Imai=INV(Ima)
990  MAT Ca=Ct*Imai
1000 MAT Cab=Ca*B
1010 MAT W=D*Wo
1020 MAT Caw=Ca*W
1030 Ys=Zs-R/(Q*Cab(1,1))
1040 Us=(Ys-Caw(1,1))/Cab(1,1)
1050 MAT Bu=B*(Us)
1060 MAT Bu=Bu+W
1070 MAT Xi=Imai*Bu
1080 PRINT "Us = ";Us;"    Xls = ";Xi(1,1);"    Ys = ";Ys
1090 REM ----- READ PREVIOUS CONTROL HISTORY -----
1100 U$="N"
1110 INPUT "USE PREVIOUS CONTROL HISTORY? Y or N",U$
1120 IF U$="N" THEN GOTO 1180
1130   INPUT "INPUT FILE NAME ",F$
1140   ASSIGN #1 TO F$
1150   FOR I=0 TO 191
1160     READ #1,I+1;S1,S2,U(I),S4,S5,S6,S7,S8,S9
1170   NEXT I
1180 Initialize:REM ----- INITIALIZE CONTROL HISTORY -----
1190 Niter=0
1200 Jyo=Juo=0
1210 MAT X=Xi
1220 FOR K=1 TO 192
1230   IF U$<>"N" THEN GOTO 1260
1240     U(K-1)=Us
1250     IF (Q(K)=0) OR (K>184) THEN U(K-1)=0
1260   Wo(1,1)=To(K-1)
1270   IF K=1 THEN Wo(2,1)=Ts(191)
1280   IF K<>1 THEN Wo(2,1)=Ts(K-2)
1290   MAT W=D*Wo
1300   MAT Bu=B*(U(K-1))
1310   MAT Ax=A*X
1320   MAT X=Ax+Bu
1330   MAT X=X+W
1340   MAT Y=Ct*X
1350   Ys(K)=Y(1,1)
1360   Xls(K)=X(1,1)
```

```
1370    Jyo=Jyo+.5*Q(K)*(Y(1,1)-Z(K))^2
1380    Juo=Juo+R(K-1)*U(K-1)
1390  NEXT K
1400    Jo=Jyo+Juo
1410  Costate:REM ----- CALCULATE COSTATE VARIABLES -----
1420  PRINTER IS 6
1430  IF Niter<10 THEN PRINT Niter,Jo,Hu,10^Itau
1440  IF (Niter>=10) AND (Niter<100) AND (FRACT(Niter/10)=0)
THEN PRINT Niter,Jo,Hu,10^Itau
1450  IF (Niter>=100) AND (Niter<1000) AND (FRACT(Niter/100)=
0) THEN PRINT Niter,Jo,Hu,10^Itau
1460  IF (Niter>=1000) AND (Niter<10000) AND (FRACT(Niter/100
0)=0) THEN PRINT Niter,Jo,Hu,10^Itau
1470  IF (Niter>=10000) AND (Niter<100000) AND (FRACT(Niter/1
0000)=0) THEN PRINT Niter,Jo,Hu,10^Itau
1480  PRINTER IS 16
1490  Niter=Niter+1
1500  MAT P=(0)
1510  FOR K=192 TO 1 STEP -1
1520    MAT Atp=At*P
1530    Y(1,1)=Ys(K)
1540    MAT Y=Y-(Z(K))
1550    MAT Y=Y*(Q(K))
1560    MAT P=C*Y
1570    MAT P=P+Atp
1580    MAT Ptb=Bt*P
1590    S(K-1)=Ptb(1,1)
1600    IF Pr=1 THEN PRINT USING "2A,3D,4A,4D.4D";"S(",K-1,")
 = ",S(K-1)
1610  NEXT K
1620  IF Pl=1 THEN GOSUB Plot
1630  IF St=1 THEN GOSUB Store
1640  IF (Dj=0) AND (Niter<>1) THEN GOSUB Store
1650    Ntrial=1
1660    Fc=0
1670  Tau:REM ----- UPDATE CONTROL HISTORY -----
1680    Tau=10^Itau
1690    Hu=0
1700    FOR K=0 TO 191
1710      Un(K)=U(K)-Tau*(S(K)+R(K))
1720      Un(K)=MAX(0,Un(K))
1730      Un(K)=MIN(Um,Un(K))
1740      IF (Un(K)<>0) AND (Un(K)<>Um) THEN Hu=Hu+(S(K)+R(K)
)^2
1750    NEXT K
1760  State:REM ----- RECALCULATE STATE VARIABLES -----
1770    MAT X=Xi
1780    Ju=Jy=0
1790    FOR K=1 TO 192
```

```
1800      Wo(1,1)=To(K-1)
1810      IF K=1 THEN Wo(2,1)=Ts(191)
1820      IF K<>1 THEN Wo(2,1)=Ts(K-2)
1830      MAT W=D*Wo
1840      MAT Bu=B*(Un(K-1))
1850      MAT Ax=A*X
1860      MAT X=Ax+Bu
1870      MAT X=X+W
1880      MAT Y=Ct*X
1890      Ysn(K)=Y(1,1)
1900      Xlsn(K)=X(1,1)
1910      Ju=Ju+R(K-1)*Un(K-1)
1920      Jy=Jy+.5*Q(K)*(Y(1,1)-Z(K))^2
1930      IF Pr=1 THEN PRINT USING "4A,3D,5X,4A,2D.2D,4X,4A,2
D.2D";"K = ",K,"U = ",U(K-1),"Y = ",Y(1,1)
1940    NEXT K
1950    J=Ju+Jy
1960    PRINT USING "#,6D.3D";Jo,J,Hu
1970    IF ((Ntrial=1) OR (Fc=1)) AND (J>Jo) THEN GOTO Ac1
1980    IF Fc=1 THEN GOTO Ac2
1990    IF Ntrial=1 THEN GOTO Aab
2000    IF J<J1 THEN GOTO Aa
2010    GOTO Ab
2020 Ac1:  Fc=1
2030       Itau=Itau-.25
2040       PRINT USING "4X,2A,4D.4D";"C ",10^(Itau+.25)
2050       GOTO Tau
2060 Ac2:  Itau=Itau-.25
2070       MAT U=Un
2080       MAT Ys=Ysn
2090       MAT Xls=Xlsn
2100       Dj=J-Jo
2110       Jo=J
2120       Juo=Ju
2130       Jyo=Jy
2140       PRINT USING "4X,2A,4D.4D";"C ",10^(Itau+.25)
2150       GOTO Costate
2160 Aab:  Itau=Itau+.25
2170       MAT Ysn1=Ysn
2180       MAT Xlsn1=Xlsn
2190       MAT Un1=Un
2200       J1=J
2210       Ju1=Ju
2220       Jy1=Jy
2230       Ntrial=2
2240       PRINT USING "4X,2A,4D.4D";"AB",10^(Itau-.25)
2250       GOTO Tau
2260 Aa:   Dj=J-Jo
2270       Juo=Ju
```

```
2280        Jyo=Jy
2290        Jo=J
2300        Itau=Itau+.25
2310        MAT U=Un
2320        MAT Ys=Ysn
2330        MAT Xls=Xlsn
2340        PRINT USING "4X,2A,4D.4D";"A ",10^(Itau-.25)
2350        GOTO Costate
2360 Ab:    Dj=Jl-Jo
2370        Jo=Jl
2380        Juo=Ju
2390        Jyo=Jy
2400        Itau=Itau-.5
2410        MAT U=Unl
2420        MAT Ys=Ysnl
2430        MAT Xls=Xlsnl
2440        PRINT USING "4X,2A,4D.4D";"B ",10^(Itau+.5)
2450        GOTO Costate
2460 Store:     REM ----- STORE DATA -----
2470   INPUT "ENTER FILE NAME:",F$
2480   ON ERROR GOTO 2770
2490   CREATE F$,193,44
2500   ASSIGN #1 TO F$
2510   S1=Xi(1,1)
2520   S2=Ys
2530   S3=Us
2540   S4=Um
2550   S5=Juo
2560   S6=Jyo
2570   S7=Hu
2580   S8=Itau
2590   S9=Niter
2600   PRINT #1,1;S1,S2,S3,S4,S5,S6,S7,S8,S9
2610   FOR K=1 TO 192
2620     S1=Xls(K)
2630     S2=Ys(K)
2640     S3=U(K-1)
2650     S4=S(K-1)
2660     S5=R(K-1)
2670     S6=Q(K)
2680     S7=Z(K)
2690     S8=To(K-1)
2700     S9=Ts(K-1)
2710     IF Pr=1 THEN PRINT S1;S2;S3;S4;S5;S6;S7;S8;S9
2720     PRINT #1,K+1;S1,S2,S3,S4,S5,S6,S7,S8,S9
2730   NEXT K
2740   ASSIGN * TO #1
2750   St=0
2760   RETURN
```

```
2770   OFF ERROR
2780   IF ERRN=54 THEN GOTO 2500
2790   BEEP
2800   DISP ERRM$
2810   PAUSE
2820   GOTO 2470
2830   END
2840 Plot: REM ----- PLOT AND PRINT RESULTS -----
2850 A$=F$
2860 INPUT "FILE NAME",A$
2870 Xi=Xi(1,1)
2880 Yi=Ys
2890 Ui=Us
2900 Ju=Juo
2910 Jn=Jo
2920 Djn=Dj
2930 Prin=16
2940 INPUT "ENTER PRINTER NUMBER ",Prin
2950 PRINTER IS Prin
2960 PRINT LIN(5),TAB(6),A$,LIN(2);
2970 Zc=Z(1)
2980 Rc=R(1)
2990 Qc=Q(1)
3000 Su1=Sun1=Sud1=Nn1=Nd1=Disd1=Disn1=0
3010 Su2=Sun2=Sud2=Nn2=Nd2=Disd2=Disn2=0
3020 FOR I=1 TO 192
3030   IF I>96 THEN GOTO 3140
3040   Su1=Su1+U(I-1)*.90
3050   IF (I>24) AND (I<72) THEN GOTO 3100
3060   Sun1=Sun1+U(I-1)*.90
3070   Nn1=Nn1+1
3080   Disn1=Disn1+(Ys(I)-Z(I))^2
3090   GOTO 3230
3100   Nd1=Nd1+1
3110   Sud1=Sud1+U(I-1)*.90
3120   Disd1=Disd1+(Ys(I)-Z(I))^2
3130   GOTO 3230
3140   Su2=Su2+U(I-1)*.90
3150   IF (I>120) AND (I<168) THEN GOTO 3200
3160   Sun2=Sun2+U(I-1)*.90
3170   Nn2=Nn2+1
3180   Disn2=Disn2+(Ys(I)-Z(I))^2
3190   GOTO 3230
3200   Nd2=Nd2+1
3210   Sud2=Sud2+U(I-1)*.90
3220   Disd2=Disd2+(Ys(I)-Z(I))^2
3230 NEXT I
3240 PRINT "      INITITAL CONDITIONS:                OPTIMIZ
ATION RESULTS:"
```

```
3250 PRINT USING "5X,25A,3D.D,11X,19A,5D";"   Air Temperatur
e (C) = ",Xi,"  # of Iterations = ",Niter
3260 PRINT USING "5X,25A,3D.D,11X,19A,5D";" Globe Temperatur
e (C) = ",Yi,"        Ju (cost) = ",Ju
3270 PRINT USING "5X,25A,2D.2D,11X,19A,5D";"       Heat Inpu
t (kW) = ";Ui,"        Jy (cost) = ",Jn-Ju
3280 PRINT USING "5X,25A,2D.2D,11X,19A,5D";"    Heat Capacit
y (kW) = ";Um,"         J (cost) = ",Jn
3290 PRINT
3300 PRINT "       AMBIENT CONDITIONS:"
3310 PRINT USING "14X,25A,3D.D";"  Mean Temperature (C) = ";
SUM(To)/192
3320 PRINT USING "10X,29A,5D";"Tot. Hor. Sol. (kJ/m2/day) =
";SUM(Ts)*20/1000
3330 PRINT
3340 PRINT "       SYSTEM PERFORMANCE:"
3350 PRINT "                                          First Day
    Second Day"
3360 PRINT USING "10X,24A,5X,5D,10X,5D";"Total Energy      d
ay   ",Sud1,Sud2
3370 PRINT USING "10X,24A,5X,5D,10X,5D";" Consumption    nig
ht   ",Sun1,Sun2
3380 PRINT USING "10X,24A,5X,5D,10X,5D";"    (MJ)        tot
al   ",Su1,Su2
3390 PRINT
3400 PRINT USING "10X,24A,5X,2D.2D,10X,2D.2D";"    RMS
     day   ",(Disd1/Nd1)^.5,(Disd2/Nd2)^.5
3410 PRINT USING "10X,24A,5X,2D.2D,10X,2D.2D";" Discomfort
   night   ",(Disn1/Nn1)^.5,(Disn2/Nn2)^.5
3420 PRINT USING "10X,24A,5X,2D.2D,10X,2D.2D";"    (C)
   total   ",((Disd1+Disn1)/96)^.5,((Disd2+Disn2)/96)^.5
3430 PRINT LIN(6);
3440 PRINTER IS 16
3450 REM ----- PLOT RESULTS -----
3460   PLOTTER IS 7,5,"9872A"
3470   PLOTTER 7,5 IS ON
3480   PRINTER IS 7,5
3490   PRINT "VS 5;";
3500   PRINTER IS 16
3510   LIMIT 30,235,30,180
3520   SCALE -28,196,-17.5,27.5
3530   CLIP 0,192,-17.5,27.5
3540   LINE TYPE 1
3550   AXES 16,5,0,0,1,1
3560   UNCLIP
3570   CSIZE 4
3580   LORG 8
3590   LDIR 0
3600   FOR I=0 TO 25 STEP 5
```

```
3610      MOVE -2,I
3620      LABEL USING "DD";I
3630    NEXT I
3640    FOR I=-.5 TO -1.5 STEP -.5
3650      MOVE -2,10*I
3660      LABEL USING "SZ.D";I
3670    NEXT I
3680    LORG 5
3690    FOR I=4 TO 48 STEP 4
3700      MOVE 4*I,-1
3710      LABEL I
3720    NEXT I
3730    MOVE 96,-3
3740    LABEL "Time (hrs)"
3750    LINE TYPE 4
3760    MOVE 24,25
3770    DRAW 24,-15
3780    MOVE 72,25
3790    DRAW 72,-15
3800    MOVE 120,25
3810    DRAW 120,-15
3820    MOVE 168,25
3830    DRAW 168,-15
3840    MOVE 0,20
3850    DRAW 192,20
3860    MOVE 0,-10*R(12)
3870    DRAW 24,-10*R(12)
3880    MOVE 24,-10*R(48)
3890    DRAW 72,-10*R(48)
3900    MOVE 72,-10*R(96)
3910    DRAW 120,-10*R(96)
3920    MOVE 120,-10*R(144)
3930    DRAW 168,-10*R(144)
3940    MOVE 168,-10*R(180)
3950    DRAW 192,-10*R(180)
3960    LINE TYPE 5,2
3970    MOVE 0,Xls
3980    FOR K=1 TO 192
3990      DRAW K,Xls(K)
4000    NEXT K
4010    MOVE 80,24
4020    DRAW 92,24
4030    LORG 2
4040    LINE TYPE 1
4050    CSIZE 3.5
4060    LABEL " Tair"
4070    MOVE 80,22.5
4080    DRAW 92,22.5
4090    LABEL " Tglobe"
```

```
4100    LORG 5
4110    MOVE 96,15
4120    LABEL USING "4A,2D";"Tds=",Zc
4130    LORG 5
4140      MOVE 12,-14
4150      LABEL USING "2A,Z.D";"q=",Q(12)
4160      MOVE 12,-16
4170      LABEL USING "2A,Z.D";"r=",R(12)
4180      MOVE 48,-14
4190      LABEL USING "2A,Z.D";"q=",Q(48)
4200      MOVE 48,-16
4210      LABEL USING "2A,Z.D";"r=",R(48)
4220      MOVE 96,-14
4230      LABEL USING "2A,Z.D";"q=",Q(96)
4240      MOVE 96,-16
4250      LABEL USING "2A,Z.D";"r=",R(96)
4260      MOVE 144,-14
4270      LABEL USING "2A,Z.D";"q=",Q(144)
4280      MOVE 144,-16
4290      LABEL USING "2A,Z.D";"r=",R(144)
4300      MOVE 180,-14
4310      LABEL USING "2A,Z.D";"q=",Q(180)
4320      MOVE 180,-16
4330      LABEL USING "2A,Z.D";"r=",R(180)
4340    LDIR PI/2
4350    CSIZE 4
4360    MOVE -13,20
4370    LABEL "(C)"
4380    MOVE -18,20
4390    LABEL "Temperature"
4400    MOVE -13,5
4410    LABEL "(kW)"
4420    MOVE -18,5
4430    LABEL "Heat Input"
4440    MOVE -21,-10
4450    LABEL "Output"
4460    MOVE -26,-10
4470    LABEL "Co-state"
4480    MOVE 0,Ys
4490    FOR K=1 TO 192
4500      DRAW K,Ys(K)
4510    NEXT K
4520    MOVE 0,U(0)
4530    FOR K=1 TO 191
4540      DRAW K,U(K-1)
4550      DRAW K,U(K)
4560    NEXT K
4570    DRAW 192,U(191)
4580    MOVE 0,S(0)*10
```

```
4590    FOR K=1 TO 191
4600      DRAW K,S(K)*10
4610    NEXT K
4620    DRAW 192,0
4630    PENUP
4640    PLOTTER 7,5 IS OFF
4650    P1=0
4660    RETURN
4670    END
```